Distribution Agreement

In presenting this thesis or dissertation as a partial fulfillment of the requirements for an advanced degree from Emory University, I hereby grant to Emory University and its agents the non-exclusive license to archive, make accessible, and display my thesis or dissertation in whole or in part in all forms of media, now or hereafter known, including display on the world wide web. I understand that I may select some access restrictions as part of the online submission of this thesis or dissertation. I retain all ownership rights to the copyright of the thesis or dissertation. I also retain the right to use in future works (such as articles or books) all or part of this thesis or dissertation.

Signature:

_____ _____

Kenneth M. McCullough Date

Cell-Type Specific Behavioral and Molecular Characterization of Fear Controlling Amygdala Sub-Populations

By

Kenneth M. McCullough

Doctor of Philosophy

Graduate Division of Biological and Biomedical Science
Neuroscience

_____
Kerry Ressler, M.D., Ph.D.
Advisor

_____
Shawn Hochman, Ph.D.
Committee Member

_____
Astrid Prinz, Ph.D
Committee Member

_____
Donald Rainnie, Ph.D.
Committee Member

_____
Malú Tansey, Ph.D.
Committee Member

Accepted:

_____
Lisa A. Tedesco, Ph.D.
Dean of the James T. Laney School of Graduate Studies

_____

Date

Cell-Type Specific Behavioral and Molecular Characterization of Fear Controlling Amygdala Sub-Populations

By

Kenneth M. McCullough

B.A., Lewis & Clark College, 2010

Advisor: Kerry Ressler, M.D., Ph.D.

An abstract of

A dissertation submitted to the Faculty of the

James T. Laney School of Graduate Studies of Emory University

in partial fulfillment of the requirements for the degree of

Doctor of Philosophy

in Graduate Division of Biological and Biomedical Science, Neuroscience

2017

Abstract

Cell-Type Specific Behavioral and Molecular Characterization of
Fear Controlling Amygdala Sub-Populations

Behavioral and molecular characterization of cell-type specific populations governing fear learning and related behaviors is a promising avenue for the identification of more targeted therapeutics for the treatment of fear-related disorders such as Posttraumatic Stress Disorder. In the amygdala, a number neuronal of sub-populations within previously identified nuclei have been identified by their distinct mRNA and protein expression profiles. These sub-populations appear to differentially regulate fear behaviors by supporting the learning and expression of fear or by inhibiting fear expression and supporting fear extinction. Here, we approach the identification, behavioral characterization and molecular characterization of potentially behaviorally relevant amygdala sub-populations in three ways. First, we perform an in-depth analysis of the expression and co-expression of six mRNA markers that may relate to behaviorally relevant functional sub-populations within the central amygdala (CeA). Second, we perform an in-depth behavioral and molecular characterization of one such CeA population, the dopamine receptor 2 (*Drd2)* expressing population. Third, we behaviorally and molecularly characterize a fear inhibiting population, the Thy-1 population, found within the basolateral amygdala (BLA).

In our characterization of CeA sub-populations, we find that within the lateral compartment of the central amygdala (CeL), Somatostatin (*Sst),* Tachykinin *(Tac2)* Neurotensin *(Nts)* and Corticotropin releasing factor (*Crf)* mRNAs mark a single convergent population; however, within the medial compartment of the central amygdala (CeM) these RNAs mark independent populations. Additionally, protein kinase C delta (*Prkcd)* and *Drd2* mRNAs mark non-overlapping sub-populations within the capsular compartment of the central amygdala (CeC) and CeL. Further characterization of the CeA *Drd2* population identifies this population as a fear-supporting population whose activity is sufficient to enhance fear expression and block fear extinction. Cell-type specific characterization of actively translating RNAs using translating ribosome affinity purification (TRAP) reveals that *Sst5r, Npy5r, Fgf3, ErbB4, Fkbp14, Dlk1, Ssh3* and *Adora2a* are each differentially regulated within *Drd2* neurons following fear conditioning. Pharmacological manipulation of *Drd2* neurons through D2R and $A_{2A}R$ recapitulate fear-supporting profile observed with direct chemogenetic activation. Finally, using optogenetics and chemogenetics we identify the Thy-1 population of the BLA as a fear-inhibiting population. Isolation and sequencing of RNA from Thy-1 neurons reveals *Ntsr2, Dkk3, Rspo2,* and *Wnt7a* as being upregulated in Thy-1 neurons compared to other amygdala neurons. Pharmacological activation of NTSR2 is sufficient to recapitulate fear-suppression profile observed using direct manipulations of this population. Our efforts have clarified the identities of sub-populations of the CeA and provided important molecular characterizations of crucial fear-controlling populations of the CeA and BLA.

Cell-Type Specific Behavioral and Molecular Characterization of Fear Controlling Amygdala Sub-Populations

By

Kenneth M. McCullough

B.A., Lewis & Clark College, 2010

Advisor: Kerry Ressler, M.D., Ph.D.

A dissertation submitted to the Faculty of the

James T. Laney School of Graduate Studies of Emory University

in partial fulfillment of the requirements for the degree of

Doctor of Philosophy

in Graduate Division of Biological and Biomedical Science, Neuroscience

2017

Acknowledgements

Hey Kerry! You rock. Thank you for being the best advisor I could ask for. Everyone in the Ressler Lab, you are also the best and thank you for all of your advice and friendship. Dennis, obviously you taught me everything I know about science, so I wouldn't be here without you. My committee members, thank you for your help and guidance. Filomene, I look forward to our future adventures. Lastly, friends and family especially Jim, John, Adam, Lolly, Kevin, Melly, Andrew, Alex and Ellie thank you for constant love and support (woof!).

Index

Chapter Index

Figure Index

Supplemental Figure Index

Index of Tables

Chapter 1: Introduction: Bridging the Gap: Towards a Cell-Type Specific Understanding of Neural Circuits Underlying Fear Behaviors.

1.1 Context, Author's Contribution and Acknowledgement of Reproduction.

The following chapter reviews the current understanding of the neural circuits governing fear and anxiety-like behaviors. This chapter will discuss recent findings that elucidate the neural underpinnings of fear behaviors utilizing optogenetics, chemogenetics and other next generation techniques. The work presented here was conceptualized, organized, researched and written by the dissertation author under the guidance of Dr. Kerry Ressler. The chapter is reproduced from McCullough, K.M., Morrison, F.G., and Ressler K.J.. Bridging the Gap: Towards a cell-type specific understanding of neural circuits underlying fear behavior. *Neurobiology of Learning and Memory* (2016)

1.2 Abstract

Fear and anxiety-related disorders, such as Posttraumatic Stress Disorder (PTSD) in humans, are remarkably common and debilitating, and are often characterized by dysregulated fear responses. Rodent models of fear learning and memory have taken great strides towards elucidating the specific neuronal circuitries underlying the learning of fear responses. The present review addresses recent research utilizing optogenetic approaches to parse circuitries underlying fear behaviors. It also highlights the powerful advances made when optogenetic techniques are utilized in a genetically defined, cell-type specific, manner. The application of next-generation genetic and sequencing approaches in a cell-type specific context will be essential for a mechanistic understanding of the neural circuitry underlying fear behavior and for the rational design of targeted, circuit specific,

pharmacologic interventions for the treatment and prevention of fear-related disorders such as PTSD.

1.3 Introduction

Disorders whose major symptoms relate to the dysregulation of fear responses are usually characterized by over-generalization of fear and inability to extinguish fearful responses. Such dysregulation leads to a pathological expression of fear behaviors that can be quite debilitating, leading to a range of intrusive, hyperarousal, avoidance, cognitive, and depression symptoms. The treatment of fear-related disorders often involves cognitive-behavioral therapies, in particular exposure therapy, which mirrors behavioral extinction processes used in rodent models, relying on the repeated and non-reinforced presentation of cues previously associated with noxious stimulus.

Advances in cognitive-behavioral therapy approaches targeting traumatic memories have been made using cognitive enhancers, for example by targeting emotion-related synaptic plasticity via the NMDA, Dopamine, and Cannabinoid receptors (Singewald, Schmuckermair, Whittle, Holmes, & Ressler, 2015). Pharmacological interventions may be used to generally enhance plasticity within neural circuitry including that responsible for behavioral extinction. Across several fear- and anxiety-related disorders, the administration of cognitive enhancers, such as d-cycloserine, in conjunction with exposure-based psychotherapy has been shown to enhance the beneficial effects of behavioral therapy sessions in a rapid and long-lasting manner (Rodrigues et al., 2014). Despite these advances, insufficient knowledge of the underlying molecular and cellular mechanisms mediating fear acquisition, expression, and extinction continues to limit the *specificity* and *effectiveness* of further therapeutic breakthroughs. Therefore, a greater understanding of

the neural circuitry mediating fear processing will catalyze further progress in the development of more selective treatments for fear- and anxiety-related disorders.

In this review, we will begin by discussing the understanding of the circuitry governing the acquisition and extinction of classically conditioned fear behaviors. We will continue by discussing the advent of optogenetic approaches and the contributions this technique has made to our knowledge of fear circuits. We will discuss the use of genetic techniques to determine which and how cell populations are recruited into memory traces. With a special focus on studies that involve behavioral manipulations, we will examine recent advances in the manipulation of identified cellular sub-populations housed within canonical fear and emotional learning related circuitries. Finally, we will provide a brief review of methods for cell-type specific isolation of RNA for sequencing.

As the basic neural circuitry governing fear behaviors continues to be elucidated at a rapid pace, it is necessary to act prospectively by applying these findings towards the discovery of applicable treatments for patients suffering from fear and anxiety related disorders. By uncovering cell-type specific markers for neural circuitry governing fear and anxiety behaviors in rodent models modern researchers have an opportunity to concurrently open avenues for more targeted pharmacological therapies in humans. Cell type specific markers may be conserved across species and targeting these convergences will maximize translational value of discoveries. This review is meant to highlight the need for further cell-type specific approaches in order to make rapid progress towards more selective and targetable pharmacological treatments of fear-related disorders in humans.

1.4 Background on Circuitry and Fear

Pavlovian Conditioning

Pavlovian fear conditioning is a popular and powerful technique for studying learning and memory in animal models. This is primarily due to it being a rapidly acquired behavior with consistent and easily measured behavioral outputs that rely on a well-characterized core neural circuit. Fear conditioning, also discussed as threat conditioning (LeDoux, 2014), occurs through the pairing of an initially innocuous conditioned stimulus (CS, e.g., an auditory tone during auditory fear conditioning or the context of training during contextual fear conditioning) with an aversive unconditioned stimulus (US, e.g., a mild foot shock). Following several CS-US pairings, the subject will exhibit fear response behaviors or conditioned responses (CRs) to presentations of the CS alone. The most common fear responses investigated are freezing (the cessation of all non-homeostatic movement) and fear potentiated startle (FPS, in which the amplitude of an animals' startle to a noise burst is potentiated upon combined presentation of the CS and noise burst) (R. J. Blanchard & Blanchard, 1969; Fanselow, 1980).

In addition to measures of freezing and fear potentiated startle, there is a multitude of tests to parsimoniously examine an animal's motivational state. Briefly, in contrast to freezing or startle responses, tests demanding an active or passive avoidance response require an additional instrumental learning procedure to either perform or inhibit performance of an action such as shuttling in order to avoid a shock (*Methods of Behavior Analysis in Neuroscience.*, 2009; Picciotto & Wickman, 1998; Sousa, Almeida, & Wotjak, 2006). These learning paradigms utilize additional important circuitries and may provide further insights into the etiologies of fear related disorders (Izquierdo & Medina, 1997).

The present review will focus primarily upon conditioned fear responses such as freezing and FPS following either the acquisition or extinction of fear; however, understanding the neural substrates governing additional motivated behaviors is likewise important for understanding the spectrum of fear-related processes.

Notably, fear responses are adaptive only when the CS clearly predicts the US. When these stimuli are no longer paired, such as during extinction (when the CS is repeatedly presented without any US reinforcement), a subject will learn that the CS is no longer predictive of the US, and CRs will decrease. Importantly, extinction is generally considered to be a new learning event that modulates rather than modifies the original learned fear association; for an excellent discussion of extinction see Myers and Davis, 2007 (Myers & Davis, 2007). In this review, we refer to 'fear conditioning' or training as the period when CS – US pairings are presented; 'fear extinction' as a period when multiple or continuous CS presentations occur in the absence of the US, resulting in a decrement in CRs; 'fear expression' refers to eliciting CRs to a CS; and 'extinction expression' refers to the testing for suppression of CRs to a CS after extinction learning.

Fear learning: Basic Circuitry and Key Players

The circuitry attributed to controlling elements of fear conditioning is ever expanding and we will discuss several additional areas in the course of this review; however, the core 'canonical' circuitry remains well understood and centers on the core amygdala nuclei. For recent in-depth reviews of the current understanding of the neural circuitries governing fear and anxiety see: (Duvarci & Pare, 2014; Ehrlich et al., 2009; Myers & Davis, 2007; Pape & Pare, 2010; Pare, Quirk, & Ledoux, 2004). The core nuclei within the amygdala consist of the lateral (LA), basolateral (BA), and central (CeA)

amygdala, which may be subdivided into the dorsolateral LA (LAdl), ventromedial LA (LAvm), ventrolateral LA (LAvl), anterior BA (BAa), posterior BA (BAp), central or capsular CeA (CeC), lateral CeA (CeL), and medial CeA (CeM). These nuclei may be even further subdivided. In the present review, the basolateral complex (BA + LA) will be abbreviated BLA.

Experimentally, dissections of CeC/CeL/CeM and LA/BA circuitries often fail to sufficiently discriminate between nuclei for a number of reasons, foremost due to their small sizes and close proximity. Specifically the CeC and the CeL tend to be conflated and the anterior aspect of the BAa is usually treated as representative of the whole BA or BLA. These, previously unavoidable, imprecisions may need to be corrected in time as more rigorous descriptions of micro-circuitries are performed. Furthermore, molecularly determined cell-type specific identification will lead to more powerful approaches to understanding microcircuit function in the future.

In the case of auditory fear conditioning (in which an auditory tone CS is paired with the US), salient information regarding the CS and US converge on the LA. Auditory information flows into the LA from the secondary auditory cortex (AuV) and auditory thalamus: medial geniculate nucleus/posterior intralaminar nucleus (MGn/PIN) (LeDoux, Ruggiero, & Reis, 1985; Linke, Braune, & Schwegler, 2000). Information regarding the US is communicated via the somatosensory cortex, somatosensory thalamus and periaqueductal grey (PAG) (LeDoux, Farb, & Ruggiero, 1990; McDonald, 1998). The LA integrates the information regarding both the tone and shock, and is a major site of learning related plasticity (Muller, Corodimas, Fridel, & LeDoux, 1997). Projections from the LA can modulate CeA activity directly or indirectly through projections to the BA. Additional

inhibitory controls come from the intercalated cell nuclei (ITC). The ITC are made up of islands of GABAergic neurons surrounding the BLA. ITC nuclei receive strong inputs from the LA and BA and may receive additional inputs from extrinsic regions such as the medial prefrontal cortex (mPFC) (Giustino & Maren, 2015; Sierra-Mercado, Padilla-Coreano, & Quirk, 2011). ITC nuclei act as regulators of information flow between the BLA and CeA by providing feed-forward inhibition to multiple nuclei of the CeA (Blaesse et al., 2015; Brigman et al., 2010; Busti et al., 2011; Ehrlich et al., 2009; Giustino & Maren, 2015; Likhtik, Popa, Apergis-Schoute, Fidacaro, & Pare, 2008; Marcellino et al., 2012; Millhouse, 1986; Palomares-Castillo et al., 2012). Interestingly, the dorsal ITC (ITCd) receive inputs from LA neurons and provide feed-forward inhibition of the CeL, while more ventral medial ITCs receive input from BA neurons and inhibit CeM populations (Pare & Duvarci, 2012). The CeM is generally regarded as the main output station of the amygdala on account of its projections to the brain stem effector regions of fear behaviors such as the PAG, lateral hypothalamus and paraventricular nucleus of the thalamus (PVT) (Campeau & Davis, 1995; Gentile, Jarrell, Teich, McCabe, & Schneiderman, 1986; LeDoux, Iwata, Cicchetti, & Reis, 1988; Pitkanen, Savander, & LeDoux, 1997; Repa et al., 2001).

Outside of the core amygdalar nuclei lie many important regions; here we will discuss just a few: the hippocampus (HPC), medial prefrontal cortex (mPFC), nucleus accumbens (NAc), bed nucleus of the stria terminalis (BNST) and hypothalamus. Broadly speaking, the dorsal HPC (dHPC) is thought to be critical for encoding the contextual elements of fear conditioning while the ventral HPC (vHPC) is involved in encoding the valence of specific memories (McDonald & Mott, 2016; Pikkarainen, Ronkko, Savander, Insausti, & Pitkanen, 1999). On this account, during the testing phase of auditory fear

conditioning, freezing to the auditory CS is generally performed in a context separate from the conditioning context while in contextual fear conditioning, contextually evoked freezing is measured in the training context. The HPC connects to the BLA and the mPFC (Lesting et al., 2011), and post-training lesions of the HPC impair retrieval of contextual elements of fear (Abraham, Neve, & Lattal, 2014). Within the mPFC, the infralimbic (IL) and prelimbic (PL) cortices are intimately implicated in fear extinction and fear acquisition respectively (Sierra-Mercado et al., 2011). The IL and PL send strong inputs to the amygdala and may gate inputs from the BLA into the CeA (Quirk, Likhtik, Pelletier, & Pare, 2003). The NAc and BLA have robust reciprocal connections. These inputs have been strongly implicated in motivated cue responses, especially to appetitive cues (Ambroggi, Ishikawa, Fields, & Nicola, 2008; Di Ciano & Everitt, 2004; Stuber et al., 2011). The BNST, part of the 'extended amygdala', is a set of nuclei strongly implicated in the regulation of stress responses, which receives reciprocal connections from many regions including the amygdala, HPC and mPFC (Davis, Walker, Miles, & Grillon, 2010; Dong, Petrovich, & Swanson, 2001; McDonald, 1998). The ventromedial hypothalamus makes reciprocal connections with the CeA and makes up a key link in a parallel fear processing and defensive behavior network (Kunwar et al., 2015; LeDoux, 2014; Lee et al., 2014).

1.5 Optogenetic Tracing of Fear Circuitry

The dawn of modern genetic tools has allowed for remote control of genetically defined cellular sub-populations and has thus greatly enhanced the specificity of manipulations delineating the role of specific nuclei or connections between nuclei involved in fear responses.

Optogenetics is based upon the use of genetically encoded, optically responsive ion channels or pumps. Initially discovered by Negel and colleagues, and greatly expanded by Boyden, Deisseroth, Zhang and others, channelrhodopsin and subsequently other opsins were rapidly developed to become powerful tools for millisecond time-scale control of neural systems (Boyden, 2011; Boyden, Zhang, Bamberg, Nagel, & Deisseroth, 2005; Nagel et al., 2003; Zhang, Wang, Boyden, & Deisseroth, 2006). In the work described in the present review, most manipulations use optical stimulation with channelrhodopsin 2 (ChR2) or optical inhibition using halorhodopsin (NpHR) or archaerhodopsin (Arch). Although there are important differences between the many opsins available, we will generally broadly group them into either stimulatory or inhibitory function for the purpose of brevity. Several other strategies for genetically encoded control of neural circuits have been developed recently, most notably designer receptors exclusively activated by designer drugs (DREADDs), which are genetically encoded modified G protein coupled receptors (GPCRs) that may be activated by an otherwise inert ligand clozapine-N-oxide (CNO) (Alexander et al., 2009; Krashes et al., 2011; Rogan & Roth, 2011). DREADDs come in a variety of forms including those coupled to Gs, Gq, and Gi. While a full complement of tools is valuable for research in behavioral neuroscience, optogenetics has dominated the literature for the last five years.

Below we will provide a review of some of the recent data using optogenetics to study the circuitry underlying fear behaviors and will focus on studies that provide data examining the behavioral consequences of optogenetic manipulations. We will discuss research in the context of the nuclei that were primarily interrogated for function in

behavioral studies. For a summary of papers highlighted please see Table 1 and for a schematic of discussed projections see Figure 1.

Inputs to Lateral Amygdala

Morozov et al. (2011) found that projections from the temporal association cortex (TeA) to the LA receive feed-forward inhibition from GABAergic lateral ITC (ITCl) neurons in the external capsule, which was relieved by blockade of GABAergic transmission or removal of the external capsule. Anterior cingulate cortex (ACC) projections to the LA, however, received no such feed-forward inhibition (Morozov, Sukato, & Ito, 2011). This suggests that inputs from different regions receive heterogeneous inhibitory controls that might be differentially modulated during learning.

The hippocampus is necessary for encoding contextual elements of fear conditioning and some information flow is directed through the entorhinal cortex (EC) (Kitamura et al.). When interrogated optogenetically, strong glutamatergic projections from the BLA to the EC were confirmed. Interestingly, inhibition of these terminals during training was sufficient to block contextual fear learning even though this pathway is not necessary for the expression of contextual fear (Sparta et al., 2014). This confirms that unique combinations of activity are necessary for the encoding, expression and extinction of learned fear.

Examining the cortical regions involved in auditory processing of a CS, Nomura et al. (2015) demonstrated that unilateral optical inhibition of the auditory cortex is sufficient to act as a CS for both positive and negative valence training paradigms (Nomura et al., 2015). This study highlights the need to consider interoceptive stimuli as possible confounding variables in studies utilizing optogenetic activation and silencing manipulations. In another

study, optogenetic activation of sensory inputs to the LA from the medial part of the medial geniculate nucleus (MGn) and secondary auditory cortex (AuV) paired with a foot shock was sufficient to act as a CS during fear conditioning. Additionally, optogenetic reactivation of these sensory inputs to the LA during testing sessions was sufficient to produce spontaneous freezing (J. T. Kwon et al., 2014). Direct activation of LA neurons is sufficient to act as a marginal US in the absence of any aversive stimulus when paired with a CS (Johansen et al., 2010), thus confirming that US induced activation of LA neurons is involved in associative fear learning, while also highlighting that non-specific activity is not sufficient to form strong associative memories.

Studies focused on Basolateral Amygdala

Limited work examining LA-BA-CeA connectivity using optogenetics has been completed as the close proximity of these nuclei makes exclusive targeting difficult. Tye et al. (2011) demonstrated that activation of BLA terminals in the CeA was sufficient for acute anxiolysis while inhibition was anxiogenic. Interestingly, these results were not recapitulated by activation of somata in the BLA (Pare & Duvarci, 2012; Tye et al., 2011) This confirms the presence of direct projections from the BLA to the CeA without determining their function in the greater context of the circuit. In rats using an inhibitory avoidance task, optical stimulation or optical inhibition of the BLA for 15 minutes after training greatly enhanced or blunted the retention of that learning respectively (Huff, Miller, Deisseroth, Moorman, & LaLumiere, 2013). These data confirm the BLA is involved in the consolidation of fear and anxiety-related emotional learning.

A study from Namburi et al. (2015) attempted to more clearly define the role of different projections from the BLA in valence specific behaviors. Retrograde transported

fluorescent beads (retrobeads) were infused into the CeA or nucleus accumbens (NAc) of mice trained to associate a tone with an aversive foot shock or a rewarding sucrose delivery. Using whole-cell patch clamping, the authors found that NAc projecting BLA neurons exhibited synaptic strengthening following training to a rewarding cue and synaptic weakening in response to aversive cue training. Conversely, CeA projecting BLA neurons experienced synaptic strengthening after an aversive training and weakening after reward training. Using a similar approach with a rabies virus to retrogradely express ChR2 in NAc or CeA projectors, the authors found that stimulation of NAc projecting cell bodies was sufficient to support appetitive optical intracranial self-stimulation. Conversely, optical activation of CeA projecting cell bodies supports aversive real time place aversion. Additionally, optically inhibiting CeA projecting BLA neurons mildly blunted fear acquisition and supported reward conditioning (Namburi et al., 2015).

In this same study by Namburi et al. (2015), following the functional dissection of CeA vs. NAc projecting BLA neurons, cell bodies were then manually dissociated and collected based upon their projection specific uptake of retrobeads. RNA from these cells was sequenced and several genes specifically upregulated in CeA projectors vs. NAc projectors were uncovered (Namburi et al., 2015; Nieh, Kim, Namburi, & Tye, 2013). This publication is an excellent example interrogation of cell populations in a projection specific manner.

Additional evidence that target specific projections from the BLA may play a role in the consolidation of select types of memory comes from Huff et al. (2016). The authors activated or inhibited projections from the BLA to the vHPC during a modified contextual freezing conditioning task so as to determine whether these projections are necessary for

encoding context or foot-shock memory. In this task animals were placed in conditioning context A on day 1 then on day 2 placed in context A, immediately foot shocked, and removed. This training paradigm appears to separate consolidation of contextual memory on day 1 from foot-shock memory on day 2. Interestingly, activation of these projections following contextual training had no effect upon fear memory; however, activation following foot-shock enhanced fear learning. This suggests that afferents from BLA to vHPC may be primarily involved in encoding aversive, but not contextual elements of fear conditioning (Huff, Emmons, Narayanan, & LaLumiere, 2016).

Studies Focused on Medial Prefrontal Cortex

A number of groups have used optogenetics to confirm the differential roles of the reciprocal projections from the PL and IL of the mPFC to the amygdala in fear expression and fear extinction, respectively (Arruda-Carvalho & Clem, 2015). The PL is involved in the expression of fear following conditioning while the IL is involved in the expression of extinction to a specific cue (Arruda-Carvalho & Clem, 2014; Cho, Deisseroth, & Bolshakov, 2013; Do-Monte, Manzano-Nieves, Quinones-Laracuente, Ramos-Medina, & Quirk, 2015; Felix-Ortiz, Burgos-Robles, Bhagat, Leppla, & Tye, 2015; H. S. Kim, Cho, Augustine, & Han, 2016; Senn et al., 2014). In a foundational piece of work using precise, limited infusions of $GABA_A$ agonist muscimol Sierra-Mercado et al. (2011) demonstrated that inactivation of the PL during fear extinction blocked fear expression; however, fear extinction, as measured 24-hours later was not affected (Sierra-Mercado et al., 2011). Conversely, when the IL was temporarily inactivated during fear extinction no effects were observed on fear expression; however, the next day there was significant deficit in extinction learning

observed. Taken together this data demonstrate that the PL is necessary for fear expression while the IL is necessary for fear extinction.

In rats and mice, optical activation of glutamatergic neurons in the IL during fear extinction was found to blunt fear expression and enhance extinction; conversely inhibition of the IL blocked fear extinction (Do-Monte et al., 2015; Riga et al., 2014). In rats, optical inhibition of excitatory neurons in the IL during extinction retrieval or extinction expression had no effect on freezing, suggesting that consolidated extinction memories are stored elsewhere and the IL may not be necessary for their expression (Do-Monte et al., 2015). Opposing this result is work in mice demonstrating that unilateral inhibition of all neurons in the IL is sufficient to blunt extinction recall while activation of excitatory neurons is sufficient to enhance extinction expression (H. S. Kim et al., 2016). There may be some species differences in the specific projections between the mPFC and amygdalar nuclei to account for these differences; however, taken together these studies confirm the important role of the IL in extinction and highlight the need for its continued study (Amir, Amano, & Pare, 2011; Cho et al., 2013).

The Central Nucleus of the Amygdala

Ciocchi et al. (2010) demonstrated that optical activation of the CeM is sufficient to drive spontaneous freezing while inactivation of the CeL was likewise sufficient to drive unconditioned freezing (Ciocchi et al., 2010). This confirms the role of the CeM as a main output nucleus in the fear pathway under the inhibitory control of CeL. Activation of BLA inputs to the CeA is sufficient to acutely suppress anxiety-like behavior as measured in the open-field test, while inhibition increases those behaviors. Activation of BLA projections to the CeA increases activity in CeL neurons and causes feed-forward inhibition of CeM

neurons (Tye et al., 2011). These studies confirm the known circuitry for BLA to CeL to CeM and suggest that more complex control mechanisms maybe in place based on evidence that the direct activation of BLA somata did not elicit the changes in anxiety-like behaviors that stimulation of projections alone did.

The Intercalated Cell Masses

Although excellent work examining activity and plasticity in ITC with fear learning has confirmed their role as dynamic regulators of information flow between nuclei, optogenetic characterization of the ITC has proven difficult on account of their small size and distribution (Busti et al., 2011). Kwon et al. (2015) recently performed an in-depth characterization of the dorsal ITC (ITCd), which receive strong inputs from the LAdl. Performing either weak or strong fear conditioning, the authors found learning-related strengthening of GABAergic inputs onto ITCd only after weak fear conditioning, suggesting that the ITCd is involved in gating sub-threshold behavioral learning. This plasticity is dependent upon dopamine receptor 4 (D4) and blockade of D4 or knock-down with shRNA is sufficient to transform previously subthreshold training into supra-threshold trainings, greatly enhancing fear expression. Interestingly, treatment of animals with corticosterone precipitates PTSD-like enhancements in fear learning and blocks ITCd plasticity, suggesting that during stress, previously subthreshold learning is not gated by ITCd, thus allowing for its consolidation and enhancement of fear responses (O. B. Kwon et al., 2015).

The ITC represents an intriguing target for cell type specific manipulations. Expressing the mu opioid receptor (MOR), dopamine receptor 1 (D1), and forkhead box protein 2 (FoxP2), these islands have a wealth of targets for transgenic approaches (Soleiman, 2015). Work by Likhtik et al. (2008) in rats used dermorphin, a peptide that is a

high affinity agonist of MOR, conjugated to a toxin, saporin, to selectively ablate medial ITCs (mITC). Medial ITC's provide feed-forward inhibition to the CeA and are located at the BLA-CeA border. Behaviorally, rats were fear conditioned and extinguished followed by ablation of mITC. When tested for extinction retention a week later, peptide-toxin infused rats exhibited significant deficits in extinction expression when compared to scrambled controls. This suggests that the mITC are necessary for the retention and/or expression of fear extinction (Likhtik et al., 2008). The success of this cell-type specific manipulation suggests that with additional tools selective, non-ablative manipulation of the ITCs is possible.

Bed Nucleus of the Stria Terminalis

The BNST, a core element of the 'extended amygdala' has been noted for its crucial role in sustained fear and anxiety-like behavior; in fact it may act as a back-up for producing many of the same behavioral outputs often attributed to the amygdala (Davis et al., 2010). Limited optical analysis of direct connections between amygdala and BNST has been done to date. Kim et al. (2013) found that optically stimulating glutamatergic BLA inputs to the anterior dorsal BNST (adBNST) elicited strong anxiolytic-like behavior. Conversely, optical inhibition of these populations is anxiogenic as measured with the elevated plus maze task. Anxiolytic behaviors are likely induced by activation of feed-forward inhibition from adBNST to oval BNST (S. Y. Kim et al., 2013). This study hints at a potentially complex interplay between core and extended amygdala function that may come to light with future study.

1.6 Search for the Memory Engram

While the studies described above confirm the basic circuitries involved in fear responses and fear learning, many fundamental questions about these processes remain. As it appears select ensembles of neurons, not entire nuclei, are involved in the encoding of distinct memories; one major area of investigation has been to discover how these ensembles are recruited and whether they are static over time. This line of research, when combined with cell-type specific techniques, may prove to be a more efficient avenue to discover behaviorally relevant sub-populations than the candidate gene approach now utilized.

Building on foundational research demonstrating that distinct ensembles of neurons encode memory traces of unique contexts, more recent work has focused on labeling neurons during different experiential epochs (Guzowski, McNaughton, Barnes, & Worley, 1999). Reijmers (2007) et al. introduced a transgenic line known as the Tet-tag mouse that allows for the activity dependent tagging of neuron populations. The Tet-tag mouse system utilizes tetracycline transactivator (tTA) protein expression driven under the c-fos promoter and tetracycline response element (TRE) control of lacZ to permanently mark neurons active during a specific time period. The labeling period is determined by when the experimenter removes doxycycline from the mouse's diet. Doxycycline blocks binding of tTA to the TRE so, removal of doxycycline allows binding of tTA to the TRE. The labeling period is then closed by returning the mouse to doxycycline chow, which inhibits the function of tTA. Using this system, Reijmers et al., confirmed that BLA neurons active during fear conditioning are subsequently reactivated during fear recall (Reijmers, Perkins, Matsuo, & Mayford, 2007). This result has been confirmed in many areas using both

appetitive and aversive training paradigms (Tonegawa, Liu, Ramirez, & Redondo, 2015). These data suggest that stable networks of neurons within previously described nuclei are consistently recruited for the encoding and expression of a learned fear behavior.

It is auspicious to use this work as a springboard for understanding many of the current efforts in the study of learning and memory to determine which cell populations are recruited for select elements of fear behaviors. Efforts to illuminate distinct cell populations that regulate select fear behaviors must consider not only the different genetically defined populations within nuclei, but also the internal determinants within a neuron that promote its recruitment to a memory trace. Furthermore, these factors likely differ between brain regions.

Within the hippocampus, much progress has been made towards labeling individual place memory 'engrams' (or physical manifestations of stored memory trace) using the Tet-tag system. This system may be used to produce ChR2 (or any transgene) in neural populations active during a certain training period. These populations may then be reactivated or silenced in an alternate context or any number of other experimental conditions. In a series of papers (Ramirez et al. 2013, Redondo et al. 2014, Ryan et al. 2015), the Tonegawa group performed an in-depth analysis of engrams formed in the HPC and the BLA during either negatively and positively valenced activities such as contextual fear conditioning and mating. Together these studies demonstrated that labeling a portion of the neurons in the dentate gyrus (DG) or BLA that are active during contextual fear conditioning with ChR2, and subsequently reactivating them later, results in light-induced freezing in a naïve context. Conversely activating the engram of a neutral context in an aversively trained context interferes with context-elicited freezing, thus suggesting that the

simultaneous activation of multiple place engrams causes mixed behavioral responses. Similar patterns were found when looking at engrams generated during appetitive tasks such that reactivation of appetitive engrams caused place preference in a neutral context. Interestingly, when engrams encoded in contexts paired with an aversive or appetitive task are reactivated during retraining with tasks of the opposite valence, DG engrams could be recoded to be associated with a new valence while BLA engrams continued to code for behavioral outputs consistent with the valence of the original conditioning. Finally, memories that were formed during contextual fear conditioning may be blocked by inhibiting protein synthesis with the drug anisomycin directly after training or reconsolidation; however, the reactivation of engrams formed during that training session still elicited freezing. This distinction suggests that the content of an engram may be represented in its pattern of projections while the encoding and retrieval of a memory requires molecular processes underlying memory consolidation (Liu et al., 2012; Ramirez et al., 2013; Ramirez et al., 2015; Ryan, Roy, Pignatelli, Arons, & Tonegawa, 2015).

Trouche et al. (2016) used a similar system to express Arch, an inhibitory opsin, in a hippocampal place engram and observed several interesting phenomena. In an experimental context (A), neurons originally labeled during encoding of that place engram increased their firing in response to re-exposure to context A, while another population exhibited firing suppression. When tagged neurons were silenced in context A, an alternative population was found to compensate and increased firing to context A; behaviorally, mice with silenced engrams acted as if they were in a new context. Over six days of trials the alternative ensemble created a second engram to that first elicited by context A. Importantly, if context A was initially paired with cocaine this remapping

protocol abolished cocaine conditioned place preference, thus blocking the recall of the initial association between context A and cocaine administration. These observations contain important suggestions that HPC engrams are not fixed and that previously associated place memories may be altered to subsequently rid the subject of previously acquired associations (Trouche et al., 2016).

Complementing these findings, work from Josselyn and colleagues has demonstrated that memory traces are not necessarily allocated to pre-determined ensembles of neurons within a nucleus. Allocation is based upon naturally oscillating expression levels of CREB, which bias neural ensembles towards being recruited to an engram in an excitability dependent manner. Neurons that have high levels of CREB at the time of training are more likely to be recruited to a memory engram (J. H. Han et al., 2007; Yiu et al., 2014). CREB increases neuronal excitability and many of the molecular processes underlying synaptic plasticity and memory consolidation. By experimentally increasing levels of CREB or neuronal excitability using optogenetics or DREADDs in a sub-population of neurons of the LA, Yiu et al., (2014) were able to increase targeted neuronal recruitment into a memory trace. Both optogenetic and chemogenetic manipulations also increased the strength of the memory as measured by the ability of a context to elicit conditioned freezing during a fear expression session (Yiu et al., 2014).

1.7 Cell Type Specific Targeting of Behavioral Processes

An understanding of the neural circuits underlying behavior is clearly valuable for the study of the biology of learning and memory as highlighted in the above sections. However, without translationally tractable strategies for identifying targets to modulate fear responses and learning in humans, the value of further dissection of this circuitry will

remain somewhat esoteric. One promising strategy is the manipulation of genetically defined neuronal populations whose global modulation may have beneficial results in the regulation of specific behavior or learning processes. Here we will review a number of papers that utilize cell-type specific techniques to interrogate neural circuits underlying behavior; for a summary of papers highlighted please see Table 2 and for a schematic of described populations and projections see Figure 2.

The majority of studies mentioned thus far have focused on differences between 'genetically defined' glutamatergic or GABAergic sub-populations between nuclei; however, it has become obvious that not all excitatory and inhibitory neurons are created equal. In work by Herry et al. (2008), multiple excitatory cell populations in the BA that differentially respond to fear expression vs. fear extinction were found in actively behaving mice. One population was found to increase its firing rate in response to the presentation of the CS directly after auditory fear conditioning and then to decrease firing as the CS-US association was extinguished; these identified neurons were functionally labeled as "Fear $_{ON}$" neurons, whose activity supports fear expression. Another distinct population was found to have little activity in response to presentation of the CS just after FC but instead increased activity as the CS-US association was extinguished; these were accordingly labeled "Fear $_{OFF}$" or "Fear $_{Extinction}$" neurons, whose activity supports the suppression of fear behaviors. Interestingly, "Fear $_{ON}$" neurons were found to receive inputs from the vHPC and project to the mPFC while "Fear $_{OFF}$" neurons had only reciprocal connections with the mPFC. Finally, the selective inactivation of the BA with muscimol prevented both fear extinction and fear renewal, suggesting that the BA is necessary for signaling behavioral transitions rather than the storage of fear memories themselves (Herry et al., 2008).

This study set firm ground-work by demonstrating that within previously identified nuclei, such as the primarily glutamatergic BA, there are sub-populations of neurons that have divergent roles in behavior and learning. Unfortunately, without knowing the genetic identities of these neuron populations, it is impossible to selectively manipulate them during behavior. In order to uncover more specific, targetable populations, it will be necessary to identify additional, less globally expressed, sub-population markers, specifically genes or proteins that are differentially expressed in the population of interest compared to other neurons.

A retrospective example of this type of strategy may be observed in the modulation of the direct and indirect pathways of the striatum. The striatum is well known for its role in informational integration and motor control. This system relies upon global modulation by dopamine; direct pathway neurons express dopamine receptor 1 (D_1), a Gs-coupled GPCR, while indirect pathway neurons express dopamine receptor 2 (D_2), a Gi-coupled GPCR (Smith, Bevan, Shink, & Bolam, 1998). In the case of Parkinson's disease, rebalancing this striatal system by increasing global dopamine with L-DOPA administration is a palliative approach. The differential expression patterns within these two pathways have allowed for these circuitries to be directly manipulated using optogenetics as demonstrated by Kravitz et al. (2012). Using different promoter-cre mouse lines to virally express ChR2 specifically in either the direct or indirect pathway neurons, the authors demonstrated that activation of the direct pathway is reinforcing while activation of the indirect pathway is punishing as measured with place preference or place avoidance tasks (Kravitz, Tye, & Kreitzer, 2012). Taken together these studies demonstrate the feasibility of identifying genetically-defined cell populations that differentially support aversive and

appetitive behavior. In the present section, we will examine genetically identified cell populations within the amygdala (both core and extended regions) and related areas that have confirmed roles in fear behaviors.

Differential Molecular Markers of Central Amygdala Cell Types: *PKCd, Sst,* and *Tac2*

Recently, a growing number of inhibitory microcircuits have been reported. These circuits often function through mutual inhibition where the inhibition of one inhibitory population by another leads to the disinhibition of a third 'output' population that reads out the signaling tone of the circuit. These types of circuits are especially fruitful as several cell-type specific markers for sub-populations of inhibitory neurons have been described.

To interrogate the micro-circuitries of the CeA, Ciocchi et al. (2010) and Haubensak et al. (2010) used single unit recordings to interrogate population firing in the CeL of awake behaving mice. The authors identified two populations of neurons whose activity changed after fear conditioning; one that increased firing in response to the CS (CeL_{ON}, ~ 30%) and another that decreased firing during the same period (CeL_{OFF}, ~ 25%). These populations were further found to be mutually inhibitory. The CeL_{OFF} population was found to project to and inhibit a CeM population projecting to the PAG, a region associated with the behavioral freezing responses during fear expression. Importantly this CeL_{OFF} population expressed a relatively cell-type specific serine- and threonine-kinase gene, protein kinase C delta (*PKCd*), thus allowing for genetic targeting and manipulation of this population, which lead to confirmation of its role within the CeM fear controlling circuitry underlying fear conditioning behavior (Ciocchi et al., 2010; Haubensak et al., 2010).

Pursuing the observation that increases in tonic activity in *PKCd*-expressing (PKCd+) neurons strongly correlate with fear generalization, Botta et al. (2015) examined

the contributions of PKCd+ neurons to acute fear responses and anxiety-like behaviors. Following a discriminative training protocol where the US is paired with one CS (CS+), but not another CS (CS-), PKCd+ neurons were activated using optogenetics during alternate CS+/CS- presentations. Optical stimulation drove fear generalization as measured by an increase in the ratio of freezing to CS- / CS+ stimuli. Optical stimulation of PKCd+ neurons was also accompanied by increased anxiety-like behaviors as measured by decreased time spent in the open arm of an elevated-plus maze (EPM) and decreased time spent in the center of an open field. These behavioral changes were attributed to excitability changes driven by α_5 subunit containing $GABA_A$ receptors located on the extra-synaptic dendritic region. Increased tonic activity of PKCd+ neurons caused by a reduction in extrasynaptic inhibition after fear conditioning was associated with decreased α_5-$GABA_AR$ mediated conductance, and furthermore this change was significantly correlated with anxiety-like behaviors in the EPM. Finally, cell-type specific knock-down of α_5-$GABA_AR$ with a shRNA was sufficient to increase anxiety-like behavior and fear generalization (Botta et al., 2015; Ciocchi et al., 2010; Haubensak et al., 2010; Wolff et al., 2014). These results suggest overlap between the circuits mediating anxiety-like behaviors and the generalization of cued fear behaviors.

An important clue as to the identity of the observed PKCd-, CeL_{ON} population, comes from Halhong Li et al. (2013). Somatostatin (SOM+) neurons located within the CeL are largely non-overlapping with PKCd+ neurons (~13% overlap). At basal conditions, excitatory input from the LA onto SOM+ neurons is comparatively weak compared to SOM- populations; however, after fear conditioning this relationship switches; consistent with enhanced excitatory drive after learning. Interestingly, selectively silencing of SOM+

neurons with a Gi-DREADD during fear conditioning abolished this switch and blunted fear acquisition, thus suggesting that post-synaptic activity is required for the observed synaptic strengthening and that this switch is necessary for fear learning. Mutual inhibition between the SOM+ and SOM- (partially PKCd+) populations was uncovered. Finally, optical activation of SOM+ neurons was sufficient for the generation of spontaneous freezing in naïve animals while optical inhibition was sufficient to block freezing during a fear expression test (H. Li et al., 2013). This study identifies SOM+ neurons of the CeL as containing a complementary population to the PKCd+ population in the CeL disinhibitory circuit controlling CeM output. SOM+ neurons inhibit PKCd+ neurons during fear conditioning, allowing for increased activity in the CeM and the expression of fear behaviors.

The tachykinin 2 (*Tac2*)-expressing cell population, appears to be found in both the CeL and CeM, depending upon anterior-posterior position of reference. At more posterior locations within the CeL, *Tac2* mRNA expression partially overlaps with that of both somatostatin (*Sst* or SOM) and *corticotrophin releasing factor (Crf),* but not *Prkcd (PKCd)*; however, more anteriorly, the large CeM *Tac2* population is expressed in an independent population (unpublished data). Andero et al. (2014) recently identified *Tac2* as a dynamically regulated gene whose expression rapidly rises after fear conditioning, and returns to baseline by 2 hours post training. After fear conditioning, the protein product of *Tac2*, neurokinin B (NkB), is strongly upregulated. Notably, intra-amygdala application of an NkB receptor (Nk3R) antagonist, osanetant, blunts fear consolidation when given directly following fear conditioning. Over-expression of the *Tac2* gene is sufficient to enhance fear learning, and this manipulated enhancement can be blocked with the Nk3R

antagonist. Finally, silencing *Tac2*-expressing neurons in the CeA during fear conditioning using Gi-DREADD is sufficient to blunt fear acquisition. This study identified the *Tac2* and Nk3R expressing populations as excellent targets for cell-type specific manipulation of fear learning and behaviors, which may be particularly interesting in their role in the output nuclei of the CeA (Andero, Dias, & Ressler, 2014).

The Parabrachial Nucleus and Calcitonin Gene-Related Peptide

So far we have exclusively discussed thalamic inputs to the LA as the major contributors of US information to the CeA. Recently, Han et al. (2015) examined an alternative US input pathway to the CeA; a circuit from parabrachial nucleus (PBN) to the CeL was found to also transmit information regarding the US. Han et al. found that the external lateral subdivision of the PBN (PBel) expressed high levels of *Calca,* the gene encoding for calcitonin gene-related peptide (CGRP), which regulates pain transmission and can directly produce unconditioned freezing when infused in the CeA. Using cre-dependent tetanus toxin expression to silence synaptic transmission in PBel CGRP neurons throughout contextual fear conditioning and subsequent expression tests, the authors demonstrated that silencing these neurons in the PBel was sufficient to decrease freezing in all phases of contextual fear conditioning and expression, suggesting that these inputs to the CeL are necessary for learning in response to painful stimuli. Mice in which PBel CGRP neurons were silenced had normal withdrawal responses from nociceptive stimuli; however, escape behaviors and freezing were reduced suggesting that nociception was normal, but behavioral responding to painful stimuli was blocked. Optogenetic activation of PBel CGRP neurons was also sufficient to drive both context and auditory-cued fear conditioning when used as a US during training. Finally, targeting the CGRP receptor

(CGRPR) expressing population of the CeL, the authors demonstrated that activation of these neurons was sufficient to create generalized fear responding when used as the US in contextual and cued fear conditioning (S. Han, Soleiman, Soden, Zweifel, & Palmiter, 2015). This work highlights the observation that the canonical thalamic route for US information to the CeA must be updated to include information flow from the PBN. Furthermore, both the CGRP and CGRPR cell populations may be amenable to cell-type specific modulation, an interesting avenue for further investigation.

BLA Inhibitory Neuronal Sub-Populations: PV and SOM

Within the basolateral amygdala, several cell-type specific targets have been discovered. Wolff et al. (2014) identified a partial inhibitory micro-circuit within the BLA demonstrating some similarities to inhibitory circuits in the CeA. In this study, the selective activation or inhibition of the parvalbumin expressing (PV+) population specifically during the US presentation of fear conditioning blocked or enhanced fear learning to a CS, respectively. Combined with work demonstrating that inhibition of PV+ neurons leads to enhanced excitability in principal neurons, these data suggest that the selective modulation of the PV+ neuronal population may be necessary for fear learning. In awake behaving mice, the authors further observed spike suppression of PV+ neurons during US presentation confirming the physiological relevance of optogenetic manipulations. Interestingly, when looking at CS-induced activity, the authors observed the opposite pattern of activity wherein PV+ neurons increased their responding to the CS. Furthermore, optogenetic activation of PV+ neurons during the CS, but not US, actually enhanced fear learning. This prompted the discovery of a polysynaptic disinhibitory circuit including somatostatin positive (SOM+) populations whereby during CS presentation, PV+ neurons

increase activity, inhibiting SOM+ neurons, thus leading to disinhibition of principle neurons receiving cortical or thalamic auditory inputs (Wolff et al., 2014). These data align well with an additional disinhibitory circuit found in the auditory cortex also involving PV+ neurons (Letzkus et al., 2011). Notably, these types of disinhibitory circuits have been discovered in many areas of the brain suggesting that disinhibition may in fact be a major mechanism of associative learning and memory (Letzkus, Wolff, & Luthi, 2015). It is possible that globally manipulating the tone of such inhibitory circuits may provide a possible therapeutic method for many associative learning disorders; however much remains to be understood about GABAergic regulation, oscillatory networks, and different interneuron populations for such approaches to be feasible in a reliable and predictive manner.

Thy1-Population of Pyramidal BA Neurons

Given the great success with targeting inhibitory populations in the amygdala, equal success might be expected from excitatory populations; however, to date comparatively few of these have been uncovered. Jasnow et al. (2013) described a BA population marked by the Thy1.2 promoter cassette derived lines: Thy1-ChR2 line 18 and Thy1-eYFP line H. These lines mark a common developmental population originating from the pallial zones of the telencephalon (Porrero, Rubio-Garrido, Avendano, & Clasca, 2010). From an evolutionary perspective, populations with common developmental origins are likely to have complementary roles, especially those generating neocortical circuits often implicated in top-down regulation of older striatal-like populations such as the CeA (Swanson, 2003). Using these transgenic lines the authors demonstrated that this BA Thy1 population was entirely glutamatergic and, within the temporal lobe, localized almost exclusively within

the anterior BAa. Optical activation of this population during presentation of the US blocks the consolidation of fear learning. Likewise optical activation of the Thy1 population during presentation of the CS during extinction dramatically enhanced extinction consolidation. Finally the authors found that activation of BA Thy1-ChR2 neurons generated polysynaptic feed-forward inhibition of evoked excitatory potentials in the CeM generated by electrical stimulation of the LA (Jasnow et al., 2013). Taken together these data confirm the presence of functionally segregated glutamatergic populations within the BA, that putatively may align with the functionally defined $Fear_{Extinction}$ population defined (and discussed above) by Herry et al (Herry et al., 2008). These data further highlight the need for the generation of additional cell type specific markers in this area.

Hypothalamic Sub-Populations: OT, ESR1, SF1

Originating in the hypothalamus, oxytocin (OT) expressing neuronal inputs projecting into the CeA have been shown to play important roles in modulating distinct elements of fear behaviors (Cassell, Freedman, & Shi, 1999; Viviani et al., 2011). Knobloch et al. (2012) demonstrated in rats that activation of glutamatergic fibers from OT expressing hypothalamic nuclei elicit co-release of oxytocin onto CeL neurons and also increase inhibition of CeM populations in an OT dependent manner. Importantly, activation of OT fibers was sufficient to block context dependent freezing in previously contextually fear conditioned rats (Knobloch et al., 2012; Sparta et al., 2014). This study highlights the importance of extra-amygdala populations in fear behaviors and encourages a broadening of our view of possible cell type specific targets.

Another possible target for cell-type specific modulation is the estrogen receptor 1 expressing (ESR1+) population of neurons that is enriched in the ventrolateral division of

the ventromedial hypothalamus (VMHvl), medial amygdala (MeA) and BAp. Lee H et al. (2014) recently identified the ESR1+ population in the VMHvl as being active during aggressive behaviors between male mice. Cell-type specific strong optical activation of this ESR1+ population or ESR1- population elicited either attack or no behavioral change, respectively, in males in the resident intruder task. Optical inhibition of the ESR1+ population was sufficient to rapidly block or stop an aggressive encounter. The authors observed that low intensity stimulation or low viral infection efficiencies were sufficient to provoke mounting or close inspection of both male and female intruders by male mice and that by increasing the intensity of photostimulation or number of neurons infected, these behaviors could be transitioned to attack behaviors. Together these experiments suggest that ESR1+ neurons of the VMHvl control a range of social interaction behaviors in a recruitment-dependent manner (Lee et al., 2014). This study begins to demonstrate the wealth of extra-amygdalar targets for modulation of a variety of defensive behaviors. Furthermore, it suggests the importance of understanding the role of the BAp ESR1+ cell populations. As fear-related disorders in humans encompass a wide variety of perturbed and dysregulated behaviors, these targets may be of great translational value, and may be an important target in understanding sex differences in emotion-related behaviors.

Another genetically identified sub-population found to be intimately involved in social behaviors was found by Kunwar et al. (2015). The steroidogenic factor 1 (SF1+) population of the dorsal medial and central ventromedial hypothalamus (VMHdm/c) is non-overlapping with the previously discussed ESR1+ population. Optical stimulation of SF1+ neurons causes freezing behaviors and occasional activity bursts similar to those observed in escape behaviors. These behaviors had a similar dependency on stimulation

intensity as the ESR1+ populations; higher intensity stimulation, higher frequency stimulation or increased numbers of virally infected neurons more often generated activity bursts. Interestingly, very low intensity stimulation was found to be aversive and precipitated conditioned place avoidance. Additionally, SF1+ stimulation produced persistent defensive behaviors, anxiety-like behaviors and elevations of serum corticosterone. Finally, genetically targeted ablation of SF1 neurons blunted predator avoidance and anxiety-like behaviors (Kunwar et al., 2015). This study demonstrates that the SF1+ is intimately involved in aversive and anxiety-like behaviors and represents a tractable target for cell-type specific modulation of fear and anxiety-related behaviors.

Alternative Targets

In addition to the populations discussed above, several other promising gene targets, which to this point have remained out of reach or incompletely characterized, may now be accessible for future pursuit. Many neuropeptides have extensive literatures associating them with behavioral learning (Bowers, Choi, & Ressler, 2012). The corticotrophin releasing factor (CRF) population of the CeL has yielded several clues to its role in behavior suggesting that activity in this population may support fear learning (Gafford & Ressler, 2015). Neuropeptide S (NPS) appears to exert strong anxiolytic influences on the amygdala and supports fear extinction through its receptor (NPSR1). NPSR1 has strong expression specificity in the medial aspect of the BAa and the LAdl (Jungling et al., 2008). Interestingly, in humans, polymorphisms in the *NPSR1* and *5HTTLPR* genes epistatically confer risk of enhanced startle responses in anxiety-promoting contexts (Glotzbach-Schoon et al., 2013). An analogous *NPSR1* SNP to that found in humans was also recently found in mice and rats bred for high anxiety traits; this SNP increases GR

responsiveness of gene transcription (Slattery et al., 2015). These are just a few of the large number of identified pathways that participate in behavioral modulation that are ripe for analysis with cell-type specific tools.

Connections between the BA and the NAc have long been implicated in supporting reward learning and responding to previously reward-paired cues; however, much less attention has been paid to this connection in the context of fear learning (Di Ciano & Everitt, 2004). Stuber et al. (2011) directly investigated this connection via viral infection of BLA cell bodies followed by optical manipulations of terminals in the NAc. Optical stimulation of BLA terminals in the NAc was sufficient to support intracranial self-stimulation (ICSS) and ICSS was prevented with blockade of D1 receptors, suggesting that BLA afferents synapse selectively on D1 expressing neuronal populations (Di Ciano & Everitt, 2004; Stuber et al., 2011). These results suggest a variety of roles for the BLA across motivated behaviors. Although these projections have mostly been studied in light of appetitive tasks, they may play a crucial role in fear extinction by rebalancing the valence assigned to a previously learned association.

1.8 Cell-Type Specific Transcriptome Sequencing

In the case of several cell-type specific markers mentioned above, direct manipulation of the protein product of the identifier gene is possible; however, in most cases this is either impossible or translationally impractical. In these cases it is necessary to identify additional pharmacologically tractable targets for remote control of these populations in a closed system. To efficiently molecularly phenotype these populations the most expedient route is cell-type specific RNA sequencing.

Guez-Baber et al. (2011) reported a strategy (see (Guez-Barber et al., 2012) for protocol) for the isolation of striatal neurons expressing c-fos after cocaine exposure in rats. Through this process, neurons are rapidly dissociated, fixed and sorted using fluorescence activated cell sorting (FACS). Collection and sequencing of high quality RNA from sorted samples allows for either activity dependent or cell type specific interrogation of neuronal RNA content (Guez-Barber et al., 2011). This protocol has since been adapted for cell-type specific RNA interrogation to great success. This method has the advantage that it allows for the comparison of the cell population of interest compared to all other neurons, as well as for the rapid collection of large numbers of cells. Other methods of cell-type specific RNA isolation do not allow for the collection of control RNA specifically from marker-negative neurons (Guez-Barber et al., 2011). Additionally, FACS is a valuable tool when combined with mouse lines expressing transgenes under activity dependent promoters (ex. the Tet tag mouse described in earlier sections). In the case of the Tet tag mouse, neurons active during the dox-off period will express Beta-galactosidase; alternatively neurons labeled acutely by cfos-shEGFP may be collected within a few hours. Both of these labels may be targeted and used as fluorescent markers for FACS (Cruz et al., 2013). Alternatives to FACS to achieve similar ends include manual cell-sorting (Namburi et al., 2015), (Hempel, Sugino, & Nelson, 2007), laser-capture microdissection (Luo et al., 1999; Yao et al., 2005), and single cell expression analysis (Toledo-Rodriguez et al., 2004).

Another technology that allows cell-type specific RNA interrogation is translating ribosome affinity pull-down (TRAP). This technique utilizes transgenic expression of a modified ribosomal subunit appended to GFP (L10a-GFP) to selectively pull down ribosomes and the RNAs being translating at the time of collection (M. Heiman, R. Kulicke,

R. J. Fenster, P. Greengard, & N. Heintz, 2014). This method yields very high quality RNA and is methodologically less intensive than previously mentioned techniques such as FACS. When a conditional TRAP expressing line (e.g. Rosa26-f-s-TRAP (Zhou et al., 2013)) is crossed with any cell-type specific promoter-cre line, the resulting double transgenic mouse will express L10a-EGFP in the population of interest. This technique may also be used in a similar activity-dependent manner to FACS sorting (Cell-type specific activity dependent interrogation necessitates a novel line or combination of previously available lines) (Drane, Ainsley, Mayford, & Reijmers, 2014). However, cell-type specific RNA pull-down is not possible without the ability to genetically target populations, thus limiting its usefulness to the selection of established cre-drivers that are currently available.

In cases where genetic markers for functionally specified cell populations are not available, it is possible to interrogate gene changes in a projection-specific manner. We previously discussed Namburi et al. (2015) where the authors parsed the RNA content of CeA vs. NAc projecting BLA neurons (Namburi et al., 2015). To interrogate gene changes in specifically LA projecting thalamic and cortical populations Katz et al. (2015) retrogradely labeled these projecting neurons and performed laser micro-dissection of cell bodies. RNA content of these neurons was analyzed either at baseline or after fear conditioning, and the authors found projection-specific differences in gene changes (Katz & Lamprecht, 2015). This type of projection-specific RNA sequencing might easily be combined with FACS using retrobeads for sorting, or with TRAP by infusing a trans-synaptic transported cre virus (AAV-EF1a-mCherry-IRES-WGA-Cre, available through UNC viral vector core) into the f-s-TRAP mouse.

1.9 Summary

Cell-type specific interrogation of the behavioral and molecular profiles of select neuronal populations within the brain is likely the most expedient avenue towards the identification of selective compounds that modulate distinct circuitries involved in fear and anxiety related behaviors and associated disorders. In rodent models, optogenetics has rapidly confirmed and expanded the known neural circuitries underlying fear related behaviors. By identifying and manipulating genetically marked sub-populations of previously described nuclei, recent progress has been made towards circuit specific control of fear. In order to fully elucidate the molecular profiles of previously identified sub-populations, cell-type specific isolation may be employed to generate RNA expression profiles for these neurons. Taking this combinatorial approach, additional targets for pharmacological manipulation of fear-related populations may subsequently be more rapidly generated. Novel, cell-type specific, cognitive enhancers may provide unique avenues for the treatment of fear- and anxiety-related disorders.

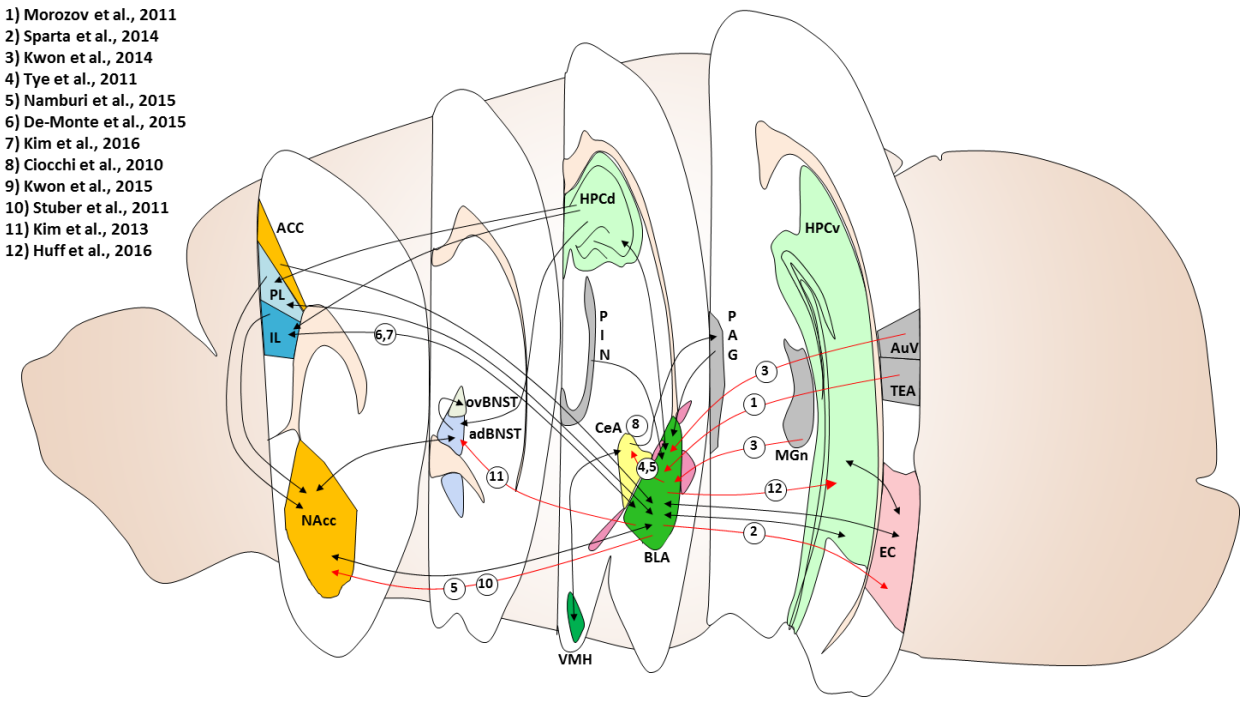

Figure 1-1. Neural circuits involved in fear and anxiety-related behaviors in rodents.

Optogenetic, electrophysiological, and pharmacogenetic techniques have elucidated many specific circuitries underlying rodent fear and anxiety-related behaviors. Cross sectional views taken from different anterior-posterior positions within the rodent brain are marked with relevant brain regions and their distal projections. Projections highlighted in red are discussed in the present review; these highlighted circuits account for only a portion of identified circuitries, some of which are labeled with black arrows. ACC, anterior cingulate cortex; adBNST, anterodorsal nucleus of the BNST; AuV, secondary auditory cortex; BLA, basolateral amygdala; CeA, central amygdala; EC, entorhinal cortex; HPCd, dorsal hippocampus; HPCv, ventral hippocampus; IL, infralimbic division of the mPFC; MGn, medial geniculate nucleus; NAcc, nucleus accumbens; ov, oval nucleus of the BNST; PAG,

periaqueductal gray; PIN, intralaminar thalamic nuclei; PL, prelimbic division of the mPFC; TEA, temporal association cortex; VMH, ventromedial hypothalamus.

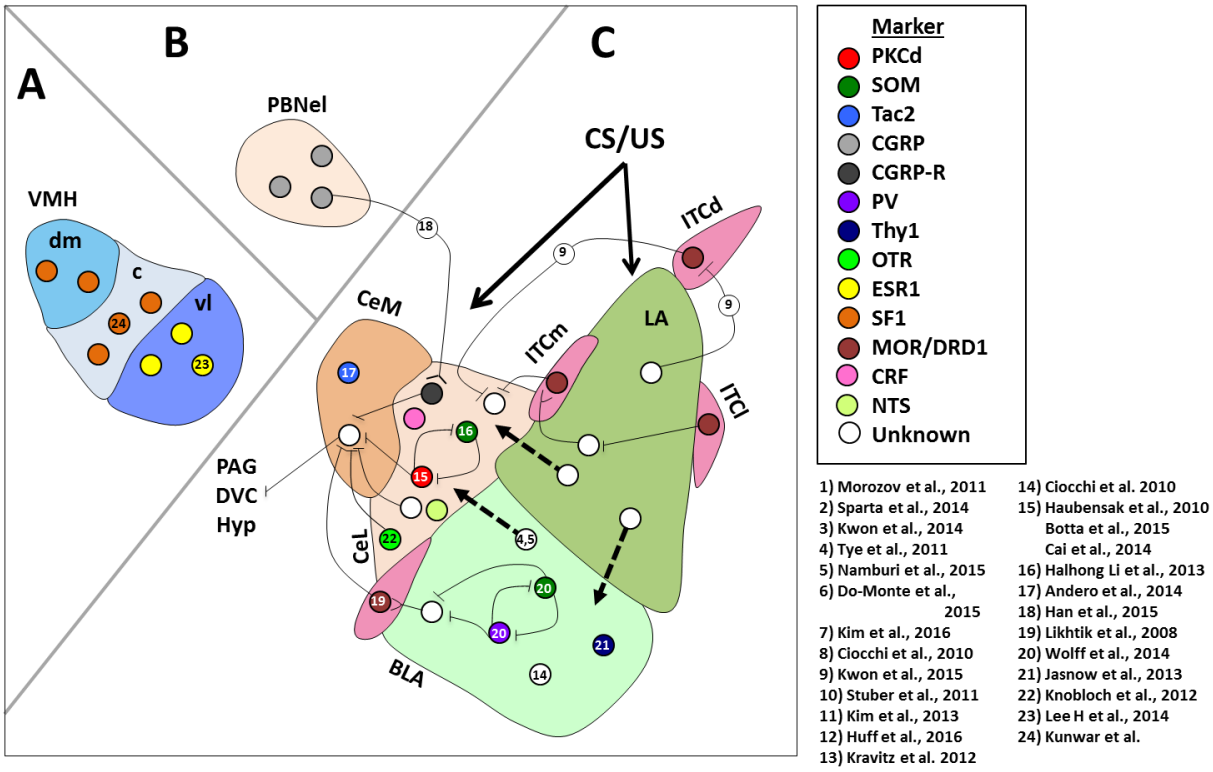

Figure 1-2. Microcircuits and specific neuronal populations in the amygdala, ventromedial hypothalamus (VMH) and parabrachial nucleus (PBN) involved in fear and anxiety-related behaviors.

Table 1. Description of publications using optogenetics to query basic fear-related circuitries.

Publication	Investigated Circuitry
Morozov et al. (2011)	Inputs from TeA → LA receive feed forward inhibition from ITC while ACC → LA inputs do not.
Sparta et al. (2014)	BLA→ EC projections are necessary for the acquisition but not the expression of conditioned fear.
Kwon et al. (2014)	Activation of MGm→ BLA and AuV→ BLA projections is sufficient to act as a conditioned CS.
Tye et al. (2011)	Activation/ inhibition of BLA→ CeA terminals is sufficient for anxiolysis/ anxiogenesis, but activation of cell bodies is not.
Namburi et al. (2015)	Synaptic strengthening of BLA→ CeA projections after fear learning and of BLA→ NAc projections after appetitive training.
Do-Monte et a. (2015)	IL activity in rats is necessary for encoding but not retrieval of extinction memory.
Kim et al. (2016)	Inhibition/ activation of IL activity in mice is sufficient for enhancement/ blocking of extinction retrieval.
Ciocchi et al. (2010)	Activation of CeM is sufficient to produce spontaneous freezing.
Kwon et al. (2015)	Inputs from LAdl to ITCd generate feed-forward inhibition of CeL. ITCd receives additional GABAergic inputs to gate its activity during sub-threshold training
Stuber et al. (2011)	Activation of BLA→ NAc is sufficient to support ICSS.
Kim et al. (2013)	Activation/ inhibition of BLA→ adBNST projections is anxiolytic/ anxiogenic.

Table 1.1. Description of publications using optogenetics to query basic fear-related circuitries.

Table 2. Description of publications using cell-type specific methodologies to query fear related circuitry.

Publication	Investigated Circuitry
Kravitz et al. (2012)	Optical activation of D1 direct/D2 indirect pathway supports place preference/place avoidance.
Ciocchi et al. (2010) and Haubensak et al. (2010)	Identified PKCd + population as decreasing firing during fear conditioning, relieving inhibition of PAG projecting CeM population, supporting fear expression.
Botta et al. (2015)	Activity in CeL PKCd population supports fear generalization and tonic activity in these neurons is dynamically regulated by extrasyaptic α_5-$GABA_AR$.
Cai et al. (2014)	Activation of CeL PKCd neurons is acutely anxiolytic.
Halhong Li et al. (2013)	SOM+ neurons of CeL represent opposing population to PKCd population; increasing activity with fear learning. Activity in these neurons is sufficient to support spontaneous freezing.
Andero et al. (2014)	CeA Tac2 neurons are necessary for fear acquisition. Antagonism of Tac2 receptor is sufficient to block fear consolidation.
Han et al. (2015)	PBN→ CeA transmits US information. Inhibition of PBN CGRP neurons blocks FC while activation is sufficient for generation of fear responses.
Likhtik et al. (2008)	Ablation of ITCm is sufficient to impair expression of extinction.
Wolff et al. (2014)	PV and SOM neurons in the BLA create disinhibitory circuit gating cortical and thalamic inputs to principal neurons.
Jasnow et al. (2013)	Activation of BLA Thy1-ChR2 population is sufficient to block fear acquisition and enhance fear extinction.
Knobloch et al. (2012)	Activation of hypothalamic OT fibers in CeL is sufficient to increase feed-forward inhibition of CeM in an OT dependent manner.
Lee H et al. (2014)	ESR1 neurons in the VMHvl generate investigative/ mounting/ attack behaviors in an intensity/ recruitment dependent manner.
Kunwar et al. (2015)	SF1 neurons of the VMHdm/c generate freezing/escape behaviors in an intensity/recruitment dependent manner.
Huff et al. (2016)	Activation of BLA→ vHPC projections is sufficient to support aversive learning, but not contextual learning.

Table1.2. Description of publications using cell-type specific methodologies to query fear related circuitry.

Chapter 2: Co-Expression Analysis of *Prkcd, Sst, Tac2, Crf, Nts and Drd2* Sub-Populations Within the Central Amygdala.

2.1 Context, Author's Contribution and Acknowledgement of Reproduction.

The following chapter is an effort to examine the expression and co-expression of mRNAs that appear to be mark specific sub-populations of the CeA that have a function relevant to fear behaviors. Markers were chosen based upon evidence in the literature and experience of the authors. The results of this paper are consistent with results found in the literature using different techniques and animal models. The dissertation author contributed to the paper by designing and running experiments, analyzing the data, and was the main contributor to the writing of the paper. The chapter is reproduced from McCullough K.M. & Ressler K.J. Co-Expression analysis of *Prkcd, Sst, Tac2, Crf, Nts and Drd2* Sub-Populations within the central amygdala. *In Preparation*

2.2 Abstract

Molecular identification and characterization of fear controlling neural circuitries is a promising path towards the development of targeted treatments for fear-related disorders, including anxiety and Posttraumatic Stress Disorder. Discrimination between cellular markers unique to a specific neural population and those additionally marking previously identified populations is necessary for efficient progress. Here we used three-color *in situ* hybridization analysis with RNAscope technology to determine the extent to which a variety of markers denote unique sub-populations of neurons within the central nucleus of the amygdala, a known output structure mediating fear processing. We sought to identify the extent of cellular specificity vs. co-localization identified by expression of somatostatin (*Sst*), neurotensin (*Nts*), corticotropin releasing factor (*Crf*), tachykinin 2 (*Tac2*), protein kinase c delta (*Prkcd*), and dopamine receptor 2 (*Drd2*) genes within amygdala cells. Expression and co-expression was examined across capsular (CeC), lateral (CeL), and

medial (CeM) compartments of the central amygdala. The greatest expression of *Prkcd* and *Drd2* were found in CeC and CeL. *Crf* was expressed primarily in CeL while *Sst, Nts*, and *Tac2* were distributed between CeL and CeM. Within the CeC and CeL, *Prkcd* and *Drd2* label large non-overlapping and often topographically distinct populations that do not overlap with *Sst, Nts*, *Crf* and *Tac2*. High levels of co-localization were identified between *Sst, Nts, Crf,* and *Tac2* within the CeL while little co-localization was detected between any RNA markers within the CeM. This work begins to clarify the differential and overlapping populations of CeA neurons, important for further understanding the behavioral roles of CeA neural populations and providing potential target populations for regulating fear-related behaviors.

Abbreviations:

CeA	Central amygdala
CeC	Capsular division of the central amygdala
CeL	Lateral division of the central amygdala
CeM	Medial division of the central amygdala
Crf	Corticotropin releasing factor
Drd2	Dopamine receptor 2
Nts	Neurotensin
Prkcd	Protein kinase C delta
Sst	Somatostatin
Tac2	Tachykinin 2

2.3 Introduction

The amygdala has a wide array of distinct cell populations distinguished by their molecular, electrophysiological and functional properties. Recent evidence suggests that distinct sub-populations play differential roles in fear acquisition vs. fear extinction learning. The molecular characterization of known populations is a promising route for

identification of translationally relevant treatments for fear and anxiety-related disorders (McCullough, Morrison, & Ressler, 2016).

Previous work has shown that the central lateral amygdala (CeL) contains a mutually inhibitory circuit that gates fear expression via the inhibition of central medial amygdala (CeM) output neurons (Ciocchi et al., 2010; Ehrlich et al., 2009; Herry et al., 2008; Letzkus et al., 2015). Notably, the CeL is often combined with the central capsular division (CeC) in analyses, despite these regions having unique projection patterns and potentially different roles in fear and anxiety. Given the small size and close proximity of these nuclei discrimination is technically challenging, especially in mice. Although direct manipulations and measurements may be unable to specifically target these nuclei with the current technologies, careful distinction and analysis remains important going forward. In the present manuscript we will discuss these two regions separately (Bourgeais, Gauriau, & Bernard, 2001; Jolkkonen & Pitkanen, 1998).

A number of gene-targeted populations have been identified in the literature as playing specific roles in behavior. The most prominent of these were chosen for further examination of their specificity and co-expression. The Protein Kinase C Delta (PKC-δ, *Prkcd*) expressing population has previously been shown to directly inhibit CeM output neurons, reducing their activity in response to conditioned stimuli (CS) following fear conditioning and thus playing an important role in fear extinction learning among other behaviors (Cai, Haubensak, Anthony, & Anderson, 2014; Ciocchi et al., 2010; Haubensak et al., 2010; Herry et al., 2008). The somatostatin (SOM, *Sst*) expressing population appears to be an opposing counterpart of the PKC-δ population, whose activity increases in response to CS following fear conditioning and whose activity is both sufficient and necessary for the

production of fear and defensive behaviors (H. Li et al., 2013; Penzo, Robert, & Li, 2014; Yu, Garcia da Silva, Albeanu, & Li, 2016). The Tachykinin 2 (TAC2, *Tac2*) population plays a complementary role to the SOM population, with activity that is also both necessary and sufficient for fear learning (Andero et al., 2016; Andero et al., 2014). Importantly, each of molecule used here as a marker for a CeA sub-population has an important role in modulating neuronal activity; however, these roles will not be addressed in this work.

In addition to SOM and TAC2, other neuropeptides have been implicated as playing critical roles in fear circuitry. In particular corticotropin releasing factor (CRF, *Crf*) and neurotensin (NTS, *Nts*) expressing neurons are expressed in populations ideally situated and connected to participate in the central amygdala fear controlling circuit (Day, Curran, Watson, & Akil, 1999; Marchant, Densmore, & Osborne, 2007; Petrovich & Swanson, 1997). Both NTS and CRF have been shown to play important roles in fear learning and expression (Gafford & Ressler, 2015; Merali, McIntosh, Kent, Michaud, & Anisman, 1998; Shilling & Feifel, 2008; Thompson, Erickson, Schulkin, & Rosen, 2004; Yamauchi et al., 2007). Dopamine has also been established as playing a critical role in fear and extinction learning. Specifically, the differential distributions of dopamine receptors may have important implications for mediating fear behaviors (Abraham et al., 2014; de la Mora, Gallegos-Cari, Arizmendi-Garcia, Marcellino, & Fuxe, 2010; O. B. Kwon et al., 2015). The dopamine receptor 2 (DRD2, *Drd2*), but not dopamine receptor 1, is expressed selectively in the CeL suggesting an important role for DRD2 in fear behaviors (Perez de la Mora et al., 2012).

Considering the preponderance of CeA cell populations that play parallel or complementary roles in fear behaviors, it is important to determine the extent to which these populations overlap. While much work has been completed identifying markers for

behaviorally relevant neuronal populations, less has been done to examine the extent to which these populations are unique. In the present investigation, three-color *insitu* hybridization using RNAscope technology was used to determine the extent of overlap in expression of *Prkcd, Sst, Nts, Tac2, Crf,* and *Drd2*. This next-generation *insitu hybridization* technique offers unprecedented specificity of probe binding and amplification compared to traditional fluorescent *insitu hybridization,* which allows analysis of co-localization within single cells across a wide range of probe combinations. The present work represents the most in-depth and comprehensive analysis of co-expression of these transcripts to date.

The results of this investigation suggest that within the CeC, *Prkcd* and *Drd2* label large non-overlapping populations. Within the CeL, *Sst, Tac2, Nts* and *Crf* populations largely overlap. Of these *Sst* labels the largest population that contains the others markers to varying extents. Within the CeL, the *Prkcd* and *Drd2* populations largely do not overlap with each other or the other populations examined. The CeM has moderately sized *Sst, Tac2, Nts* and *Crf* populations, but is largely devoid of *Prkcd* and *Drd2* labeled cells. Notably, unlike within the CeL, within the CeM, the *Sst, Tac2, Nts,* and *Crf* populations largely do not overlap suggesting important differences in the functional populations labeled by these markers in the CeL and CeM.

2.4 Results

Before characterizing distinct and overlapping populations of gene expression markers within the amygdala, a number of quality control studies were performed. All staining was performed in tissue collected from adult male C57BL/6 mice at baseline conditions approximately 2 hours following the beginning of the light cycle. Patterns observed with *in situ* staining for co-localization of three marker experiments was identical

to that observed from single- labeling of each marker. Staining patterns were consistent with those observed in the literature and with those produced by the Allen Brain Institute. All six probes produced strong staining in the central CeA.

Each marker was examined individually to characterize its distribution across sub-compartments of the CeA. Determination of sub-compartment location was primarily accomplished through examination of DAPI staining patterns. We found that the most common and referenced mouse brain atlases (Paxinos and Allen Institute) differ somewhat on the locations of CeA sub-compartments across the anterior-posterior (A-P) axis of the amygdala (Supplemental Figure 1). Thus, the reference atlas provided through the Allen Brain Institute (www.brain-map.org) was used throughout our studies as a primary guide.

Distribution of Labeled Cells.

The distribution of total cells expressing mRNAs of interest was examined across CeA sub-compartments (Figure 1A and 1B). *Prkcd* staining was almost entirely contained within the CeC (51%) and CeL (43%), with only minority populations found within the CeM (6%). *Prkcd* staining was consistently dense and highly localized within the CeC and CeL. Notably, *Prkcd* cell bodies are found primarily within anterior ventral CeC, posterior dorsal CeC and posterior CeL . *Drd2* was strongly expressed within the CeC (48%) and CeL (35%) with a smaller population within the CeM (17%). Importantly, in contrast to *Prkcd* labeled cells, *Drd2* mRNA labeled cells are found most strongly in anterior dorsal CeC and anterior CeL, while found more sparsely at more posterior positions. *Crf* was primarily expressed within CeL at all A-P positions (75%) with smaller populations in CeM (19%) and CeC (6%). *Sst, Tac2,* and *Nts* labeled populations in both CeL (58%, 49%, and 34% respectively) and CeM (36%, 49%, and 58%) with only small numbers of cells labeled in CeC (6%, 2%

and 8%). These mRNAs only moderately label anterior CeL while very high densities are found within posterior CeL.

Prevalence of Labeled Cells

Single- labeling by marker mRNAs was examined to determine their prevalence within a sub-compartment (Figure 1C). This was completed by determining the proportion of labeled cells to the total number of DAPI positive cells within a compartment. *Drd2* and *Prkcd* label large proportions of cells within the CeC (31% and 21%, respectively) while other markers *Sst, Tac2, Nts* and *Crf* label minority populations (5%, 1%, 3%, and 2% respectively). *Prkcd, Drd2, Sst, Tac2, Nts* and *Crf* each label significant populations within the CeL (17%, 21%, 26%, 13%, 14%, and 20%). *Sst, Tac2,* and *Nts* label moderate populations within the CeM (10%, 10%, and 13%) while *Prkcd, Drd,* and *Crf* label smaller proportions of CeM cells (1%, 6% and 4%).

Co-localization of CeA Markers

Co-localization between markers was examined within each CeA sub-compartment. Triple-labeled images were analyzed only for co-localization between pairs of markers due to practical limitations on the number of probe combinations. Additionally, although co-localization was examined at a variety of A-P positions (-.8 to -1.8), data is presented here collapsed across A-P -1.2 to -1.8. This may lead to an underestimation of the co-localization of some markers at certain positions (discussed below), but nonetheless provides an important picture of overall co-localization between markers in CeA.

Sst appears to mark the largest population of CeL cells (Figure 1C and Figure 2C). This population overlaps to a great extent with *Tac2* (Figure 2D) within the CeL, but not the

CeC or CeM (Figure 2F). Quantification of co-expression reveals that the total *Sst* labeled population is statistically larger than the co-expressing *Sst/ Tac2* population in all sub-compartments; however, within the CeL the *Tac2* population is not statistically different from the co-expressing *Sst/Tac2* population (Figure 2G). These data suggest that the larger *Sst* population may entirely contain the *Tac2* population at this A-P range. *Prkcd* exhibits a typical dense CeC and CeL expression (Figure 2E). Within the CeL, total *Sst, Tac2* and *Prkcd* populations are larger than populations co-expressing those markers, suggesting these RNAs mark separate populations (Figure 2H and 2I). Within CeC and CeM, total populations are generally statistically larger than co-expressing populations except in cases where total population is very small.

Crf labels a large population of CeL cells with sparser labeling in the CeM (Figure 3C). *Nts* marks a large population within the CeL and a moderate population within the CeM (Figure 3D). Quantification of co-expression reveals the total *Crf* population is statistically larger than the co-expressing *Crf/Nts* population in the CeL and CeM; however, within the CeL the *Nts* population is not statistically different from the co-expressing *Crf/Nts* population (Figure 3G). This suggests that within the CeL, the *Nts* population may be contained within the *Crf* population while within the CeM these populations are distinct. *Prkcd* demonstrates a similar expression pattern to that seen in Figure 2 (Figure 3E). The *Prkcd* population is separately expressed from the *Crf* and *Nts* populations in all areas where an appreciable number of marked cells are found (Figure 3H and 3I).

Examination of co-expression of *Nts* and *Sst* reveals similar patterns. Within the CeL, the *Nts* population appears to be contained within the *Sst* population (Figure 4A- 4F). While within the CeM, these mRNAs mark distinct populations (Figure 4F). Likewise, when *Crf*

and *Tac2* are examined for co-expression, neither of the total labeled populations is statistically larger than the co-labeled *Crf/Tac2* populations suggesting they are the same (Figure 4G-4L). However, within the CeM these RNAs mark separate populations (Figure 4L).

These results suggest a hierarchical organization within the CeL wherein *Sst > Crf ~Tac2 >Nts* in terms of number of labeled neurons. This is in contrast to the CeM where all total labeled populations are found to be significantly different from their co-labeling with any other marker. Meaning each population is significantly different from every other.

Examination of co-expression at a variety of A-P positions reveals that the zone of highest co-expression between *Sst, Tac2, Nts* and *Crf* is constrained to A-P -1.4 to -1.8. Examination of more anterior positions (A-P -0.8 to -1.2) demonstrates that these populations are co-expressed at lower rates and found in different sub-compartments in the anterior CeA.

At anterior positions (A-P∼-.9), *Drd2* labels a large population of CeC cells while *Prkcd* cells are found in a more constrained cluster in the ventral aspect of the CeC (Figure 5C and 5E). At this A-P position *Nts* is found primarily within the CeM (Figure 5D). These populations largely do not overlap (Figure 5F).

At a similar A-P position (∼-.8) *Crf* densely labels the CeL (Figure 5I). Very little *Tac2* staining is found within the CeL; however, labeled *Tac2* cells are found in the CEM and the dorsal aspect of the main intercalated mass (Im) located ventrally to the BLA (Figure 5J). *Prkcd* is found in the ventral CeC (Figure 5K). These populations largely do not overlap.

Slightly more posteriorly (A-P∼-1.2), the densely labeled CeL seen in more posterior sections begins to appear (Figure 5M-5R). *Crf* continues to densely label the CeL and more

sparsely the CeM (Figure 5O). *Prkcd* begins to form the typical CeC and CeL expression pattern (Figure 5Q); however, *Tac2* does not densely label the CeL at this position and markers continue to be co-expressed at low levels (Figure 5P and 5R).

Overall, these results highlight that the zone of dense co-expression in CeL is constrained to more posterior aspects of the CeA. The overall percentages of co-expression for all mRNA pairs examined at anterior and posterior positions is presented in Table 1A and 1B.

2.5 Discussion

The central amygdala plays a pivotal role in the control of a wide range of behaviors. As such, the connectivity, cytoarchitecture and expression profiles of cells in the various subdivisions of this nucleus have been widely studied, especially in rats (Cassell et al., 1999; Jolkkonen & Pitkanen, 1998; McDonald, 1982, 1984, 1998). To date, a number of molecularly identified populations have been described as playing distinct roles in the control of behavior. Additionally, several publications have described the distributions of these populations using immunohistochemistry or *in situ* hybridization (Andero et al., 2016; Andero et al., 2014; Cassell et al., 1999; Cassell, Gray, & Kiss, 1986). However, minimal data is available on the extent to which these population markers overlap, especially in mice, leading to ambiguity in the specificity of identified and manipulated populations. This publication provides a necessary link by examining the co-expression of *Prkcd, Sst, Nts, Tac2, Crf,* and *Drd2* in the CeA of mice. To this point, the depth of analysis of co-expression presented here has not been possible. Improvements in *insitu hybridization* technology (RNAScope) has allowed for this unprecedented level of expression based description.

The present method for identifying cells expressing an mRNA used a binary system so that all cells reaching minimum cut off were considered to be expressing. Additionally, all animals were the same age and sacrificed under the same conditions at the same time. This approach was used to characterize the baseline identity of cells; however, it ignores a wealth of data concerning levels of expression at the time of sacrifice and dynamic (e.g. circadian or following behavior) changes in expression level. One clear example is that both *Tac2* and *Sst* are clearly expressed at different levels in different populations. Cells appear to express *Tac2* and *Sst* at both high (bright) and moderate/low (dimmer) levels within the same sub-nucleus. Future studies examining static difference and dynamic changes in RNA expression level may yield important information regarding the functional roles of these mRNAs.

Data presented here confirms immunohistochemical analyses in rat by demonstrating that within the CeL there is a high degree of overlap between *Sst, Nts, Tac2,* and *Crf*. Remarkably this overlap is observed only within a constrained posterior section of the CeL between A-P -1.4 and -1.8. Examination of these populations across the A-P axis suggests that *Crf* most consistently marks a CeL population while *Sst, Nts,* and *Tac2* most consistently label cells in the anterior CeM before densely marking the CeL at posterior positions. Within the posterior CeL, these populations are highly overlapping. *Sst* expressing cells represent the largest population containing the majority of cells expressing *Nts, Tac2,* and *Crf*. This is in contrast to the CeM where these populations are consistently non-overlapping.

An important consideration for examination of these populations across the A-P axis is the presence of inconsistency among available mouse brain atlases. For example, at

anterior positions, the Allen Brain Atlas identifies the location of the dense *Crf* population as the CeL while the Paxinos & Franklin (2001) atlas identifies this region as the interstitial nucleus of the posterior limb of the anterior commissure (IPAC). While these may be semantic differences, the consistency of nucleus identification has important implications for the quantification of co-expression. Our decision to adhere more closely to the Allen Brain Atlas Reference Atlas may have led to an underestimation of the extent of co-expression of examined markers within the CeL.

Drd2 consistently marks a large CeC and CeL population that appears to be contiguous with the amygdalostriatal transition area (Ast). This is in contrast to *Prkcd,* which at anterior positions marks a very ventral population of CeC cells before moving more dorsally to mark a very constrained population of CeC and CeL cells at posterior positions. Consistent with previously published work, neither the *Prkcd* nor the *Drd2* population is highly overlapping with any others examined. This finding validates the identification of these populations as potentially unique markers for functionally distinct sub-populations.

Prior literature identifying functionally distinct populations has been inconsistent in the delineation of within which sub-compartment of the CeA a neuronal population has its distinct role. Such a specific delineation is especially critical in the case of *Sst, Nts, Tac2,* and *Crf* where the identification of these populations within the CeL may be redundant to previous work. Conversely, lack of co-expression in the CeM highlighted by the present findings may indicate a more specialized role for these cells in this sub-compartment. Future studies using intersectional approaches may yield clear and parsimonious descriptions of the distinct functional roles of single- expressing and co-expressing

populations in the CeL and CeM (Dymecki, Ray, & Kim, 2010; Hirsch, d'Autreaux, Dymecki, Brunet, & Goridis, 2013; Jensen & Dymecki, 2014; Okaty et al., 2015). Additionally, unlike in the CeL where examined populations label a majority of total cells, in the CeM, examined populations make up less than half of examined cells, indicating many additional populations remain to be described.

These results represented a much-needed beginning in the examination of the many possible markers for CeA sub-populations in mice. The receptors of the protein products of several of the mRNAs examined may also provide promising markers for specific sub-populations (*Crfr1, Crfr2, Tacr2, Sstr1-5*). Additionally, further research into the co-expression of various neuropeptides and other identified markers such as vasoactive intestinal peptide, cholecystokinin, neuropeptide Y, enkephalin, and substance P (which have all also been shown to play important roles in fear and anxiety behaviors) will, in the future, be necessary to identify the extent to which additional populations co-localize within the CeA.

2.6 Methods

RNA Scope Staining

Staining for RNA of interest was accomplished using RNA Scope Fluorescent Multiplex 2.5 labeling kit. Probes utilized for staining are: mm-Nts-C1, mmNts-C2, mm-Tac2-C2, mm-Sst-C1, mm-Sst-C2, mm-Crh-C1, mm,Prkcd-C1, mm-Prkcd-C3, mmDrd2-C3. Brains were extracted and snap-frozen in methyl-butane on dry ice. Sections were taken at a width of 16μm. Procedure was completed to manufacturers specifications.

Image Acquisition

Images were acquired with experimenter blinded to probes used. Sixteen-bit images of staining were acquired on a Leica SP8 confocal microscope using a 10x objective. Within a sample images were acquired with identical settings for laser power, detector gain, and amplifier offset. Images were acquired as a z-stack of 10 steps of .5 μm each. Max intensity projections were then created and analyzed.

Data Analysis

The expression and co-expression of mRNA of different markers of interest was quantified in three areas central capsular amygdala (CeC), central lateral amygdala (CeL), and central medial amygdala (CeM). Images (approximate area) of regions were taken bilaterally from a minimum of one section from each of four animals for each marker pair (n= >8 amygdala/ marker pair). Individual cells were identified based upon DAPI staining of nucleus. Cells were determined to be expressing marker when more than five fluorescent dots or an area of staining sufficient to contain five dots were clearly associated with a single nucleus. The width of a cell was considered to be twice the diameter of the nucleus. The distribution of cells across CeA nuclei was determined by dividing the number of labeled cells in a nucleus by the total number of labeled cells across all nuclei. The percentage of cells in a nucleus expressing a certain mRNA was determined by dividing the number of positive cells in a nucleus by the total number of DAPI labeled nuclei in the nucleus.

Statistical Analysis

Determination of the percentage of cells within a sub-compartment expressing marker of interest was accomplished by dividing the total number of cells expressing the marker by

the total number of DAPI positive nuclei in the area. Determination of the percentage of a labeled population found in a certain sub-compartment was accomplished by dividing the number of labeled cells in a compartment by the total number of labeled cells found in all compartments. Statistical analysis of the whether a labeled population was different than the co-expressing component of that population was performed using the non-parametric Mann-Whitney test with Graphpad's 'Prism' software package.

2.7 Figures

A

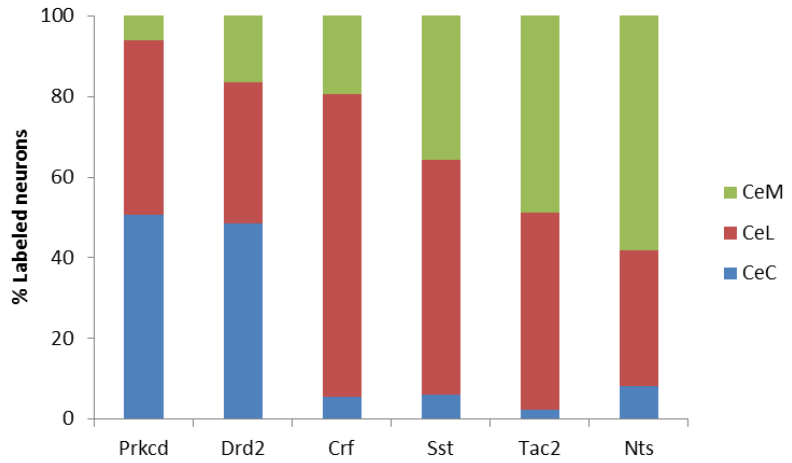

B

Distribution of Examined RNAs across CeA sub-compartments

Gene	*Prkcd*	*Drd2*	*Crf*	*Sst*	*Tac2*	*Nts*
% labeled cells found in CeC	50.7	48.5	5.6	6.0	2.3	8.3
% labeled cells found in CeL	43.2	35.0	75.0	58.3	48.8	33.6
% labeled cells found in CeM	6.1	16.6	19.4	35.7	48.9	58.1

C

Percentage of expression of mRNAs in total cells of CeA sub-compartment

Gene	*Prkcd*	*Drd2*	*Crf*	*Sst*	*Tac2*	*Nts*
% total cells in CeC	21.4	31.1	2.0	5.2	1.1	3.3
% total cells in CeL	16.7	21.4	20.5	26.4	13.7	13.4
% total cells in CeM	1.3	6.0	4.2	10.1	10.4	13.4

Figure 2-1. Distribution of examined mRNAs across CeA sub-compartments.

A. Graphical representation of labeled cell distribution across CeA sub-compartments. **B.** Tabular results of data represented in A. **C.** Labeled cells as percentage of total cells in sub-compartment. Labeled cell counts presented as a percentage of total DAPI positive nuclei examined within a nucleus.

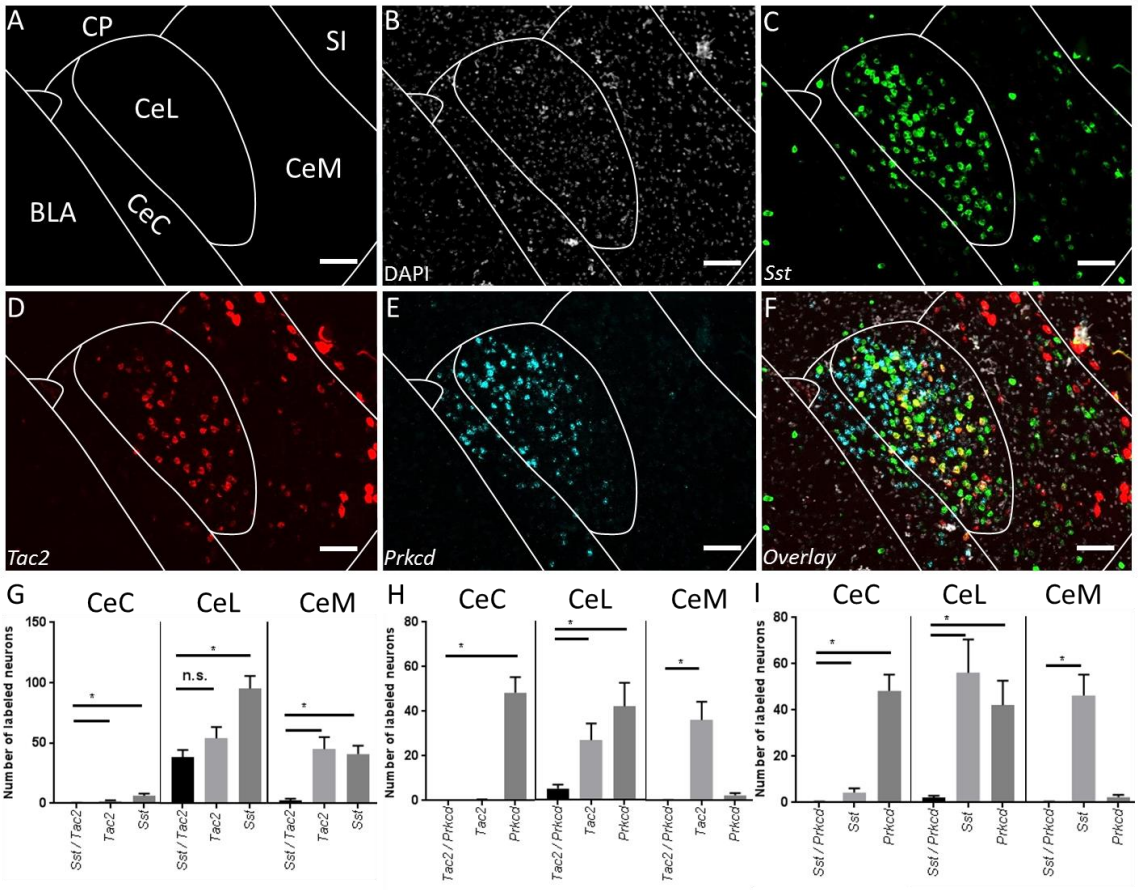

Figure 2-2. Co-expression of *Sst, Tac2* and *Prkcd (A-P -1.5).*

A. Map of area examined. **B.** DAPI stain (grey) of area examined. **C.** *Sst* expression (green) is found strongly in the CeL and CeM. **D.** *Tac2* expression (red) is found strongly in the CeL and CeM. **E.** *Prkcd (cyan)* expression is found strongly in the CeC and CeL. **F.** Overlay of B-F reveals strong overlap in expression of *Sst* and *Tac2* in CeL but not CeM. *Prkcd* does not highly co-express in any area. Scale Bar indicates 50 µm. **G.** Quantification of single-expressing cells and co-expressing *Sst* and *Tac2* cells in CeC, CeL and CeM. Bars represent the mean number of (co)expressing cells in each sub-compartment, (+ / - s.e.m.) where * = $p<.05$ difference between single- and double-labeled populations (Mann-Whitney U test.). **H.** Quantification of single- expressing cells and co-expressing *Tac2* and *Prkcd* cells in CeC, CeL and CeM. Bars represent the mean number of (co)expressing cells in each sub-

compartment. (+ / - s.e.m.) where * = p<.05 difference between single- and double-labeled populations (Mann-Whitney U test.). **I.** Quantification of single- expressing cells and co-expressing *Sst* and *Prkcd* cells in CeC, CeL and CeM. Bars represent the mean number of (co)expressing cells in each sub-compartment. (+ / - s.e.m.) where * = p<.05 difference between single- and double- labeled populations (Mann-Whitney U test.).

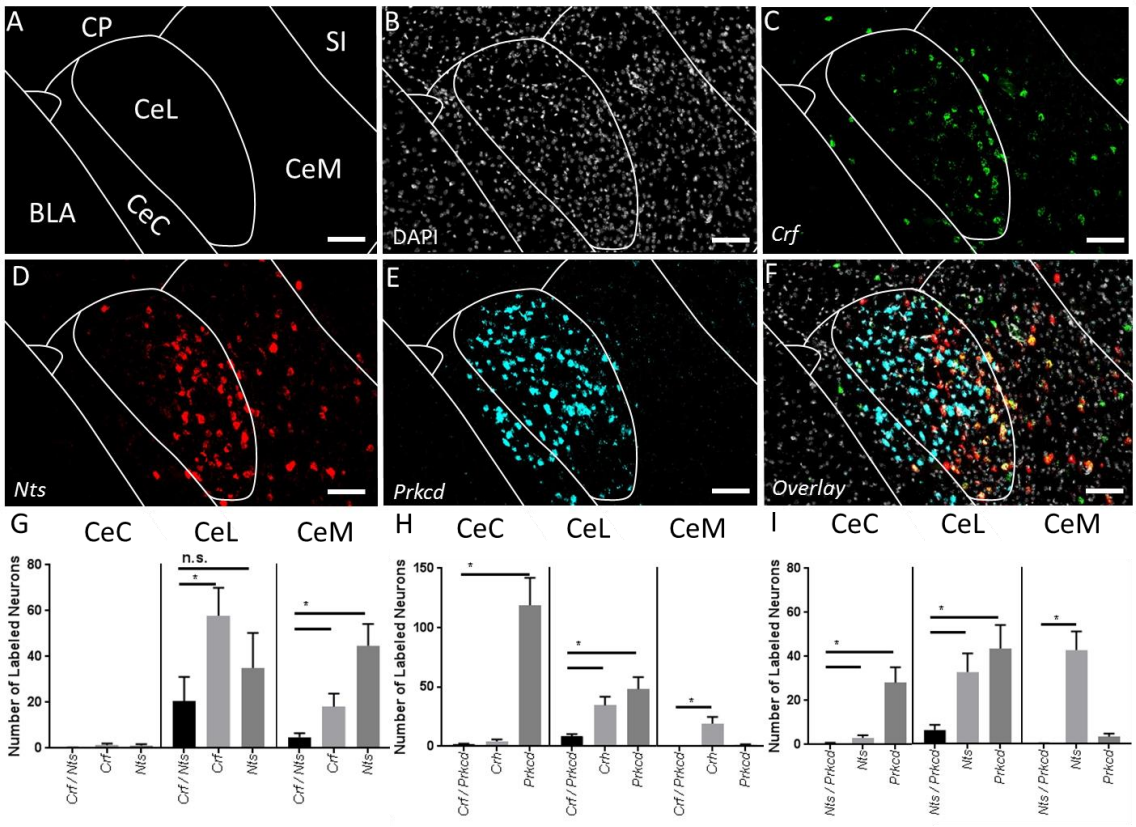

Figure 2-3. Co-expression of *Crf, Nts* and *Prkcd (A-P -1.5).*

A. Map of area examined. **B.** DAPI stain (grey) of area examined. **C.** *Crf* expression (green) is found strongly in the CeL and moderately in the CeM. **D.** *Nts* expression (red) is found strongly in the CeL and CeM. **E.** *Prkcd* expression (cyan) is found strongly in the CeC and

CeL. **F.** Overlay of B-F reveals strong overlap in expression of Crf and *Nts* in CeL but not CeM. *Prkcd* does not highly co-express in any area. Scale Bar indicates 50 μm. **G.** Quantification of single- expressing cells and co-expressing *Crf* and *Nts* cells in CeC, CeL and CeM. Bars represent the mean number of (co)expressing cells in each sub-compartment. (+ / - s.e.m.) where * = p<.05 difference between single- and double- labeled populations (Mann-Whitney U test.). **H.** Quantification of single- expressing cells and co-expressing *Nts* and *Prkcd* cells in CeC, CeL and CeM. Bars represent the mean number of (co)expressing cells in each sub-compartment. (+ / - s.e.m.) where * = p<.05 difference between single- and double- labeled populations (Mann-Whitney U test.). **I.** Quantification of single- expressing cells and co-expressing *Sst* and *Prkcd* cells in CeC, CeL and CeM. Bars represent the mean number of (co)expressing cells in each sub-compartment. (+ / - s.e.m.) where * = p<.05 difference between single- and double- labeled populations (Mann-Whitney U test.)

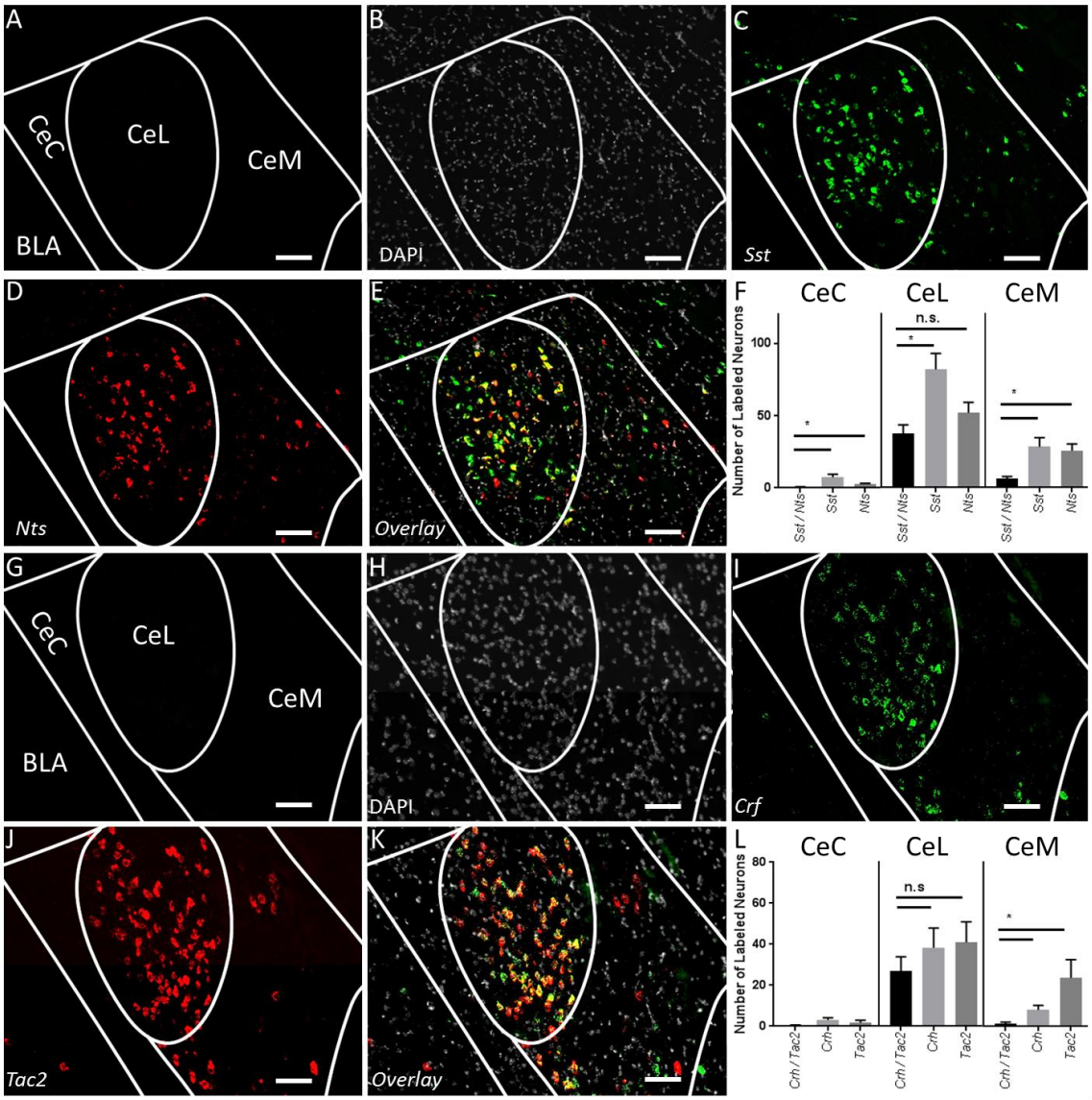

Figure 2-4. Co-expression of *Sst and Nts,* and *Crf* and *Tac2 (A-P -1.5).*

A. Map of area examined B-E. **B.** DAPI stain (grey) of area examined. **C.** *Sst* expression (green) is found strongly in the CeL and CeM. **D.** *Nts* expression (red) is found strongly in the CeL and CeM. **E.** Overlay of B-E reveals strong overlap in expression of *Sst* and *Nts* in CeL but not CeM. Scale Bar indicates 50 µm. **F.** Quantification of single- expressing cells and co-expressing *Sst* and *Nts* cells in CeC, CeL and CeM. Bars represent the mean number of (co)expressing cells in each sub-compartment. (+ / - s.e.m.) where * = p<.05 difference

between single- and double- labeled populations (Mann-Whitney U test.). **G.** Map of area examined H-K. **H.** DAPI stain (grey) of area examined. **I.** *Crf* expression (green) is found strongly in the CeL and CeM. **J.** *Tac2* expression (red) is found strongly in the CeL and CeM. **K.** Overlay of H-J reveals strong overlap in expression of Crf and Tac2 in CeL but not CeM. Scale Bar indicates 50 μm. **L.** Quantification of single- expressing cells and co-expressing *Crf* and *Tac2* cells in CeC, CeL and CeM. Bars represent the mean number of (co)expressing cells in each sub-compartment. (+ / - s.e.m.) where * = $p<.05$ difference between single- and double- labeled populations (Mann-Whitney U test.).

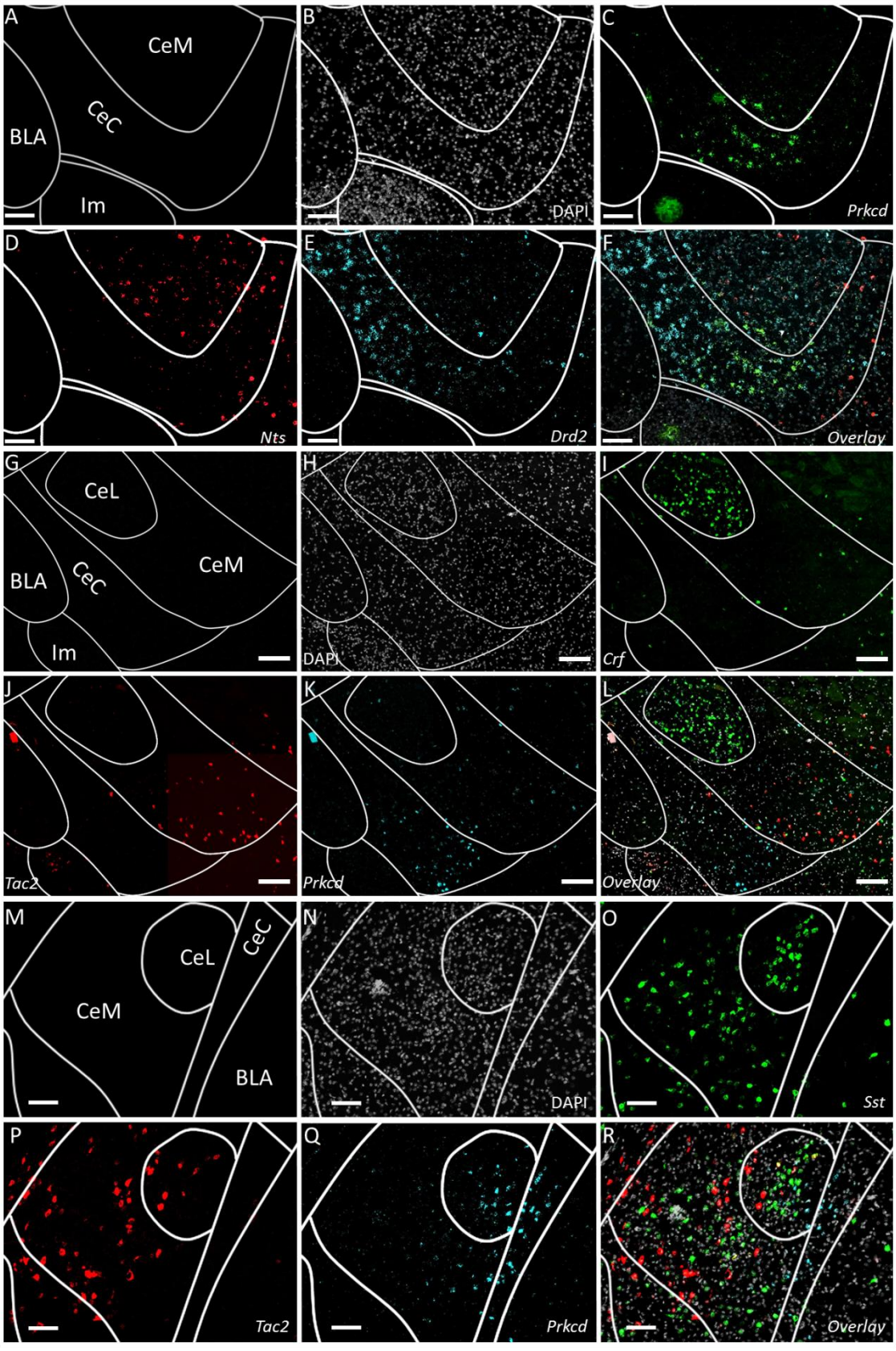
A
CeM
CeC
BLA
Im
B
DAPI
C
Prkcd
D
Nts
E
Drd2
F
Overlay
G
CeL
CeM
BLA
CeC
Im
H
DAPI
I
Crf
J
Tac2
K
Prkcd
L
Overlay
M
CeL
CeC
CeM
BLA
N
DAPI
O
Sst
P
Tac2
Q
Prkcd
R
Overlay

Figure 2-5. Co-expression of examined mRNA's in anterior CeA (A-P -.9, -.8, and -1.22).

Examination of markers at anterior positions within CeA reveals differential distributions across sub-compartments and reduced co-expression. ***A.*** Map of area examined (A-P ~ -.9). **B.** DAPI stain (grey) of area examined. **C.** *Prkcd* expression (green) is found strongly in ventral CeC. **D.** *Nts* expression (red) is found strongly in the CeM with limited expression in medial ventral CeC. **E.** *Drd2* expression (cyan) is found strongly in the more dorsal elements of the CeC. **F.** Overlay of B-F reveals limited overlap in expression of any marker examined. Scale Bar indicates 50 μm. ***G.*** Map of area examined (A-P ~ -.8). **H.** DAPI stain (grey) of area examined. **I.** Crf expression (green) is found strongly in CeL. **J.** *Tac2* expression (red) is found in the CeM. **K.** *Prkcd* expression (cyan) is found strongly in ventral CeC. **L.** Overlay of H-K reveals limited overlap in expression of any marker examined. Scale Bar indicates 200 μm. ***M.*** Map of area examined (A-P ~ -1.2). **N.** DAPI stain (grey) of area examined. **O.** *Sst* expression (green) is found strongly in CeL and CeM. **P.** *Tac2* expression (red) is found in the CeL and CeM. **Q.** *Prkcd* expression (cyan) is found strongly in CeL and CeC with limited expression in the CeM. **R.** Overlay of N-Q reveals limited overlap in expression of any marker examined. Scale Bar indicates 50 μm.

A

CeC	Expression w/*Sst* (%)	Expression w/*Tac2* (%)	Expression w/*Crh* (%)	Expression w/*Nts* (%)	Expression w/*Prkcd* (%)	Expression w/*Drd2* (%)
Sst						
Tac2						
Crh						
Nts					13.7	
Prkcd	0	0	0	3.3		22.9
Drd2	0	.2	0.7	3.7	8.8	

CeL	Expression w/*Sst* (%)	Expression w/*Tac2* (%)	Expression w/*Crh* (%)	Expression w/*Nts* (%)	Expression w/*Prkcd* (%)	Expression w/*Drd2* (%)
Sst		0.0				
Tac2						
Crh		1.1		3.1	5.9	32.7
Nts			9.5		11.5	
Prkcd		10.0	17.6	4.5		8.1
Drd2	0.0	0.0	19.2	8.2	3.1	

CeM	Expression w/*Sst* (%)	Expression w/*Tac2* (%)	Expression w/*Crh* (%)	Expression w/*Nts* (%)	Expression w/*Prkcd* (%)	Expression w/*Drd2* (%)
Sst		2.1		27.8	0	8.0
Tac2	2.1		2.2		0	2.4
Crh						8.6
Nts	48.0		4.8		.9	3.9
Prkcd						4.7
Drd2	4.2	5.3	8.5	9.7	1.6	

B

CeC	Expression w/*Sst* (%)	Expression w/*Tac2* (%)	Expression w/*Crh* (%)	Expression w/*Nts* (%)	Expression w/*Prkcd* (%)	Expression w/*Drd2* (%)
Sst		6.6	2.3	7.9	6.0	
Tac2						
Crh	1.7					
Nts						
Prkcd	1.0	.4	5.3	1.5		
Drd2	0	4.0	1.0	1.9		

CeL	Expression w/*Sst* (%)	Expression w/*Tac2* (%)	Expression w/*Crh* (%)	Expression w/*Nts* (%)	Expression w/*Prkcd* (%)	Expression w/*Drd2* (%)
Sst		40.3	35.1	45.5	2.3	3.2
Tac2	71.0		64.5		19.3	7.7
Crh	4.6	62.7		40.8	25.9	30.7
Nts	72.0		59.5		18.9	9.2
Prkcd	2.9	10.3	18.2	15.1		
Drd2	2.9	6.4	19.2	6.5		

CeM	Expression w/*Sst* (%)	Expression w/*Tac2* (%)	Expression w/*Crh* (%)	Expression w/*Nts* (%)	Expression w/*Prkcd* (%)	Expression w/*Drd2* (%)
Sst		6.5	0.0	21.2	.6	0.0
Tac2	5.9		5.4		0.8	12.0
Crh	0.0	12.2		24.3	1.4	
Nts	23.5		13.1		.4	3.6
Prkcd						
Drd2						

Table 2.1. Co-expression of examined RNA's across CeA sub-compartment in anterior and posterior CeA.

A. Co-expression of markers of interest in anterior CeA between A-P -.8 and -1.2. Parent population labeled on vertical column (total cells labeled). Co-expressed population labeled on horizontal column (total co-labeled cells). Blacked-out boxes indicate that parent population did not label greater than 5% of total cells in sub-compartment. **B.** Co-expression of markers of interest in posterior CeA between A-P -1.2 and -2.0. Parent population labeled on vertical column (total cells labeled). Co-expressed population labeled on horizontal column (total co-labeled cells). Blacked-out boxes indicate that parent population did not label greater than 5% of total cells in sub-compartment.

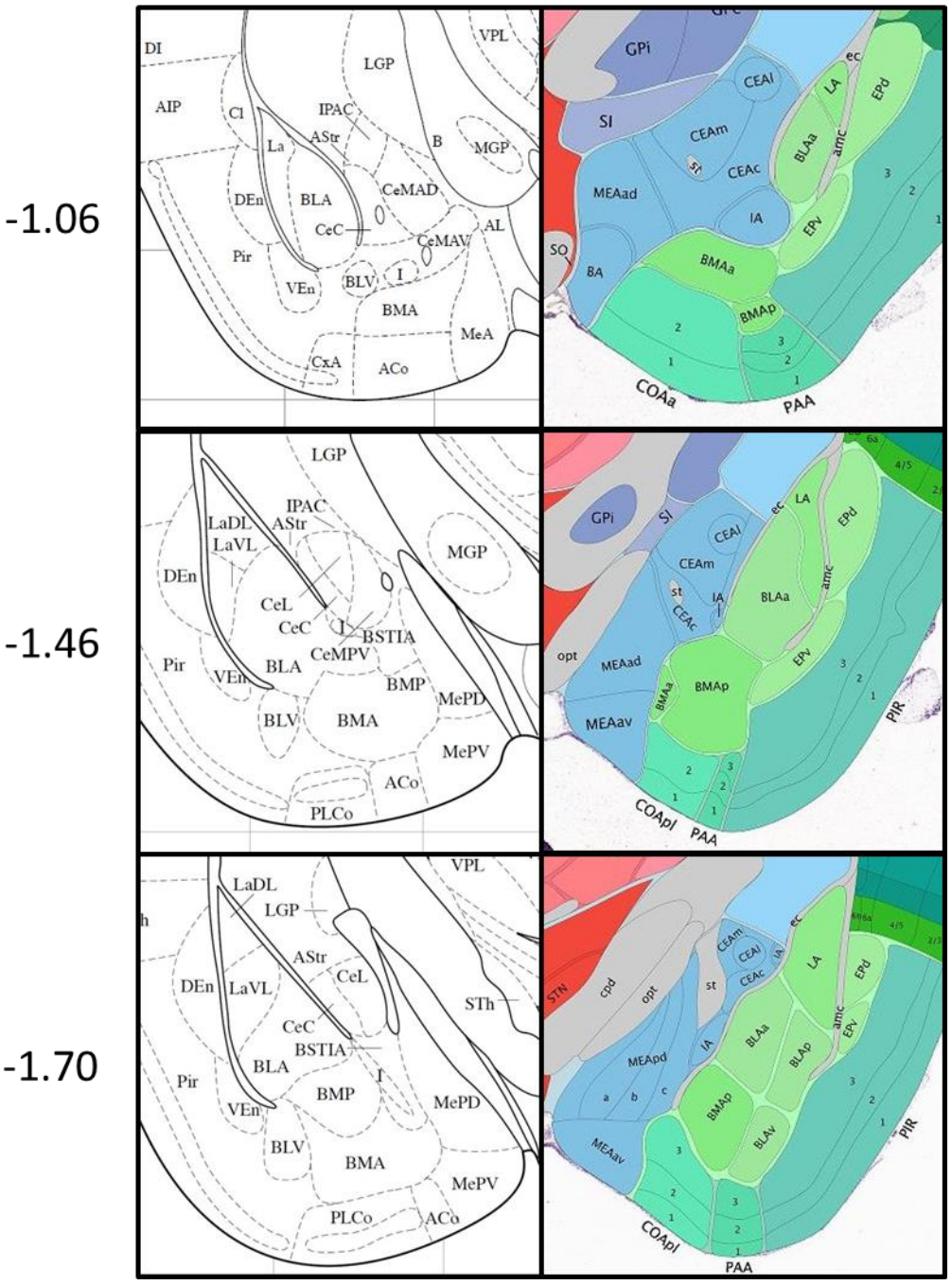

Supplemental Figure 2-1. Comparison of mouse brain atlases.

Atlases obtained from Paxinos and Franklin (2001, Left) and Allen Brain institute (2011, Right) at approximately equivalent A-P locations reveals several important differences in nucleus identification.

Chapter 3: Behavioral and Molecular Characterization of Central Amygdala Dopamine Receptor 2 Expressing Neurons' Role in Fear Behavior.

3.1 Context, Author's Contribution and Acknowledgement of Reproduction

The following chapter is an effort to behaviorally and molecularly examine the CeA *Drd2* expressing population. Data presented here indicates that *Drd2* marks a CeA population that supports fear expression and opposes fear extinction. Characterization of transcriptional changes following behavior reveals a number of targets for pharmacological manipulation. The results of this paper are consistent with results found in the literature using different techniques and animal models. The dissertation author contributed to the paper by designing and running experiments, analyzing the data, and was the main contributor to the writing of the paper. The chapter is reproduced from McCullough K.M., Gafford. G., Zimmeman. K., Morrison FG & Ressler K.J. Behavioral and Molecular Characterization of Central Amygdala Dopamine Receptor 2 Expressing Neurons' Role in Fear Behavior. Submitted.

3.2 Abstract

Behavioral and molecular characterization of cell-type specific populations governing fear learning and behavior is a promising avenue for identification of more targeted therapeutics for fear-related disorders. Here, we identify the CeA *Drd2* expressing population as a fear-supporting population. Direct manipulation of CeA *Drd2* neurons with Gs-DREADD reveals this population to support fear expression and oppose fear extinction. Characterization of this population via sequencing of RNA acquired with translating ribosome affinity purification (TRAP) identifies *Sst5r, Npy5r, Fgf3, ErbB4, Fkbp14, Dlk1, Ssh3* and *Adora2a* as differentially regulated following fear conditioning. Pharmacological manipulation of this population through D2R or $A_{2A}R$ confirm roles for *Drd2* neurons found using direct manipulation.

3.3 Introduction

The acquisition of learned fear associations is adaptive in dangerous environments; however, failure to extinguish fearful associations once a stimulus no longer predicts danger is maladaptive (A.P. Association, 2013). Pavlovian fear conditioning is a useful behavioral paradigm for studying associative fear learning where neutral conditioned stimuli (CS, e.g. a tone) are paired with innately aversive stimuli (US, e.g. a shock) until an animal expresses conditioned responses (CRs) to the CS. A commonly measured CR is freezing or the cessation of all non-homeostatic motion. Strength of acquisition of learned fearful associations is measured by the expression of CR to the CS alone. Fearful associations may be extinguished by multiple presentations of CS alone leading to a decrement in CR, this process mirrors many aspects of exposure therapy in humans. Notably, extinction creates new memories that overlay and modulate the original fearful association. The retention of consolidated extinction learning may be measured by observing the strength of CR to additional CS presentations (Maren & Fanselow, 1996; Myers & Davis, 2007).

Canonically, the amygdala is thought to be a main control hub of fear learning. CS and US information is integrated by the basolateral amygdala while the central amygdala (CeA) acts as a primary output, projecting to downstream brainstem areas directly responsible for executing select elements of fear behavior. Recent evidence suggests that genetically identifiable sub-populations within previously described sub-nuclei of the brain may play differential roles in the acquisition and extinction of learned fear associations (Ciocchi et al., 2010; Haubensak et al., 2010; H. Li et al., 2013). Identification of additional cell-type specific markers of fear controlling circuitries is crucial for further progress

towards understanding the neurobiology of behavior as well as for development of translationally relevant pharmaceutical treatments for fear disorders (McCullough et al., 2016).

The dopaminergic system is well known for its role in appetitive learning; however, more recently has it been recognized as being important in fear and extinction learning (Abraham et al., 2014; de la Mora et al., 2010). Dopamine modulates prediction error, stimulus salience, motivational states and other elements germane to associative learning (Fernandez, Boccia, & Pedreira, 2016). Broadly, dopamine receptors fall into two categories: stimulatory (Dopamine receptor 1-like; D1R & D5R), which enhance cAMP concentrations through $G_{\alpha s/olf}$, and inhibitory (Dopamine receptor 2-like: D2R, D3R & D4R), which decrease cAMP concentrations through $G_{\alpha i/o}$ (Abraham et al., 2014). Additionally, D1R and D2R bind additional G protein coupled receptor (GPCR) subunits activating PLC signaling and heterodimerize with other receptors modulating diverse signaling cascades (de la Mora et al., 2010). Perturbations in the dopaminergic system have been implicated in the disease etiologies of several human pathologies ranging from Parkinson's Disease to Schizophrenia, Depression and PTSD (Barch, Pagliaccio, & Luking, 2016; Lenka, Arumugham, Christopher, & Pal, 2016; L. Li et al., 2016). Although D2R's are clearly involved in fear and extinction learning, the literature is equivocal on their exact roles in CeA, since different study designs appear to show antagonist administration leading to opposing effects (Guarraci, Frohardt, Falls, & Kapp, 2000; Perez de la Mora et al., 2012; Ponnusamy, Nissim, & Barad, 2005). Thus, here we attempt to separate the role of CeA *Drd2* expressing neurons in behavior from that of receptor activity of D2R itself.

Determination of a genetically defined cell population's role in fear behavior is often best facilitated through the mobilization of genetically encoded modulators of neural activity. Designer receptors exclusively activated by designer drugs (DREADDs) are genetically encoded modified GPCRs exclusively activated by an otherwise inert ligand, clozapine-N-oxide (CNO) (Alexander et al., 2009; Rogan & Roth, 2011). Available DREADDs are coupled to $G_{\alpha s}$, $G_{\alpha i}$, and $G_{\alpha q}$, which increase neuronal excitability, decrease neuronal excitability or cause burst firing, respectively. DREADDs may be targeted to the cell population of choice through the viral transduction of Cre-recombinase dependent sequences into mice expressing Cre-recombinase under a cell-type specific promoter sequence.

Translating ribosome affinity purification (TRAP) relies upon genetically targeted expression of a modified ribosomal subunit, EGFP-L10a, which allows the purification of RNAs being actively translated in the cell population of interest at the time of sacrifice (Myriam Heiman, Ruth Kulicke, Robert J. Fenster, Paul Greengard, & Nathaniel Heintz, 2014). These RNAs may be sequenced, yielding a complete profile of a cell population's translational state at the time of interest. This approach offers unique opportunity for identifying cell-type specific targets that are relevant to fear.

In the present manuscript we found that *Drd2* is expressed in a population of CeA neurons. Direct enhancement of excitability in CeA Drd2 neurons using $G_{\alpha s}$-DREADDs supported fear expression and blocked fear extinction consolidation. Unbiased examination of changes in translational activity produced a diverse set of targets for future research aimed at identifying translationally relevant targets for modulation of fear learning and behavior. We identified the adenosine receptor 2a (*Adora2a*, $A_{2A}R$) mRNA as being

upregulated in *Drd2* neurons following fear conditioning. Additional markers found to be modulated with fear learning include *Sst5r, Npy5r, Fgf3, ErbB4, Gpr6, Fkbp14, Dlk1* and *Ssh3*. Consistent with the identification of the *Drd2* expressing population as a 'fear-on' population, blockade of $A_{2A}R$ (a $G_{\alpha s}$ GPCR) with Istradefylline during fear extinction blocked within-session fear expression and enhanced fear extinction consolidation. We further examined the effect of pharmacological manipulation of D2R (a $G_{\alpha i/o}$ GPCR) using antagonist, Sulpiride. Antagonism of D2R during fear extinction enhanced fear expression and increased rate of extinction. Additionally, blockade of D2R following fear extinction disrupts extinction consolidation. Consistently, *Drd2* expression increases following extinction, but not fear conditioning, suggesting dopamine supports extinction through increases in inhibitory tone onto this population through D2R. The CeA *Drd2* expressing population consistently acts to support fear behavior and modulation of receptors on this population is sufficient to enhance or interfere with this role.

3.4 Results

Examination and Cell-Type Specific Manipulation of CeA *Drd2* Population.

Dopamine Receptor 1 (*Drd1*) and Dopamine Receptor 2 (*Drd2*) mRNA expression patterns were examined utilizing RNAScope *insitu* hybridization (Figure 1A-F). Dickkopf 3 (*Dkk3*) mRNA marks BLA neurons (Figure 1C). *Drd1* and *Drd2* mark large populations within the striatum. *Drd1* but not *Drd2* appears to be expressed at high levels within the intercalated cell nuclei (ITC). *Drd2* is strongly expressed in the CeC, CeL and at lower levels in the CeM, while *Drd1* is expressed in the CeM and largely spares the CeC and CeL. Sub-compartments of the CeA have differential roles in fear expression and learning; expression

of *Drd2* in the CeC and CeL suggests dopaminergic signaling may differentially regulate these regions during learning.

To determine the precise role of the *Drd2*-expressing population in fear behavior, we directly manipulated these neurons during behavior using DREADDs. Drd2-Cre (B6.FVB (Cg)-Tg (Drd2-Cre)ER43Gsat/Mmucd) mice were obtained and Cre-expressing experimental mice and non-Cre expressing littermate controls were infected bilaterally with a Cre-dependent Gs-coupled DREADD virus. Three weeks following infection, mice were mildly fear conditioned with 5 CS/US (0.4 mA US footshock) pairings to avoid ceiling effects (Figure 1G). Thirty-minutes prior to the extinction session (15 CS), all mice were injected with CNO (1 mg/kg, i.p. in saline). Mice that expressed Cre-recombinase and thus expressed Gs-DREADD in *Drd2* neurons exhibited significantly more freezing to the tone throughout the extinction session (Figure 1H). Importantly, 24 hours later, after a wash-out period (3-9 hours), Cre-recombinase expressing mice again displayed significantly more freezing to the tone than non-carrier controls during a 30-CS extinction retention session (Figure 1I). These data suggest that enhancing the excitability of *Drd2* neurons both enhances fear expression and blunts fear extinction consolidation. Gs-DREADD expression was visualized and pattern confirmed through the strong expression of mCherry tag (Figure 1K & 1L). The direct enhancement of excitability of *Drd2* neurons through genetically targeted Gs-DREADDs both increased fear expression and blunted fear extinction consolidation, suggesting that the *Drd2* population in the CeA supports fear.

Characterization of Dynamic mRNA Changes in *Drd2* Cells After Fear Conditioning.

To further characterize the *Drd2*-expressing population, we next examined expression changes in *Drd2* neurons following fear conditioning. To identify actively transcribed transcripts, TRAP was utilized. The Drd2-Cre mouse line was crossed with the floxed-stop-TRAP (B6.129S4-Gt (ROSA)26Sortm1 (CAG-EGFP/Rpl10a,-birA)Wtp/J)) line to generate a double transgenic line, DRD2-TRAP. These animals express the L10a-GFP transgene specifically in striatal, amygdalo-striatal transition, and CeA populations, recapitulating our observed expression patterns of *Drd2* (Figures 2A-B). Animals were next either fear conditioned to (5 CS/US, 0.65 mA) or exposed to tone and chamber in the absence of any US shocks. Fear conditioned animals exhibited increases in freezing (Supplemental Figure 1). Animals were sacrificed two hours following behavior, micropunches centered over the CeA were collected, and TRAP was performed to obtain isolated mRNA from *Drd2* neurons (Figure 2C). High quality RNA was retrieved from the TRAP protocol (RIN =8.5-10). To verify the specificity of RNA pull down, qPCR analysis of samples was performed to compare bound versus un-bound samples. Ribosomal subunit S18 was found at higher levels in the bound fraction compared to the unbound fraction, confirming enrichment for ribosomes (Supplemental Figure 2A). When expression levels of *Drd2* and *Drd1a* were compared in each fraction, the bound fraction had a larger enrichment for *Drd2* versus *Drd1a* when compared to the unbound fraction (Supplemental Figure 2B) (Oude-Ophuis, Boender, van Rozen, & Adan, 2014). These data suggest that ribosomes specifically expressed in *Drd2* neurons were successfully pulled down and that RNA collected from these pull-downs demonstrated expected characteristics of *Drd2* neurons.

Sequencing RNA collected from *Drd2* neuron ribosomes revealed genes dynamically regulated following fear conditioning, many of which have been previously reported to be involved in fear and anxiety-like behaviors (Figure 2D). FDR was calculated using 5% cut-off criteria. Fold-change cut-off was set at $2^{\wedge 0.5}$. Significantly changed genes were examined for the availability of high quality agonists or antagonists using the Drug-Gene Interaction Database (DGidb). Finally, genes were examined for expression patterns similar to *Drd2,* with the requirement of strong expression in CeC and CeL. Additional markers found to be modulated with fear learning included *Ador2a, Sst5r, Npy5r, Fgf3, ErbB4, Gpr6, Fkbp14, Dlk1* and *Ssh3.* Of significantly regulated genes with available targeted pharmacological modulators, *Ador2a* was upregulated following fear conditioning and exhibited an expression pattern nearly identical to that of *Drd2*; therefore, it was chosen for further examination (Figure 2E, Image Credit: Allen Institute (Ed S Lein et al., 2007)).

Manipulation of A_{2A} Receptor During Fear Behavior.

To examine the role of the $A_{2A}R$ ($G_{\alpha s}$ coupled GPCR) in behavior, its activity was manipulated during fear behavior. The highly selective $A_{2A}R$ antagonist, Istradefylline, is selective for $A_{2A}R$ over A_1 Receptor with a Ki of 2.2 and 150 nM respectively. Additionally, Istradefylline is a potential anti-Parkinsonian drug treatment currently being tested for use in human populations. For these experiments, mice were first fear conditioned (5 CS/US, .65mA) (Figure 3A). Twenty-four hours later, mice were injected with either vehicle (10% DMSO, 1% NP-40 in saline i.p.) or Istradefylline (3mg/kg) 30 minutes prior to the extinction session. Mice that were treated with Istradefylline expressed significant reductions in freezing throughout the extinction session (Figure 3B). The next day when mice were tested for fear extinction retention, those that received Istradefylline during the

previous session expressed less freezing during the 30-CS session, suggesting that treatment with Istradefylline prior to extinction enhanced fear extinction consolidation (Figure 3C). Importantly, when animals were treated with vehicle or Istradefylline 30 minutes prior to a 10 minute open-field test, those that received drug treatment displayed no changes in anxiety-like behavior as measured by time in the center; however, drug-treated animals did exhibit increased locomotion as measured by distance traveled (Figure 3D & 3E). Locomotor changes are expected as this drug is used to treat Parkinsonism by increasing activity in indirect pathway D2 expressing neurons.; however, locomotor effects are unlikely to affect extinction consolidation and the extinction retention test was performed after drug wash-out. These results suggest that the direct antagonism of the $A_{2A}R$, which we predict to decrease *Drd2*-cell activity, may block fear expression and enhance fear extinction consolidation – the opposite effects observed with the Gs-DREADD stimulation of *Drd2*-cell activity above.

Examination of Role of D2R in Fear Learning and Extinction.

To examine the role of D2R in fear learning, we next utilized the D2R antagonist, sulpiride. Sulpiride is a commonly prescribed treatment for anxiety, depression and schizophrenia. Naïve mice were fear conditioned (5CS/US, .65 mA) and injected with sulpiride (10 mg/kg, i.p.) or vehicle (5% DMSO in saline) immediately following fear conditioning. Twenty-four hours later, mice were tested for expression of fear (Figure 4A). Mice that previously received i.p. injections of Sulpiride expressed more freezing during the first session of fear extinction, suggesting that this group more strongly consolidated fear learning.

To examine the role of D2R on the expression of learned fear, mice were fear conditioned (5 CS/US, .65mA) (Figure 4B). Twenty-four hours following the conditioning session, mice underwent fear extinction (15 CS). Thirty-minutes prior to the fear extinction session, mice were given an injection of sulpiride (10 mg/ kg, i.p.) or vehicle (5% DMSO) (Figure 4C). Mice that received sulpiride prior to extinction expressed significantly more fear during first block of fear extinction than controls, suggesting that the acute blockade of D2R enhances fear expression. Interestingly, during the extinction session, mice that were administered sulpiride demonstrated enhancement of both amount and rate of extinction compared to vehicle-injected controls (Figure 4C & Supplemental Figure 3). Enhancement of within-session extinction learning suggests that antagonism of D2R during extinction may change prediction error processing, perhaps due to initial higher rates of fear expression. No differences were detected during the second extinction session 24-hours later, though this may be due to signal loss from a behavioral floor effect (Figure 4D).

Dynamic Regulation of *Drd2* After Fear Extinction.

Drd2 expression was not significantly changed after fear conditioning in Drd2 neurons; however, it appears D2R is involved in the control and consolidation of fear and extinction learning. Therefore, *Drd2* was examined for dynamic regulation after fear extinction. Four groups of animals were trained: 1) home cage (HC), 2) 30 CS (HC30) (tone exposure alone), 3) Fear Conditioning (FC1) (5CS/US, .65mA), 4) Fear Extinction (FC30) (5 CS/US, .65mA followed 24 hours later by 30 CS extinction). FC1 group was exposed to the extinction context and a single tone in order to verify that extinction, and not exposure to a novel context and tone, is responsible for changes in *Drd2* expression. Both the FC1 and FC30 groups expressed more freezing than the HC30 control group (Figure 5A). Each

cohort of mice was sacrificed 2 hours following behavioral testing, RNAs were isolated from 1 mm micropunch centered over CeA and *Drd2* expression levels were examined via qPCR. *Drd2* mRNA expression was significantly increased in the extinction group when compared to all other groups and no change was found in either HC30 or FC1 groups compared to HC group (Figure 5B). These data demonstrate that *Drd2* mRNA is dynamically regulated after fear extinction, but not fear conditioning.

Examination of Role of D2R in Consolidation of Extinction Learning.

To further examine the role of D2R in fear extinction consolidation in a mouse model of PTSD, mice were strongly fear conditioned (5CS/US, 1mA) in Context A. One week later mice were strongly fear conditioned a second time (5CS/US, 1mA) in Context A. The next day mice were matched for fear expression to 3 CS presentations in a novel context (Context B) in order to create two groups with equivalent freezing. Mice were then, 24-hours later, fear extinguished in Context B (15 CS) (Figure 5C). Directly following extinction, mice were given injections of vehicle or Sulpiride (10mg/kg, i.p.). The next day fear renewal was measured by extinguishing mice (15 CS) in a third novel context, Context C. Interestingly, during the fear renewal test animals that had been given injections of Sulpiride following extinction in Context B exhibited enhanced freezing during session compared vehicle group as well as enhanced freezing compared to the same group the previous day during extinction in Context B (Figure 5D). Directly following fear renewal animals were given i.p. injections of Sulpiride. The next day animals were extinguished (15 CS) again in context C and given i.p. injections of Sulpiride directly following the extinction session (Figure 5E). Enhanced expression of freezing was maintained in the Sulpiride group when compared to the vehicle injected group during this session. Finally, animals

were tested for extinction retention with a final fear extinction session (15CS) in Context C. The Sulpiride injected group displayed enhanced freezing when compared to vehicle injected group on the third day of extinction in Context C (Figure 5F). Interestingly the vehicle group expressed significant extinction, as measured by reduced levels of freezing, when compared to Extinction 1 in Context C while the Sulpiride injected group showed no significant decreases in freezing over the course of 3 extinction sessions. These results suggest that the blockade of D2R during fear extinction consolidation disrupts extinction consolidation and may enhance fear renewal in a non-extinguished context.

3.5 Discussion

The currently described experiments: 1) examine the distribution of *Drd2* expressing neurons and the effects of direct chemogenetic manipulation of *Drd2* expressing neurons on fear expression, 2) characterize cell-type specific transcriptional changes following fear conditioning and identifies many dynamically regulated genes, 3) demonstrate that direct antagonism of $A_{2A}R$ blocks fear expression and enhances extinction, and 4) demonstrate that *Drd2* is dynamically expressed following fear extinction and examine the effects of manipulation of this receptor on fear learning and expression. The presented data represent an in-depth profiling of the role of CeA *Drd2* neurons in fear and extinction learning.

Overall, the behavioral data are remarkably consistent suggesting that activation of the *Drd2* neuronal population via Gs–DREADD activation or inhibition of D2R ($G_{\alpha i}$), increases fear expression and interferes with fear extinction consolidation. In contrast, decreasing activity of this population by antagonizing $A_{2A}R$ ($G_{\alpha s}$), decreases fear expression and enhances extinction. Furthermore, the dynamic increase in *Drd2* gene expression

following fear extinction may directly support this process by furthering the fear-inhibitory effects of dopamine modulation on CeA function. Interestingly, these results closely mirror findings (now in clinical trial) in mice and humans demonstrating that post-extinction treatment with L-DOPA enhances the consolidation of extinction learning (J. Haaker, Lonsdorf, & Kalisch, 2015; Jan Haaker et al., 2013). Additionally, L-DOPA enhances generalized fear extinction while D2R blockade instigates generalized enhancement of fear (increased renewal) suggesting opposing mechanisms. These effect may be facilitated through a similar circuit where enhanced DA signaling increases inhibition of CeA *Drd2* neurons through D2R.

Previous publications have provided extensive evidence for diverse roles of dopamine including decision making, prediction error, stimulus salience and addiction; however, less is known about its role in fear processing. By bypassing the complex roles of the D2R, examination of cell-type specific behavioral profiling of CeA *Drd2* neurons establishes a foundational knowledge of the function of this cell population against which pharmacological manipulations may be compared. Furthermore, profiling changes in RNAs being actively transcribed utilizing TRAP provides a unique look at the acute responses of these neurons to a learning event. The genes identified in the present set of experiments provide valuable avenues for future study. Several genes including *Adora2a, Sst5r, Npy5r, Fgf3* and *ErbB4,* have been directly implicated or are in well-established signaling pathways implicated in control of fear learning. Others such as *Gpr6, Fkbp14, Parva, Dlk1* and *Ssh3* have not been studied in the context of fear biology, but may provide valuable insights upon further investigation. Interestingly, several of these genes, most prominently *Adora2a* and *SstR5*, have been implicated in human anxiety disorders (Hohoff et al., 2010;

Saus et al., 2010). $A_{2A}R$ is known to be co-expressed with D2R and these receptors have been shown to have opposing actions, consistent with the behavioral results we find here, suggesting that both receptors may be viable candidates for modulation of a single sub-population (Aoyama, Kase, & Borrelli, 2000; Oude Ophuis, Boender, van Rozen, & Adan, 2014).

The acute enhancement of activity in CeA *Drd2* neurons using Gs-*DREADD* demonstrates that as a population, these neurons support the expression of fear, and consequently, activity in these neurons opposes the consolidation of extinction memories. Consistently, antagonism of the $A_{2A}R$, ($G_{\alpha s}$) suppresses fear expression and enhances fear extinction consolidation, ostensibly by reducing excitability of these neurons. Also, antagonism of D2R prior to extinction acutely enhances fear expression (first 3 CS of the extinction session). D2R blockade following behavioral training enhances consolidation of fear conditioning and blocks consolidation of fear extinction suggesting that increasing excitability in *Drd2* neurons drives mice towards high fear condition. These results are complicated by the observation that D2R antagonism during extinction also enhances the rate of fear extinction. Having antagonist on-board during learning may enhance prediction error or modify the valence of a CS dynamically, while antagonism exclusively during consolidation more specifically modifies the consolidation processes. For all pharmacological studies, as injections were given systemically and both $A_{2A}R$ and D2R are expressed in additional structures outside the amygdala, behavioral effects are complicated by extra-amygdalar receptor antagonism and requires further study.

Acute increases and decreases in locomotion with global $A_{2A}R$ and D2R antagonism, are consistent with reports in the literature and expected as manipulation of the indirect

pathway is a common treatment for Parkinsonism (Aoyama et al., 2000; Ponnusamy et al., 2005). The absence of effects on anxiety-like behavior and the presence of changes in extinction consolidation with the $A_{2A}R$ antagonist Istradefylline suggest that changes in freezing are due to changes in behavioral state and not due entirely to locomotor changes. These results are also consistent with reports that $A_{2A}R$ antagonism with SCH58261 produces deficits in contextual fear conditioning (Simoes et al., 2016).

Activity in *Drd2* expressing neurons appear to primarily have a fear-on function, supporting fear expression and blunting fear extinction. Consistently, enhancing excitability via D2R blockade enhances fear learning consolidation and blocks fear extinction consolidation; conversely, diminishing excitability via $A_{2A}R$ blockade reduces fear expression and enhances extinction consolidation. Furthermore, *Drd2* mRNA expression is increased following fear extinction but not fear conditioning consistent with enhanced DA signaling through this receptor facilitating inhibition of fear following extinction.

3.6 Methods

Animals

C57BL/6J mice were obtained from Jackson Laboratories (Bar Harbor, ME). B6.FVB (Cg)-Tg (Drd2-Cre)ER43Gsat/Mmucd mice were obtained from the MMRRC and produced as part of the GENSAT BAC Transgenic Project. Rosa26 fs-TRAP (B6.129S4-Gt (ROSA)26Sortm1 (CAG-EGFP/Rpl10a,-birA)Wtp/J) were obtained from Jackson Laboratories. Drd2-TRAP mice were generated by crossing Drd2-Cre and Rosa26 fs-TRAP lines. All mice were adult (8-12 week) at time of behavior. All mice were group housed and maintained on a

12hr:12hr light:dark cycle. Mice were housed in a temperature-controlled colony and given unrestricted access to food and water. All procedures performed conformed to National Institutes of Health guidelines and were approved by Emory University Institutional Animal Care and use Committee.

Surgical Procedures

Mice were deeply anesthetized with Ketamine/ Dexdormitor (medetomidine) mixture and heads fixed into stereotaxic instrument (Kopf Instruments). Stereotaxic coordinates were identified from Paxinos and Franklin (2004) and heads were leveled using lambda and bregma. For viral delivery (Figure 4), a 10µl microsyringe (Hamilton) was lowered to coordinates just above BLA and .5 µl of virus solution was infused at .1µl/min using microsyringe pump. Virus solution contained purified AAV_5-hSyn-DIO-rM3D (Gs)-mCherry (UNC Viral Vector Core). After infusion, syringes rested at injection for 15 min then slowly were withdrawn. After bilateral infusion, incisions were sutured closed using nylon monofilament (Ethicon). For all surgeries, body temperature was maintained using a heating pad. After completion of surgery, anesthesia was reversed using Antisedan (atipamezole) and mice were allowed to recover on heating pads.

Drug Administration

Clozapine-N-Oxide (Sigma) was diluted in sterile saline and administered at 1mg/kg i.p. 30 minutes prior to behavioral testing. Sulpiride (Tocris) was dissolved in pure DMSO and diluted to 5% DMSO in saline immediately prior to i.p. administration at 10 mg/kg. Istradefylline was dissolved in DMSO and diluted to 10% DMSO, 1% NP-40 in sterile saline immediately prior to i.p. administration at 3mg/kg.

Behavioral Assays

Auditory Cue-Dependent Fear Conditioning

Mice were habituated to fear conditioning chambers (Med Associates Inc., St Albans, VT) for 10 minutes each of two days prior to fear conditioning. Mice were conditioned to five (30s, 6kHz, 65-70db) co-terminating with a foot shock (1s, .65mA or .4mA for mild conditioning).

Auditory Cue-Dependent Fear and Extinction

Cue-dependent fear extinction was tested 24-hours after fear conditioning and extinction retention occurred 24-hours after fear expression. For extinction, mice were placed in a novel context and exposed to 15 or 30, 30-second tones with an inter-trial-interval of 60 seconds. Freezing was measured using Freeze View software (Coulbourn Instruments Inc., Whitehall, PA).

Open Field

Open field chambers (Med Associates) were placed in a dimly lit room. Mice were placed in the chamber for 10 minutes and allowed to explore.

Brain Collection Following Behavior

Examination of changes in *Drd2* expression following behavior experiment included 4 groups 1) a Home Cage control group that remained in their home cage throughout the experiment; 2) the primary experimental group (FC30) which was trained with five 6kHz, 70-75dB, 30-second tones, coterminating with the delivery of a 1 second, 1 mA shock unconditioned stimulus (US). Twenty-four hours later, these mice were given extinction training in which they were placed in a novel context (differing in olfactory cue, lighting

and flooring) and exposed to 30 CS presentations; 3) a group (HC30) that remained in the home cage during training but was exposed to the same 30 tone presentations as the FC30 group and 4) a group (FC1) that was fear conditioned as in the FC30 group but only exposed to one tone twenty four hours later. Brains were extracted 2 hours after fear extinction or tone exposure. Brains from HC control animals were also extracted during this time.

Real Time PCR

RNA was reverse transcribed using SuperScript 4 (Invitrogen). Quantitative PCR was performed on cDNA with each sample run in triplicate technical replicates. Reactions contained 12µl Taqman Gene Expression Master Mix (Applied Biosystems), 1µl of forward and reverse primer, 1 µl of 5ng/ul cDNA, and 6 µl water. Primers were proprietary FAM labeled probes from Life Technologies. Quantification of qPCR was performed on Applied Biosystems 7500 Real-Time PCR System. Cycling parameters were 10 minutes at 95°C, 40 cycles of amplification of 15s at 95°C and 60s at 60°C, and a dissociation step of 15s 95°C, 60s at 60°C, 15s 95°C. Fold changes were calculated as ΔΔCT values normalized to levels of GAPGH mRNA. Values presented as fold change +/- s.e.m.

RNA-Seq Library Preparation

Libraries were generated from 1 ng of Total RNA using the SMARTer HV kit (Clonetech), barcoding and sequencing primers were added using NexteraXT DNA kit. Libraries were validated by microelectrophoresis, quantified, pooled and clustered on Illumina TruSeq v3 flowcell. Clustered flowcell was sequenced on an Illumina HiSeq 1000 in 50-base paired end reactions.

Analysis of RNA Sequencing Data

RNA sequencing data was analyzed using Tuxedo DESeq analysis software. Differential expression between HC and FC groups were obtained and used for further analysis. Using the q value of less than .05 as a cut-off, only highly significant returns were used for further analysis. To ensure that genes had a large enough difference in expression to warrant pharmacological manipulation, only those with differences in expression greater than $2^{.5}$ or ~141% were considered. Next using the 'Drug Gene Interaction Database' returns were examined for having a known pharmacological agent that modifies its activity. Genes lacking viable pharmacological modulators were eliminated.

Translating Ribosome Affinity Purification

TRAP procedure was completed as described in Heintz et. al., (2014) (Myriam Heiman et al., 2014). Adult Drd2-TRAP mice were anesthetized, their brains removed and snap frozen. Bilateral 1mm punches were collected and pooled from 3 animals per sample (n= 3 and 4). Messenger RNA was isolated from eGFP-tagged ribosomes, as described in reference. RNA was assessed for quality using the Bioanalyzer Pico (Agilent, Santa Clara, CA). All samples returned RINs (RNA Integrity Numbers) of 8.5 or greater.

Statistics

Statistical analyses were performed using Prism 6 by Graph Pad. All data presented as mean +/- s.e.m. Fear extinction experiments were examined using a repeated-measures ANOVA with drug as the between-subjects factor and tone presentation as the within subject factor. Open field activity (time in center and distance traveled) was compared using a Students t test between drug infused and vehicle groups. For examination of fear

expression (4A, 4C) first bin of freezing during extinction CS presentations were compared using students t-test between drug and vehicle treated groups. For experiments examining presence of significant extinction (4C) first and last bins of CS presentations were compared using Student's t-test. For experiment examining rate of extinction (Supplementary 3) linear regressions were performed and resultant slopes compared. For qPCR delta delta CT's of data were compared by Students t-test between bound and unbound fractions. For all tests statistical significance was set at $p < .05$.

RNA Scope Staining

Staining for RNA of interest was accomplished using RNA Scope Fluorescent Multiplex 2.5 labeling kit. Probes utilized for staining are: mm-Nts-C1, mmNts-C2, mm-Tac2-C2, mm-Sst-C1, mm-Sst-C2, mm-Crh-C1, mm,Prkcd-C1, mm-Prkcd-C3, mmDrd2-C3. Brains were extracted and snap-frozen in methyl-butane on dry ice. Sections were taken at a width of 16μm. Procedure was completed to manufacturers specifications.

Image Acquisition

Images were acquired with experimenter blinded to probes used. Sixteen-bit images of staining was acquired on a Leica SP8 confocal microscope using a 10x objective. Within a sample images were acquired with identical settings for laser power, detector gain, and amplifier offset. Images were acquired as a z-stack of 10 steps of .5 μm each. Max intensity projections were then created and analyzed.

3.7 Figures

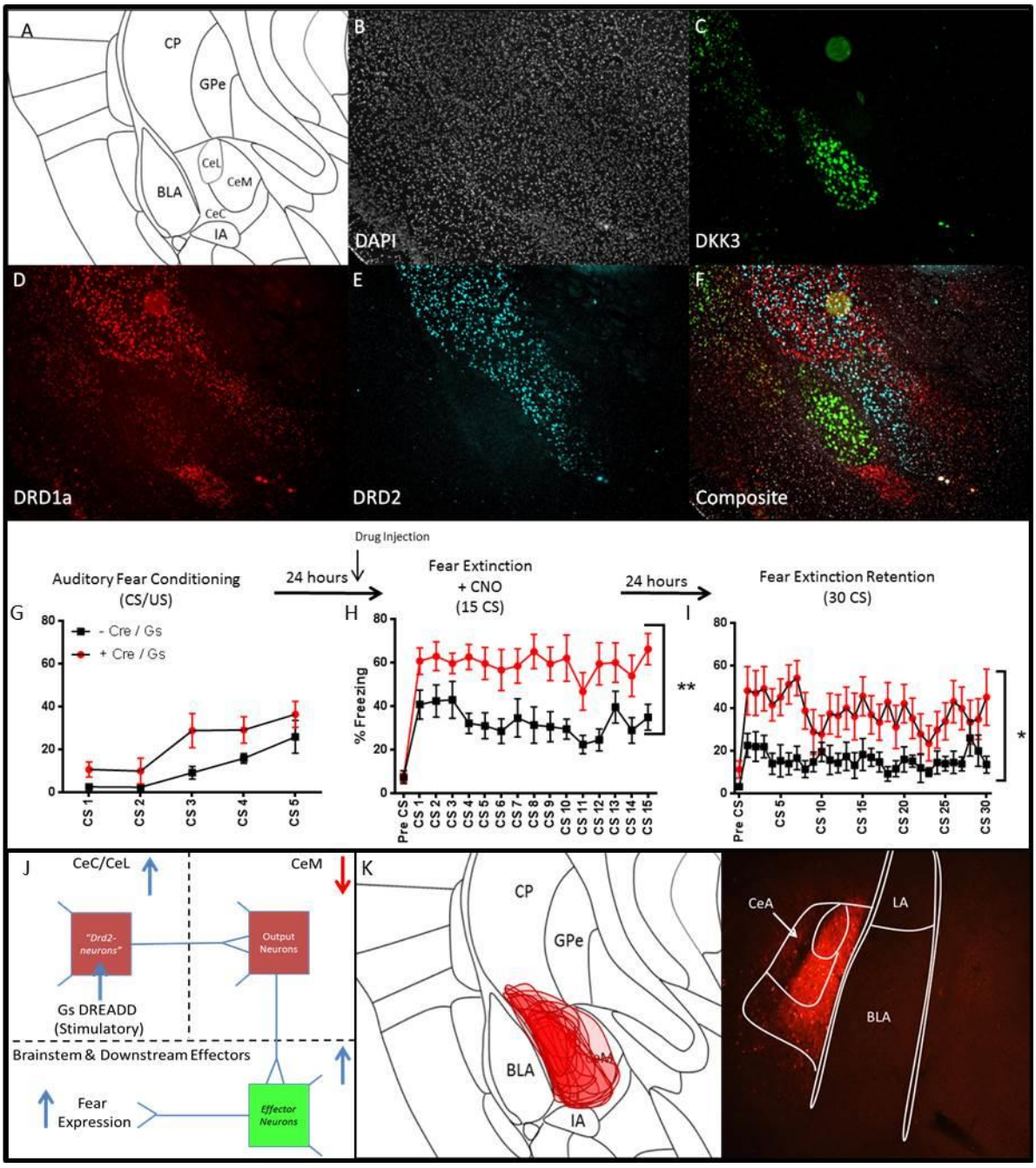

Figure 3-1. Examination and cell-type specific manipulation of CeA *Drd2* population.

Expression patterns of *Dkk3, Drd1a,* and Drd2 examined using RNAScope *insitu* hybridization and direct chemogenetic manipulation of *Drd2* neurons. **A**. Schematic of

temporal lobe. **B**. DAPI (Grey). **C**. Dkk3 (Green) is expressed in BLA. **D**. Drd1a (Red) is expressed in striatum, amygdalo-striatal transition areas, ITCs especially Im, CeM and MeA, but not CeC or CeL. **E**. *Drd2* (Cyan) is expressed in striatum, amygdalo-striatal transition areas, CeC, CeL and CeM, but not ITCs or MeA. **F**. Composite of labeling of targets in B-E. Scale Bar =200 um. Enhancing excitability of *Drd2* neurons with Gs-DREADD enhances fear expression and blocks fear extinction consolidation. **G**. Drd2-Cre positive and Cre-negative littermates were infused with AAV-hSyn-DIO-rM3D (Gs)-mCherry and fear conditioned to 5 CS/US pairings three weeks later. **H**. Mice were injected i.p. with CNO 30-minutes prior to fear expression session. Mice expressing Cre-recombinase and thus Gs-DREADD-mCherry expressed significantly more fear during entire extinction session than non-carrier controls (RM ANOVA $F(1,18)= 11.49$, ** $p < .01$). **I.** Mice expressing Gs-DREADD-mCherry expressed significantly more fear 24-hours later during extinction retention session suggesting enhancement of excitability during fear extinction resulted in deficits in fear extinction consolidation (RM ANOVA $F(1,18)= 7.512$, * $p < .05$). **J**. Hypothetical schematic for circuit mechanism by which Gs-DREADD activation of Drd2 neurons may enhance fear expression. **K**. Collapsed over-lay of expression pattern of mCherry for Cre-expressing experimental animals. Expression is generally constrained to CeC and CeL with limited expression in CeM. **L**. Representative expression pattern of mCherry-tag expression in Drd2 amygdala. Scale Bar =200 um.

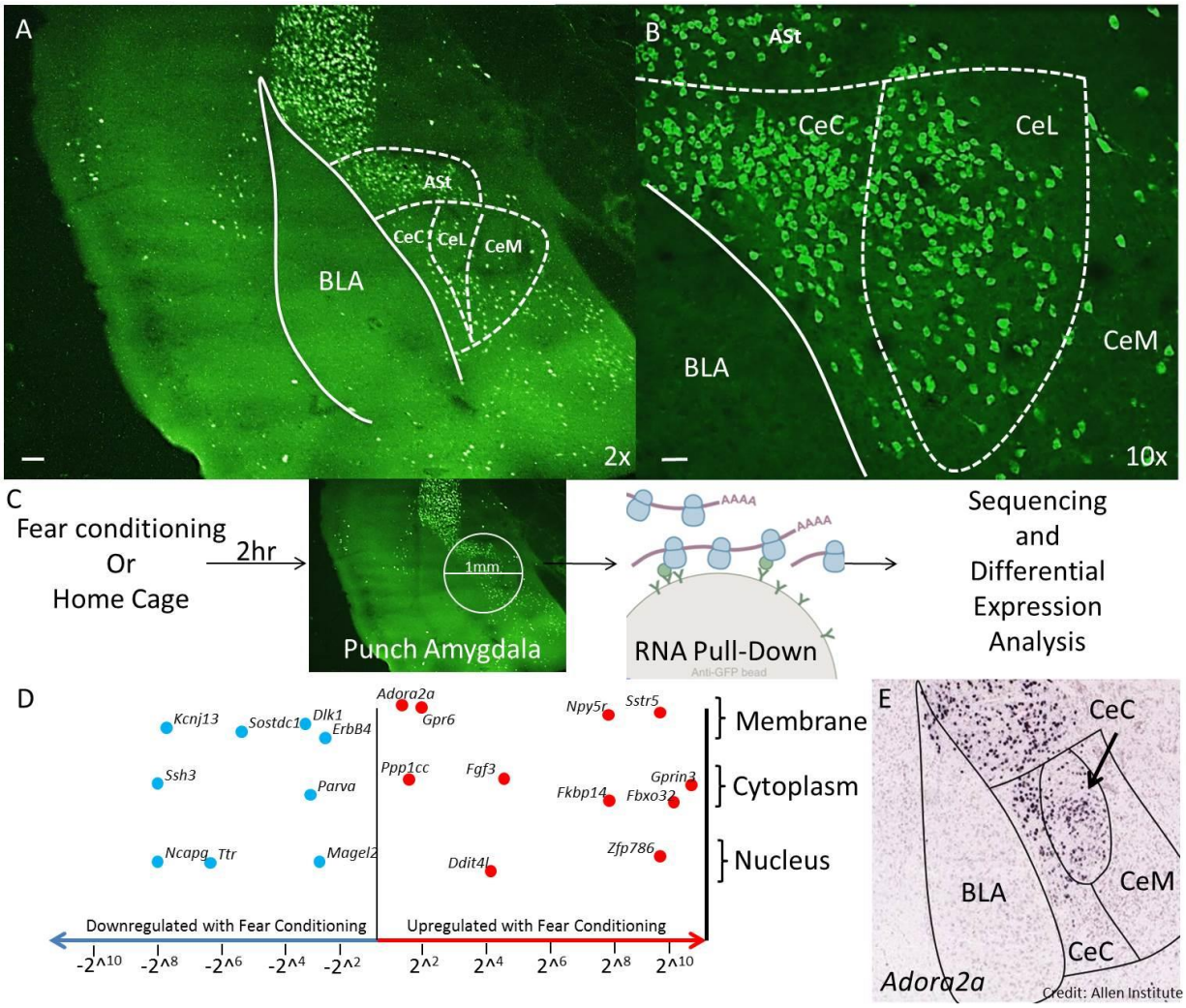

Figure 3-2. Examination of cell-type specific mRNA changes after fear conditioning.

Breeding *Drd2*-Cre line with Floxed-stop-EGFP-L10A line yields double transgenic Drd2-TRAP line. **A.** and **B.** Drd2-TRAP line has robust transgene expression (green) in striatum, amygdalo-striatal transition area (ASt), CeC, CeL and to a lesser extent CeM. This expression pattern is consistent with mRNA expression pattern found via *insitu* hybridization. Scale Bar =100 um & 20um **C.** Work-flow for TRAP following behavior. Animals are fear conditioned to 5CS/US pairings (.65 mA). Two hours following the end of behavior, mice are sacrificed and brains are collected. Punches (1mm) centered over CeA

are collected and TRAP protocol is performed on tissue. EGFP tagged ribosomal subunits are pulled down and bound RNAs are eluted. Collected RNA is sequenced and differential expression analysis is completed. **D.** Differential expression analysis comparing RNAs pulled down for fear conditioned vs. home cage control animals reveals a number of genes that are either upregulated or down regulated following behavior. **E** *Adora2a,* coding for $A_{2A}R$, was found to be upregulated following behavior and has an expression pattern similar to that of *Drd2* (Image credit: Allen Institute).

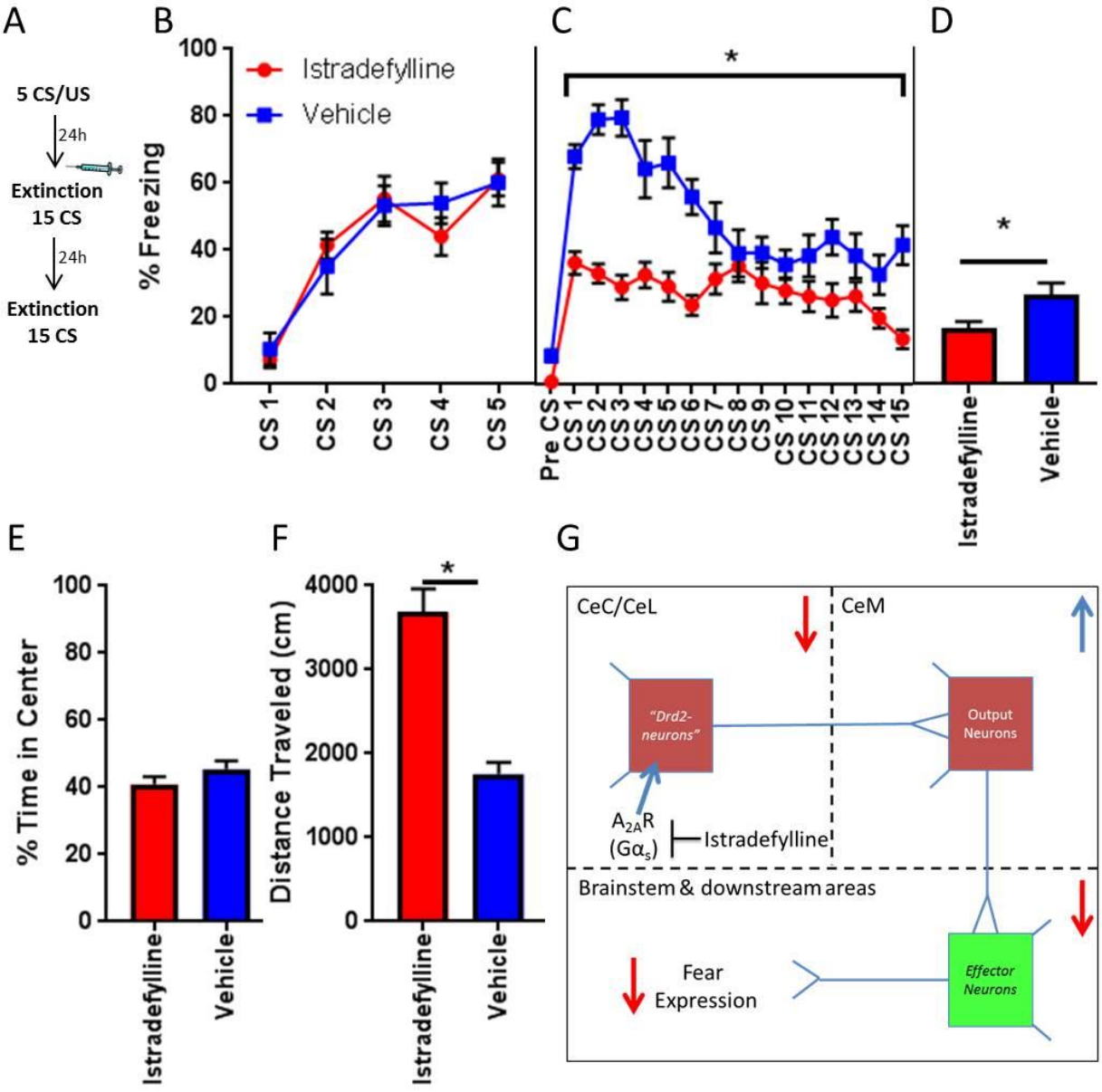

Figure 3-3. Selective blockade of $A_{2A}R$ blunts fear expression and enhances extinction consolidation.

$A_{2A}R$, a $G_{\alpha s}$ coupled GPCR, is dynamically upregulated following fear condition and antagonism of this receptor with the selective $A_{2A}R$ antagonist, Istradefylline, may oppose expression of learned fear. **A.** Behavioral schema. **B.** Cohorts of mice were fear conditioned to 5 CS/US pairings, .65 mA. **C.** Mice were injected with (3mg/kg, i.p.) Istradefylline 30

minutes before the fear extinction session. Within-extinction session, mice express significantly less freezing to tone than vehicle injected controls (RM ANOVA F (1,18)=27.94, *p<.0001). **D.** Mice that were previously injected with Istradefylline prior to the extinction session express significantly less freezing to the tone during the extinction retention session (30 CS) 24-hours later (RM ANOVA F (1,18)=5.955, * p <.05). This suggests that $A_{2A}R$ antagonism enhances the consolidation of extinction learning. **E.** Istradefylline produces no anxiety-like behavior as measured by time spent in the center of an open field compared to vehicle-injected controls when injected 30-minutes prior to a 10-minute open-field test. **F**. Istradefylline produces increases in locomotion as measured by distance traveled compared to vehicle injected controls when injected 30-minuted prior to a 10 minute open-field test (unpaired t-Test, * p < .001). **G.** Hypothetical schematic of how antagonism of $A_{2A}R$ may lead to decreases in fear expression.

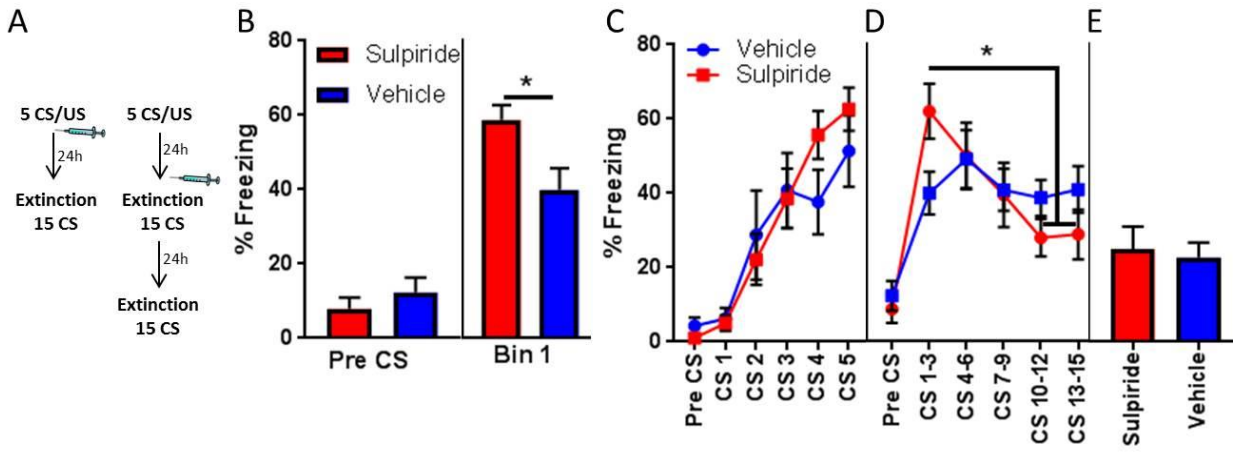

Figure 3-4. Blockade of Drd2 during extinction with common psychosis and MDD treatment, Sulpiride, enhances fear expression and within session extinction.

A. Behavioral Schema. **B.** Post fear conditioning injections of sulpiride leads to enhanced fear consolidation as measured by enhanced freezing during first block of CSs during fear extinction test 24-hours later (unpaired t-Test * = p< .05). **C.** Cohorts of mice are fear conditionined to 5 CS/US pairings. **D.** I.p. injection of sulpiride 30 miunutes before fear extinction session leads to enhanced freezing during first block of CS presentations (unpaired t-Test, * p < .05). Injection of sulpiride also enhances within-session extinction as experimnetal group exhibits significant reductions in freezing blocks 4 & 5 compared to block 1 (unpaired t-Test vs. 1^{st} bin *= p < .05). No changes in fear expression across session is observed in vehicle injected group. **E.** Pre-extinction injection of sulpiride causes no changes in the consolidation of extinction as measured 24 hours later during extinction retention session.

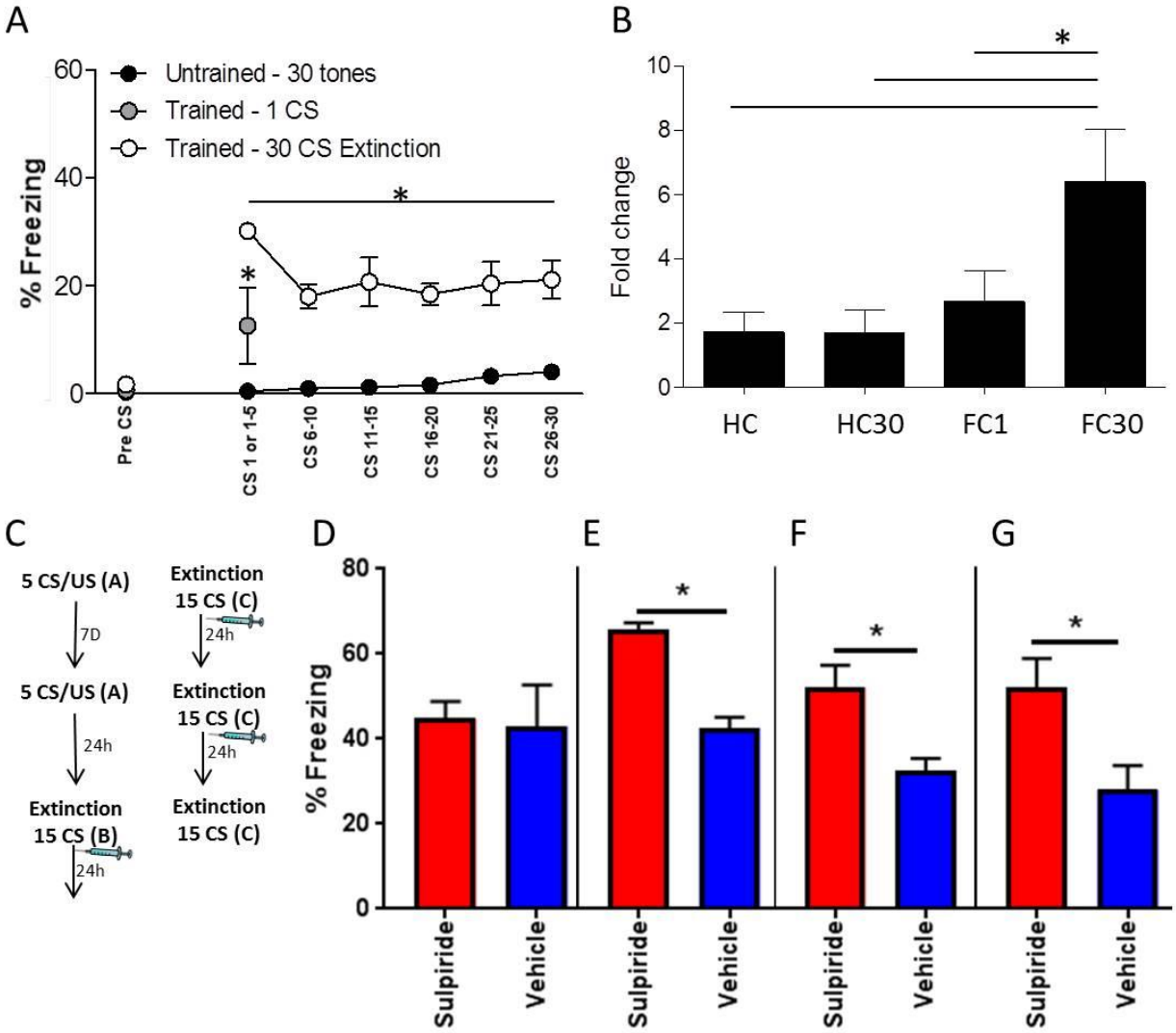

Figure 3-5. Dynamic role of Drd2 during fear extinction.

Drd2 mRNA is dynamically regulated following extinction. Antagonism of this receptor during extinction consolidation enhances fear renewal in an alternate context and blocks extinction consolidation. **A**. Four cohorts of animal were sacrificed two hours following behavior. 1) Homecage animals (HC, n=6) were sacrificed directly from homecage, 2) Homecage 30 (HC30, n=7) animals were exposed to training and extinction CSs without any US pairs, 3) Fear conditioned (FC1, n=7) animals were fear conditioned, exposed to the fear extinction context

and a single unpaired CS, 4) Extinguished (FC30, n=7) animals were fear conditioned and extinguished to 30 CSs. No significant within-subjects effect was found during fear extinction ($F(4, 48) = 32.21$, $p > 0.05$) with no significant group difference $F(1,12)=1.72$, $p > 0.05$) for the fear conditioned groups (FC1 and FC30). **B.** Quantitative RT-PCR data showing the mean Ct values ± s.e.m. normalized to GAPDH across different conditions (unpaired t-Test vs FC30, * $p < .05$). Blockade of D2/D3R during the consolidation period following extinction enhances fear renewal to tone in alternate context. Additionally, repeated Sulpiride adiministration following extinction in same context blocks fear extinction consolidation. **C**. Behavioral Schema. Following two strong fear conditioning sessions (context A) and an expression match session (3 CS in Context B), animals are fear extinguished to 15 CS in Context B. Fear renewal is measured twenty-four hours later via 15 CS extinction session in Context C immediately followed by i.p. injection of sulpiride. Two additional extinction sessions followed by sulpiride injections were performed on subsequent days. **D.** Animals express no differences in freezing during expression session in Context B. **E.** In alternate context C, animals previously injected with sulpiride express more freezing than control animals (RM ANOVA $F(1,11)=69.36$, * $p< .0001$). **E.** During second extinction session in context C, experimental animals continue to express enhanced freezing compared to controls (RM ANOVA $F(1,11)=10.04$, * $p < .01$). **F.** During third exitinction session in context C experimental animals continue to express enhanced freezing compared to controls (RM ANOVA $F(1,11)=6.829$, * $p< .05$). Additionally, control animals express significant extinction compared to first context C training session (RM ANOVA $F(1,10)=4.366$, *$p < .05$), while sulpiride treated animals exhibit no fear extinciton.

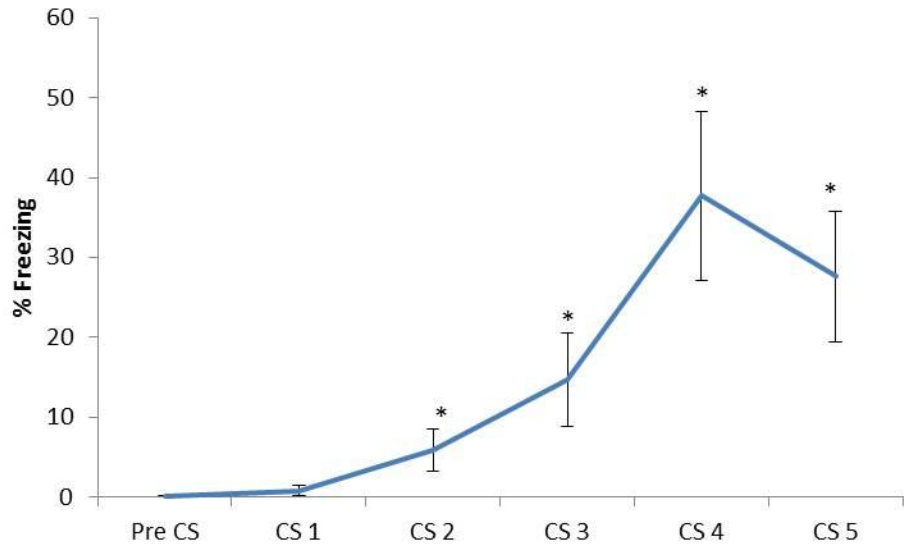

Supplemental Figure 3-1. Fear conditioning of mice for TRAP collection.

Mice express significantly more freezing after fear conditioning. (Unpaired t-Test vs CS 1, * = $p < .05$)

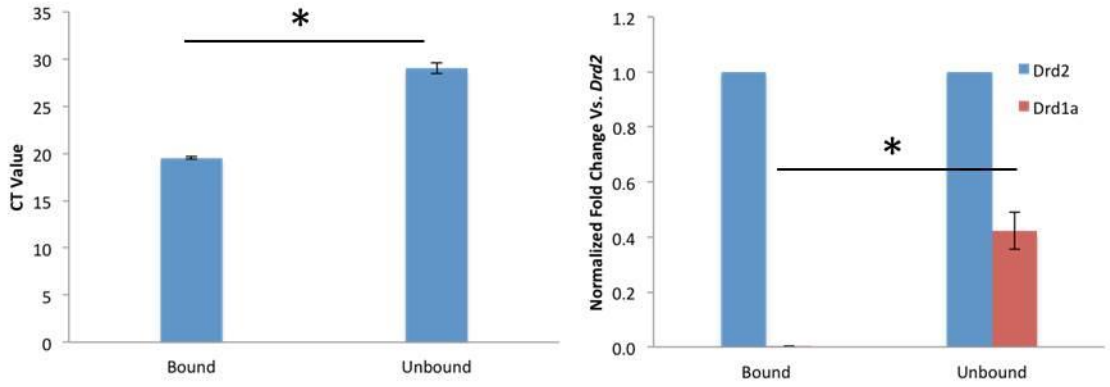

Supplemental Figure 3-2. Validation of TRAP pull-down.

A. Ribosomal subunit 18S is found at significantly higher levels in bound fraction verifying ribosomal pull down (Paired t-Test, * $p < .05$). **B**. The ratio of *Drd2:Drd1a* is significantly

higher in bound fraction vs. unbound fraction verifying RNA's were successfully isolated from Drd2 neurons (Paired t-Test, * p< .05).

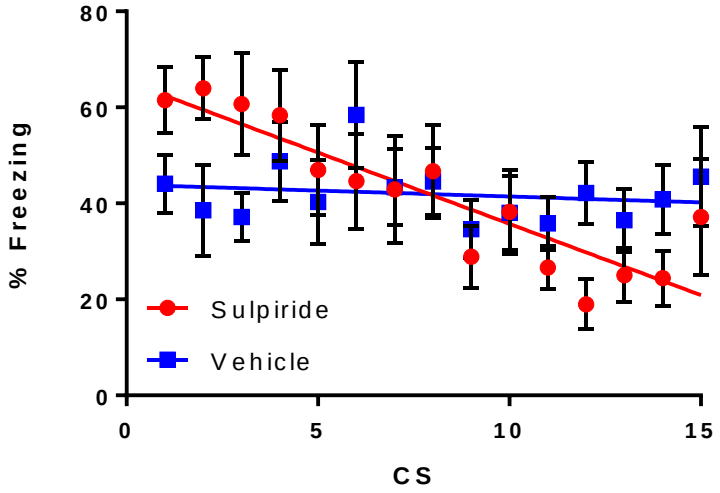

Supplemental Figure 3-3. Sulpiride effects on fear extinction rate.

Rate of extinction following sulpiride injection. **A.** Linear regression analysis reveals a significant reduction of freezing in Sulpiride injected group with CS presentations ($F(1, 14) = 50$, $p < .0001$) with $R^2 = .79$, while no interaction was found in vehicle injected group ($F(1, 14) = .44$, p=n.s.)) with $R^2 = .03$. Slopes of two groups were significantly different with ($F(1,26)$ 24, $p < .0001$).

Chapter 4: Molecular Characterization of a 'Fear-Off' Neuronal Population within the Basolateral Amygdala.

4.1 Context, Author's Contribution and Acknowledgement of Reproduction.

The following chapter is an effort to examine the Thy-1 population of the basolateral amygdala (BLA). This population was behaviorally characterized through direct manipulation using optogenetics and chemogenetics. Molecular examination of this population described how its RNA content differs from other neurons in the area. Using this data we were able to further molecularly characterize and recapitulate behavioral profiles through pharmacological manipulations. The dissertation author contributed to the paper by designing and running experiments, analyzing the data, and was the main contributor to the writing of the paper. The chapter is reproduced from McCullough K.M., Choi. D.C., Guo. J, Zimmerman. K., Walton. J. Rainnie. D. & Ressler K.J. Co-Expression Analysis of CeA Sub-Populations. *Nature Communications (2016)*

4.2 Abstract.

Molecular characterization of neuron populations, particularly those controlling threat responses, is essential for understanding the cellular basis of behavior and identifying pharmacological agents acting selectively on fear-controlling circuitry. Here we demonstrate a comprehensive work-flow for identification of pharmacologically tractable markers of behaviorally characterized cell populations. Thy1-eNpHR, Thy1-Cre and Thy1-eYFP labeled neurons of the BLA consistently act as fear inhibiting or 'Fear-Off' neurons during behavior. We use cell-type specific optogenetics and chemogenetics (DREADDs) to modulate activity in this population during behavior to block or enhance fear extinction. Dissociated Thy1-eYFP neurons are isolated using FACS. RNA sequencing identifies genes strongly upregulated in RNA of this population including *Ntsr2, Dkk3, Rspo2,* and *Wnt7a*. Pharmacological manipulation of Neurotensin Receptor 2 confirms behavioral effects

observed in optogenetic and chemogenetic experiments. These experiments identify and validate *Ntsr2* expressing neurons within the BLA as a putative 'Fear-Off' population.

4.3 Introduction

Overexpression of learned fear underlies many neuropsychiatric disorders such as phobia, panic disorder and Posttraumatic Stress Disorder (PTSD). Hallmark symptoms of PTSD such as re-experiencing memories of traumatic events, intrusive thoughts and hyper-arousal are likely precipitated by the over-consolidation of and failure to extinguish learned fear associations (A.P. Association, 2013; Kessler et al., 2005). Classical fear conditioning allows for the controlled study of neuronal processes mediating associative fear. Pavlovian fear conditioning is a learning paradigm wherein an initially neutral conditioned stimulus (CS) (e.g. a tone) is paired with an aversive unconditioned stimulus (US) (e.g. a mild footshock). After several CS+US pairings, mice display threat responses (also referred to as fear behaviors) upon presentation of the tone CS alone, here, fear behaviors are measured by quantifying freezing (when the moue ceases all non-homeostatic motion) (Johansen, Cain, Ostroff, & LeDoux, 2011). During fear extinction, the CS tone is presented in the absence of any US shock until the threat responses return to baseline (D. C. Blanchard & Blanchard, 1972; Bouton, Westbrook, Corcoran, & Maren, 2006; Johansen et al., 2011; Myers & Davis, 2007). The amygdala is well known to have an essential role in most fear behaviors specifically in the acquisition and extinction of learned associations (Goosens & Maren, 2001; Pare et al., 2004). Here, we will refer to fear conditioning as the training phase where CS/US associations are acquired, fear extinction as the early period where CS presentations in the absence of US lead to decrement in freezing, and fear extinction retention as a later period where additional CS presentations

measure the strength of retention of initial extinction event and act as additional extinction events. It should be noted that fear expression, fear extinction and extinction retention are overlapping processes where we are measuring the balance of signaling processes rather than unitary elements acting independently, thus early fear extinction measures primarily fear expression to CS and extinction while late fear extinction measures primarily extinction expression and consolidated retention of previous extinction learning.

Essential to understanding the opposing processes of fear acquisition and its extinction is the identification of neuronal circuits mediating each process (Chhatwal JP, 2007; Ciocchi et al., 2010; Herry et al., 2008; Senn et al., 2014; Wolff et al., 2014). Furthermore, development of rationally designed pharmaceuticals that act directly on fear inhibiting circuitry depends on discovering the molecular identities of neuronal populations that specifically mediate fear extinction. Within the basolateral amygdala (BLA), two electrophysiologically distinct populations of neurons have been described, one increasing firing in response to the CS to signal fear conditioning and expression (Fear-On) and the other increasing its firing to the CS during fear extinction (Fear-Off); differences in the activity in these populations have been shown to accurately predict freezing behavior of mice (Herry et al., 2008).

Identifying the molecular identities of these populations represents a major step towards full characterization of this circuit (Nieh et al., 2013). Importantly, we have previously electrophysiologically and functionally described a population marked by the Thy1 expression cassette that contains elements of the Fear-Off population (Jasnow et al., 2013). Thy1-channelrhodopsin-2 (Thy1-ChR2-eYFP) and Thy1-YFP lines mark a population of glutamatergic pyramidal neurons within the BLA, with significant specificity

for the anterior basal amygdala (BAa) (Feng et al., 2000). Optogenetic activation of this population leads to inhibition of a population of central amygdala (CeA) neurons and shunts excitatory drive from the LA. Behaviorally, brief activation of these neurons co-terminating with an unreinforced CS during extinction learning leads to enhanced extinction retention.

It is critical to further describe the behavioral and molecular phenotypes of this important population of cells, and in doing so identify a cell-type specific pharmacological substrate for enhancing fear inhibition. This work presents a work-flow to achieve this goal that may be applied to any genetically identified neuron population. Additional Thy1 transgenic lines are further functionally dissected with optogenetics and chemogenetics, demonstrating the necessity of these neurons for fear extinction learning. Furthermore, we characterize the RNA and protein expression patterns of this population, and identify neurotensin receptor 2 (NTSR2) as one of several possible pharmacologically targetable markers of this fear inhibiting neural circuitry. Our data suggest that pharmacological modulation of NTSR2 activity during behavior recapitulates effects observed from manipulation of Thy1 neurons, suggesting a consistent role for this neural population in fear inhibition.

4.4 Results

Thy1 Marks Consistent Population of BLA Neurons

Expression patterns were assessed across: Thy1-eYFP Line-H (Figure 1A) (Feng et al., 2000; Porrero et al., 2010), Thy1-eNpHR Line 2 (Figure 1B) (Gradinaru, Thompson, & Deisseroth, 2008; Zhao et al., 2008), Thy1-ChR2-EYFP Line 18 (Figure 1C) (Arenkiel et al.,

2007), and Thy1-Cre Line 1 (Figure 1D) (Campsall, Mazerolle, De Repentingy, Kothary, & Wallace, 2002). All lines produce high levels of transgene specifically within the BLA primarily the anterior BLA (BLAa), sparing the lateral amygdala (LA), central amygdala (CeA) and more caudally the basomedial amygdala (BMA). The Thy1-eYFP line was crossed with the Thy1-Cre line and infused unilaterally into the BLA with a Cre-dependent reporter virus. The resulting YFP fluorescence from the Thy1-eYFP line and mCherry from Thy1-Cre line exhibited strong overlap. Of mCherry (Thy1-Cre) labeled cells in the BLA, 93% were also YFP labeled demonstrating strong coherence in the identity of this population marked across Thy1 lines (Figure 1G-I). Because the rate of infected neurons is likely less than 100%, it is not possible to positively verify the proportion of YFP+ neurons that concurrently express Cre in this system; however, these data suggest that the Thy1-Cre+ population is contained almost entirely within the Thy1-YFP population. The reporter virus used here is extremely sensitive to recombination and may be recombined by a single molecule of Cre thereby detecting expression levels of Cre that are subthreshold for significant transgene expression in other lines (discussed in greater depth in supplement). For similar reasons, when the Thy1-Cre mouse line was crossed with reporter lines, as was done in initial characterization, a much larger population of cortical neurons is marked. Alternatively, this may suggest promiscuous expression during development with a more constrained pattern at adulthood; each possibility is discussed at greater length in supplemental discussion (Campsall et al., 2002). Co-localization between Thy1-eNpHR and other lines was not possible with this scheme because the transgene product is membrane bound making visualization of individual cell bodies within the densely populated BLA very difficult.

Separate Neuron Populations Active During Fear Processes

Thy1-ChR2-eYFP expressing neurons of the BLA appear to contain a 'Fear-Off' controlling population (Jasnow et al, 2013). To verify that the Thy1-eYFP marked population plays the same role in behavior, each of four cohorts of Thy1-eYFP mice (home cage, fear conditioned, fear extinction, and extinction retention) was put through the classical auditory fear-conditioning paradigm and sacrificed immediately following selected session (Jasnow et al., 2013). All tissue was processed and stained for c-Fos expression using immunohistochemistry (Figure 1E). Following fear extinction, a significant increase in c-Fos was observed in the YFP - but not the YFP + population. However, following the extinction retention test, a significant increase in c-Fos was observed in the YFP+ but not the YFP - population, suggesting that the BLA is involved in both fear expression and extinction, but the Thy1 population is selectively recruited during extinction and extinction expression. These data agree with previous data suggesting that Thy1+ neurons may be crucial for the encoding of fear extinction; from this lens we would expect the Fear-On (Thy1-) population to be primarily active during the early phases of fear extinction while the Fear-Off (Thy1+) population should increase activity as extinction progresses, thus during extinction retention session (which is also an additional extinction session) the YFP+ population is primarily active while the YFP- population is less activated. These behaviors do overlap during extinction and extinction retention, thus a long extinction test was used, so that during the extinction retention session the mouse is well within the extinction expression phase and a preponderance of the c-fos staining is observed in the Thy1+ population during this session.

Electrophysiological Characterization of Thy1-eNpHR Neurons

To confirm that eNpHR is capable of inhibiting Thy1 neurons, we measured the electrophysiological properties and light response of Thy1-eNpHR-eYFP neurons in BLA slice. As expected, we found strong laser illumination (wave length 593 nm, 3.6-10 mW/mm2) induced hyperpolarization of BLA principal neurons (Figure 2A). Laser illumination was sufficient to inhibit current injection induced spiking in eNpHR-YFP expressing neurons (Figure 2B). To confirm that transgene expression has no adverse effects on normal neuron firing in response to extrinsic inputs, normal action potential generation in eNpHR expressing neurons was measured with electrical stimulation of lateral amygdala (Figure 2C upper). The action potential was effectively abolished with laser illumination (Figure 2C, lower). Trains of action potentials were reliably produced by 10Hz electrical stimulation (Figure 2D, upper). These action potentials were effectively blocked by laser illumination (Figure 2D, lower). Taken together these results demonstrate that in the absence of laser light, eNpHR-eYFP expressing neurons have normal responses to synaptic input and laser light is sufficient to consistently hyperpolarize these neurons blocking the majority of generated action-potentials.

Optogenetic Silencing of Thy1 Neurons

Mice were implanted with optical fibers housed within ceramic ferrules unilaterally, just dorsal to the amygdala, aimed at the BLA of Thy1-eNpHR carrying and non-carrier controls. Fiber tip placement was confirmed using Cresyl violet staining and any mouse whose fiber was not placed over BLA was excluded from analysis (Supplementary Figure 1A). Mice were mildly fear conditioned to avoid ceiling effects (5CS + US, .4mA US foot shock). Yellow (593nm) light was tonically applied throughout the 30-second CS (Figure

3A). Inhibition of Thy1-eNpHR neurons during acquisition caused no changes in within-session behavior; however during 15 CS fear extinction session (considered a partial/ sub-optimal extinction session) in the absence of yellow laser stimulation, Thy1-eNpHR carriers expressed significantly more freezing throughout the session. These results suggest that during fear acquisition the BLA Thy1 population acts as a brake on fear learning and when it is silenced, fear acquisition is enhanced. Importantly, Thy1-eNpHR carriers and non-carriers that are cannulated and trained in an identical manner, but never receive any laser light, exhibit identical levels of freezing, confirming that any behavioral differences are caused by light-mediated silencing (Supplementary Figure 2).

To determine whether BLA Thy1 neurons play a role during fear expression, a naive cohort of Thy1-eNpHR expressing and non-carrier littermates received optic fiber implants and was fear conditioned without any laser application (Figure 3B). During short 15 CS fear extinction, laser light was applied throughout the CS. Thy1-eNpHR carriers expressed significantly more fear throughout the session starting from the first tone suggesting that inhibition of BLA Thy1 neurons reversed inhibition of the fear trace allowing for enhanced expression. Thy1-eNpHR carriers displayed significantly more freezing during 1 CS unstimulated expression test, suggesting that previous inhibition had not only enhanced fear expression, but blunted extinction as well. Mice were further extinguished (retention) to 30 CS's with laser application during the CS. Thy1-eNpHR carriers expressed enhanced fear throughout this fear extinction session. By the end of the session both groups of mice extinguished to baseline freezing levels. Finally, once a fearful association is extinguished, the inhibition of BLA Thy1 neurons during the final extinction session is not sufficient for reinstatement and does not drive spontaneous fear expression.

These changes in fear behavior were not accompanied with any anxiety or locomotor effects indicated by similar time spent in the center of an open field (Figure 3C) and distance travelled (Figure 3D) by both groups regardless of whether laser light was on or off. Placement of fiber tip was confirmed by Cresyl violet staining. (Supplementary Figure 1B).

Chemogenetic Activation of Thy1 Neurons

The Thy1-Cre line was utilized to modulate activity in Thy1 neurons using chemogenetics (Figure 4A). Designer receptors exclusively activated by designer drugs (DREADDs) are modified G-protein coupled receptors that are activated exclusively by an otherwise inert ligand, Clozapine-N-Oxide (CNO) (Fenno et al., 2014; Ferguson & Neumaier, 2012; Rogan & Roth, 2011). Here, we use a Gs coupled DREADD which is known to increase intracellular cAMP levels and enhance excitability when CNO is bound (Alexander et al., 2009; Krashes et al., 2011). Thy1-Cre mice were infected bilaterally with either AAV-DIO-Gs-DREADD-IRES-mCherry or AAV-CaMKII-eYFP. Expression of Gs DREADD infection is isolated to BLA; however, the pan-excitatory neuron expressing CaMKII-eYFP virus resulted in strong reporter expression throughout the amygdala (Figure 4B). Mice were fear conditioned (.65mA CS, 10CS+US pairings). The FVB background of the Thy1-Cre mice is not a high freezing line, thus a stronger fear conditioning paradigm (10CS + US) was necessary to achieve sufficient levels of freezing for experimental manipulation. Mice were injected with CNO twice at 1mg kg^{-1}, once thirty minutes before fear extinction and again twenty-four hours later before the extinction retention session (Krashes et al., 2011). Mice expressing the Gs-DREADD expressed similar levels of fear to the tone during the initial 15

CS fear extinction test; however, twenty-four hours later during a 30 CS extinction retention session they expressed significantly less fear (Figure 4A).

These results suggest that tonic enhancement of excitability in BLA Thy1 neurons during the extinction session is not sufficient for within-session changes in behavior. However, enhanced excitability is sufficient to enhance fear extinction consolidation, resulting in overall marked decreases in fear expression during the subsequent fear extinction retention session. However, it is possible that CNO administered before extinction retention enhances extinction expression despite having no within-session effect during extinction. Taken together these results further support the hypothesis that the BLA Thy1 neurons are a 'Fear-Off' population.

Isolation and Molecular Characterization of Thy1 Neurons

We next wished to further understand the molecular components that differentiate the Thy1+ cells from the Thy1- cells, hypothesizing that these cells may underlie genetic differences in the Fear-On vs. Fear-Off BLA populations. Furthermore, to rationally identify pharmaceuticals that selectively modulate known fear controlling circuits, it is advantageous to know the molecular expression profiles of targeted neurons. To approach this problem, we isolated Thy1 neurons using fluorescence activated cell sorting (FACS), then interrogated their molecular identity using RNA sequencing. To obtain purified samples of Thy1-eYFP neurons, 1mm punches of tissue centered over BLA were taken from Thy1-eYFP expressing mice and pooled (Figure 5A). Tissue was dissociated into a single cell suspension and fixed for staining with NeuN antibody and Hoechst; this allowed identification and isolation of specific neuronal cell bodies (Cruz et al., 2013; Guez-Barber et al., 2011; Guez-Barber et al., 2012). Voltages and gates were set using wildtype C57/B6

stained and unstained controls. Samples were analyzed for forward scatter and side scatter characteristics. A large portion of NeuN positive, Hoechst positive events were found in a small population near the bottom of the plot, so this population, corresponding to cell bodies, was chosen for further interrogation (Figure 5B, inset). We collected two populations, one strongly NeuN positive, strongly YFP negative and the other strongly NeuN positive, strongly YFP positive (Figure 5B). Although this method reduced the total yield, it increased the purity of collected neurons. Overall, of all cell bodies interrogated, 40% were NeuN positive while only ~2% were NeuN and YFP double-positive. Collected cells were confirmed to be either single or double-positive using microscopy. Following isolation, RNA was immediately collected from samples and later sequenced.

RNA sequencing revealed thousands of differentially regulated genes between Thy1-eYFP and other neurons. This list was then curated based upon a set of criteria demanding the gene must be highly significant controlling for false discovery rate ($q<.05$), and differentially regulated at a fold change greater than $2^{0.5}$ (Supplementary Figure 3). Furthermore, a list of gene hits meeting these inclusion criteria was input into the drug-able genome database (DGIdb) and interaction partners were searched for from expert curated lists, thus allowing for identification of gene targets that have high quality drug interaction partners. These top curated genes were then examined for expression patterns within the BLA using the Allen Brain Atlas or the literature.

Genes found to have increased expression in Thy1 neurons and the BLA include: *Dkk3, Tgfb, Rspo2, Nov, Dcn*, and *Chrd*; genes found to have relatively decreased expression in Thy1 neurons and the BLA include *Ankfn1* and *Pde7b* (Figure 5F-M). Data are shown only from differentially regulated genes that had high quality coronal images in the Allen Brain

Atlas (1; 2; 3; 4; 5; 6; 7; Ed S. Lein et al., 2007). Other genes that did not have high quality coronal ISH images available through the Allen Institute were examined in the literature for mRNA and protein expression. Several genes, notably *Ntsr2*, were determined to have enriched or depleted expression in BLA and thus met inclusion criteria (Sarret, Beaudet, Vincent, & Mazella, 1998; Sarret, Perron, Stroh, & Beaudet, 2003). RNA sequencing expression data were validated using quantitative PCR for select genes of interest. Follow up quantitative PCR supported a strong upregulation of *YFP*, *Thy1*, and *Ntsr2* mRNA in YFP + sample (Supplementary Figure 3). Results from qPCR validation performed on RNA used for sequencing replicate data demonstrated that the fluorescent Thy1 neurons were successfully sorted, and that RNA sequencing indeed identified differentially expressed genes that are selectively upregulated in these neurons.

This methodology strongly biases our results towards genes that are selectively upregulated in Thy1 neurons to the exclusion of genes with equal population-specificity but less regional specificity. Our goal is to discover putative drug targets selectively acting on the 'Fear-Off' population within the BLA. This goal is most efficiently achieved by narrow consideration of genes that are highly upregulated in putative Fear-Off populations.

Protein expression patterns of six genes selectively upregulated in Thy1-eYFP neurons were next examined using immunohistochemistry in tissue from Thy1-eYFP mice (Figure 6 and Supplementary Figure 5). Using confocal microscopy, the degree of co-localization between the protein of interest and Thy1-eYFP neurons was examined quantitatively. Images were taken in regions of high Thy1-eYFP density with equal numbers of volumes analyzed anteriorly and posteriorly. Genes examined are: *Ntsr2*, *Dkk3, TgfB2, Rspo2, Wnt 7a,* and *Dcn.* Across all markers examined, none had more than 1% of

YFP positive cells that did not co-localize with the marker of interest (Supplementary Figure 6). All genes exhibited staining in some cells that were not YFP positive, suggesting that the Thy1-eYFP population may be marking a majority sub-population of a larger population with a common protein expression profile.

To confirm that these apply across Thy1 transgenic lines, tissue previously used for the above chemogenetic experiments was stained using antibodies against Dkk3 and TGFB2 and co-localization was measured with Gs-DREADD expression. A majority population of co-labeled cells was revealed with a minority population of cells single labeled for the gene of interest and ~1% Thy1-Cre marked neurons remaining unlabeled. Although all markers had high levels of co-localization in the regions analyzed, neurotensin receptor 2 (*Ntsr2*) and Dkk3 displayed regional homology across all amygdala sections examined (Supplementary Figure 7). Furthermore, the availability of high quality agonist and antagonist drugs, acting specifically at NTSR2 prompted the further investigation of NTSR2 and its role in fear learning (Antonelli et al., 2007; Ferraro et al., 2008).

Pharmacological Manipulation of Neurotensin Receptor 2

The above evidence suggested that the NTSR2 is highly expressed within the Thy1 neurons within the BLA, sharing consistent regional and cellular specificity (Figure 7A). To assess NTSR2 as a target for actuating pharmacological manipulation of fear behaviors, a selective NTSR2 agonist, Beta-Lactotensin, was acquired and its effects on fear expression measured. Mice were fear conditioned (Figure 7B) and 24-hours later, two hours before fear extinction, mice were injected intraperitoneally with either saline or Beta-Lactotensin (30mg kg^{-1}) (Yamauchi, Wada, Yamada, Yoshikawa, & Wada, 2006). No within-session effect of Beta-Lactotensin on fear expression was detected; however, during extinction

retention, two hours after a second injection, a significant decrease in freezing was detected during the first ten tone presentations in mice receiving Beta-Lactotensin administration. These data suggest that Beta-Lactotensin may act to enhance NTSR2 activity, stimulating the amygdala 'Fear-Off' population and enhancing fear extinction consolidation and expression of extinction.

We next wished to confirm that the behavioral effects detected following peripheral administration of Beta-Lactotensin reflect changes in activity of BLA NTSR2 expressing neurons. Thus, we performed another experiment directly comparing agonists and antagonists at this receptor with targeted intra-amygdala injections. Beta-Lactotensin and Levocabastine, a selective NTSR2 antagonist, were applied directly to the amygdala in separate cohorts of mice before fear extinction (Figure 7C). Mice were cannulated bilaterally with cannulae aimed so that the injector tip rested just above the BLA. Based upon our halorhodopsin experiments, a weak fear conditioning (.4mA US) was necessary to avoid ceiling effects. Twenty-four hours later mice were infused bilaterally into the BLA with Beta-Lactotensin (90 μg per hemisphere), Levocabastine (1.5 μg per hemisphere) or vehicle (5% DMSO in Saline, needed to maintain common vehicle), 30 minutes before fear expression. Mice infused with Beta-Lactotensin had a strong, but non-significant trend towards reduced freezing throughout the fear extinction session suggesting that activating NTSR2 in the BLA is sufficient to decrease fear. There was no within session effect of Levocabastine infusion during fear expression; however, during the fear extinction retention session, mice that previously had been infused with Levocabastine froze significantly more than control. To confirm that observed effects on freezing were not due to changes in anxiety-like behavior or locomotion, mice were infused with their original

drug and placed in an open field chamber for ten minutes. No differences between groups were detected in either time spent in center or distance traveled (Supplementary Figure 8). Together, these data suggest that inhibiting NTSR2 within the BLA is sufficient to block fear extinction resulting in more fear expression.

Although Beta-Lactotensin has high affinity for NTSR2, it has ten-fold lower affinity for NTSR1 as well. To confirm that observed behavioral changes were not due to off-target agonism of the NTSR1 mice a separate, naïve cohort of mice were cannulated and fear conditioned at a higher shock intensity (.65mA) (Figure 7D) (Hou, Yoshikawa, & Ohinata, 2009). Mice were infused bilaterally with Beta-Lactotensin at a 3 fold lower concentration (30ug per hemisphere) or sterile saline thirty minutes before fear extinction session. Mice that received infusion of Beta-Lactotensin expressed significantly less fear than their Saline infused counterparts. Interestingly, during the pre-CS period the group infused with Beta-Lactotensin showed less fear compared to controls as well, suggesting that the agonism of the NTSR2 causes generalized inhibition of fear expression (unpaired t-test, $p < .01$). Twenty-four hours later mice were subjected to another fear extinction retention session without drug, and no detectable differences were measured between groups, possibly due to the previous full fear extinction test resulting in a floor effect. Overall, these experiments show that activation of NTSR2 within the amygdala is sufficient to decrease fear expression.

Examination of Projection Patterns of BLA Thy1-Cre Neurons

To understand how the Thy1/NTSR2 population fits into a larger fear-controlling circuitry, it is necessary to uncover the specific projections of this population. Thy1-Cre expressing mice were infused unilaterally with cre-dependent (AAV-DIO-GFP) virus into

the BLA at different anterior to posterior positions (-1.0, -1.5, -2.0). After three months, animals were sacrificed and the patterns of fluorescent protein expression were examined descriptively throughout forebrain structures for regions of apparent strong and weak YFP fluorescence. Labeled cell bodies were found primarily within 0.5mm along the A/P axis of the site of infusion (Supplementary Figures 9f, 10e and f, 11c and d). Examination of patterns made by filled terminals were made with no *a priori* hypotheses and revealed strong projections from BLA Thy1 neurons to several regions including nucleus accumbens (NAc) core and shell and bed nucleus of the stria terminalis (BNST) (Supplementary Figures 9b and c, 10a, c and g, 11b). Both of these regions mediate, among many other functions, reward and positive valence. Additional projections were found to the prefrontal cortex (PFC) [with some specificity for the Infralimbic cortex (IL)], anterior insula (AI), contralateral BLA and contralateral medial intercalated nuclei (mITC) (Supplementary Figures 9 a and d, 10 b and d, 11 a). These regions, especially IL and mITC have been strongly implicated as mediating extinction and fear suppression. Importantly, although anterior infusions spare posterior cell bodies and posterior infusions spare anterior cell bodies, few discrepancies were found in the patterns of projections between infusion sites. Importantly, and perhaps consistent with the apparent role of the Thy1 marked cell in Fear Off regulation, there is little apparent projection to CeA from these labeled cells (Supplementary Figures 9d and e, 10d-f, 11c).

When compared to cre-dependent tracing, biotinylated dextran amine (BDA) infused anteriorly into the BLA (-1.5 A/P) results in similar projection patterns; notably projections are very weak to the CeA as observed in Thy1-eYFP and Thy1-Cre animals (Supplementary Figure 12, CeA labeling in 12A is due to over-flow from infusion). Projections to IL and

BNST are observed as well. However when BDA is infused posteriorly (-2.5 AP) there are strong projections observed to all parts of the CeA as well as BNST and AI (Supplementary Figure 13). For additional discussion of Thy1-Cre expression see supplementary discussion (Supplementary Figure 14 & 15). Taken together, these data suggest that Thy1 'Fear-Off' neurons conform to projection patterns of the majority of rostral BLA neurons; however, they maintain their segregated projections more caudally where CeA projecting neurons that likely have an alternative role in behavior can be found as well.

4.5 Discussion

Data presented here: 1) further identify and characterize a functional role for the Thy1-marked amygdala neural population in behavior, 2) characterize the molecular profile of this population, 3) characterizes its circuit connectivity, and 4) uses that information to identify compounds that directly modulate activity of the population *in vivo*. This represents an executable methodology for behavioral and molecular characterization of a neuron population leading to identification of pharmacological agents that act *in vivo.*

Four Thy1 transgenic lines mark consistent regional and cellular populations specifically within the BLA. Populations marked by these lines maintain consistent roles in learned fear behavior as indicated by their recruitment during fear extinction (Thy1-eYFP), sufficiency of tonic enhancement of excitability for augmented fear extinction consolidation (Thy1-Cre) and necessity of activity for fear inhibition and extinction (Thy1-eNpHR). Previously, we have demonstrated the Thy1-ChR2 line marks a population whose activation is sufficient to enhance fear extinction (Jasnow et. al, 2013). Examination of differentially regulated genes identified using FACS and RNA sequencing reveals many genes that mark neuron populations that consistently overlap with the Thy1-eYFP

populations. Finally, using drugs selectively targeting one identified marker, NTSR2, yields behavioral results that consistently recapitulate those observed with optogenetic and chemogenetic manipulations.

As is well known, use of the Thy1.2 expression cassette may generate mice with drastically different transgene expression patterns (Feng et al., 2000). Similar expression patterns across mouse lines likely result from coincidental marking of a common developmental population originating from the pallial zones of the telencephalon (Porrero et al., 2010). Thus, we do not claim that Thy1 is a marker of only the amygdala Fear-Off population, but rather that these mouse lines conveniently mark a common developmental population generating a population of neurons including the Fear-Off pyramidal neurons within the BLA in adulthood. Additional consideration must be given to the fact that within the Thy1-eNpHR mouse brain, populations in addition to the BLA population examined are labeled, specifically hippocampal and some cortical neurons. As there are many cell bodies and processes labeled in the BLA it is impossible to determine whether extrinsic terminals are also labeled, leaving the possibility open that some effects may be due to inhibition of terminals or fibers of passage. Behavioral replication using virally induced Gs-DREADD gives evidence that activity specifically of BLA Thy1 neurons is involved in fear learning; however, further study is necessary.

Highly specific micro-iontophoresis of muscimol specifically into the BLA blocks extinction consolidation without within-session effects (Herry et al., 2008). In our hands, selective inhibition of Thy1 neurons appears to allow maintenance of activity of the previously silenced Fear-On circuitry. Thus, the fear circuit may be artificially unbalanced,

and we observe enhanced within-session fear expression in addition to previously observed deficits in extinction consolidation.

NTSR2, less studied than its high affinity partner NTSR1, is a Gq coupled signaling protein identified as a low affinity Neurotensin receptor with highly selective binding to levocabastine (Amar, Kitabgi, & Vincent, 1987). Recent reports from Tye and colleagues have demonstrated differential roles in behavior for BLA neurons projecting to the CeA and NAc. The high-affinity neurotensin receptor NTSR1 may mark a CeA projecting population that supports fear expression (Namburi et al., 2015). NTSR1 was not found to be differentially regulated in Thy1-eYFP neurons in our study, suggesting a dynamic and potentially complementary role for neurotensinergic signaling in fear learning, perhaps dependent upon differential projection patterns (Namburi et al., 2015). It is possible these populations correspond to IL/PL projecting populations reported by Senn et al. (2014); however, further study is needed[11]. Thus, we propose that NTSR1 supports fear expression and NTSR2 supports fear inhibition via their differential expression within the BLA.

Results demonstrating the fear suppressing effects of Beta-Lactotensin are very encouraging; however more research is necessary to clearly define the mechanism by which this compound is working. There have been reports of Beta-Lactotensin mediating anti-nociception, anxiolysis, and fear memory modulation (Hou et al., 2011; Lafrance et al., 2010; Yamauchi et al., 2007; Yamauchi et al., 2006). Although this is the first report examining intra-amygdala application of this compound in the context of auditory fear conditioning, future studies will need to rigorously dissect the mechanisms of this fear-suppression phenotype. Analysis of projection patterns of BLA Thy1-Cre neurons reveals a strong preference for regions commonly thought to be associated with appetitive learning

and fear suppression such as the NAc, mPFC and ITCm. Recently there has been a great deal of discussion concerning the implications of a heterogeneous BLA population with distinct sets of neurons projecting to, for example, the CeA or the NAc depending on whether they convey information with negative or positive valence respectively (Namburi et al., 2015). Here we suggest that Thy1 labeled neurons, acting as proxy for NTSR2 expressing neurons, correspond to the Fear-Off, and possibly positive valence neurons, based upon their role in behavioral and projection patterns.

4.6 Methods

Animals

Adult (8-12 week) B6.Cg-Tg (Thy1-eYFP)HJrs/J (Thy1-eYFP), B6.Cg-Tg (Thy1-COP4/EYFP)18Gfng/J (Thy1-ChR2-EYFP), FVB/N-Tg (Thy1-Cre)1Vln/J (Thy1-Cre), B6;SJL-Tg (Thy1-hop/EYFP)2Gfng/J (Thy1-eNpHR), and C57BL/6J mice were obtained from Jackson Laboratories (Bar Harbor, ME). All mice were group housed and maintained on a 12hr:12hr light:dark cycle. Mice were housed in a temperature-controlled colony and given unrestricted access to food and water. All procedures performed conformed to National Institutes of Health guidelines and were approved by Emory University Institutional Animal Care and use Committee.

Surgical Procedures

Mice were deeply anesthetized with Ketamine/ Dexdormitor (medetomidine) mixture and heads fixed into stereotaxic instrument (Kopf Instruments). Stereotaxic coordinates were identified from Paxinos and Franklin (2004) and heads were leveled using lambda and bregma. To allow for optical inhibition (Figure 3), mice were implanted unilaterally with an

optical fiber (length 5mm, .22NA, 200µm core; Thor labs) housed in a ceramic ferrule (Thor Labs) just dorsal to the BLA (-1.8mm AP, +/- 3.4 mm ML, -4.8mm DV) implants were randomized to side. Ferrules were adhered to the skull with adhesive, then a protective head cap was constructed using dental cement. For viral delivery (Figure 4), a 10µl microsyringe (Hamilton) was lowered to coordinates just above BLA and .5 µl of virus solution was infused at .1µlmin^{-1} using microsyringe pump. Virus solution contained either purified AAV$_5$-hSyn-DIO-rM3D (Gs)-mCherry or AAV$_5$-hSyn-eGFP in PBS (UNC Viral Vector Core). After infusion, syringes rested at injection for 15 min then slowly were withdrawn. After bilateral infusion, incisions were sutured closed using nylon monofilament (Ethicon). For pharmacological experiments (Figure 7) mice were implanted bilaterally with a guide cannula (length 5mm, 22 gauge, Plastics One) so that infuser tip rested just above the BLA as before. Guide cannulae were attached to the skull with adhesive and a head-cap was constructed using dental cement. After dental cement cured dummy stilets were placed into cannulae. For all surgeries, body temperature was maintained using a heating pad. After completion of surgery, anesthesia was reversed using Antisedan (atipamezole) and mice were allowed to recover on heating pads.

Laser Delivery

Optogenetic inhibition was achieved using a 50mW DPSS 593nm laser (Ikecool Inc., Anaheim, CA). Laser-coupled fiber was attached to an optical fiber patch chord via a rotary joint (Doric) and suspended above behavioral testing chambers. Patch cords were attached directly to a chronically implanted optic fiber. Animals received 30 seconds of 10mW (79.55mW/mm^2) tonic light during 'tone on' epochs of cued fear behaviors. For open field

experiments mice received tonic light for alternating 2.5-minute light-on but not light-off periods.

Drug Administration

Clozapine-N-Oxide (Sigma) was diluted in sterile saline and administered at 1mgkg^{-1} i.p. Beta-Lactotensin (NIMH) used for i.p. experiments (Figure 7C) was prepared in sterile saline and administered at 30mg kg^{-1} two hours prior to behavioral testing. Beta-Lactotensin used for initial intra-amygdala experiment (Figure 7D) was prepared in 5% DMSO in sterile saline and administered at 90ug perhemisphere thirty minutes before behavioral testing. Levocabastine (Sigma) (Figure 7D) was prepared fresh prior to administration in 5% DMSO and administered at 1.5ug per hemisphere. Beta-Lactotensin used for follow up replication (Figure 7E) was prepared in sterile saline and administered at 30ug per hemisphere thirty minutes before behavioral testing.

Behavioral Assays

Auditory Cue-Dependent Fear Conditioning

Mice were habituated to fear conditioning chambers (Med Associates Inc., St Albans, VT) for 10 minutes each of two days prior to fear conditioning. Mice were conditioned to five tones (ten for Thy1-Cre experiment, Figure 4) (30s, 6kHz, 65-70db) co-terminating with a foot shock (1s .4mA (weak), or .65mA (regular) depending on session).

Auditory Cue-Dependent Fear Expression and Extinction

Cue-dependent fear extinction was tested 24-hours after fear conditioning and extinction retention occurred 24-hours after fear expression. For extinction, mice were placed in a novel context and exposed to 15 or 30, 30 second tones with an inter trial interval of 60

seconds. Freezing was measured using Freeze View software (Coulbourn Instruments Inc., Whitehall, PA) or hand scored by two blinded experimenters (Figure 3).

Behavioral Tests For c-fos Expression Experiments

As above, animals were habituated to training chamber. As above, animals were fear conditioned to 5 CS/US pairings. For fear extinction, mice were extinguished to 30 CS tones in an alternate context. The next day for fear extinction retention testing, mice were re-exposed to a single CS in the extinction context. Mice were sacrificed as below ninety minute following cessation of behavior.

Open Field

Open field chambers (Med Associates) were placed in a dimly lit room. Mice were placed in the chamber for 10 minutes and allowed to explore. For optogenetic experiments mice received light during the second and final 2.5 minutes of the session.

Dissociation of Amygdala Tissue for FACS

For each of three replicates where RNA was collected from isolated neurons three groups of three Thy1-eYFP mice and several control C57 mice were rapidly decapitated and bilateral 1mm amygdala punches were taken within 2 minutes. To minimize RNA degradation each solution used was prepared with RNAse Out (Life Technologies Inc., Bedford, MA) and kept on ice. Each pair of amygdala punches was homogenized with a razorblade on a cold glass petri dish then transferred to cold Hibernate A (Life Technologies). Tissue was spun down and supernatant replaced with 1mL Accutase (Innovative Cell Technologies, Inc., San Diego, CA) and allowed to digest for 30 minutes while rotating at 4°C. Digested tissue was spun down and resuspended in cold Hibernate A.

Three sets of punches were combined (for a total of N=3 mice per sample) and tissue was manually dissociated by trituration using fire polished Pasteur pipettes with diameters 1.3 mm, .8mm and .4 mm in series where supernatant was collected and volume restored between each step. Cell suspensions were spun down and cell pellet resuspended in Hibernate A. Cell suspensions were filtered through pre-wetted 100um and 40um filters (BD Biosciences, Inc., San Jose, CA) in series.

Immunolabeling Cell Suspension for FACS

Cells were fixed by adding equal volumes of 100% ice cold EtOH and incubating for 15 minutes. Fixed cells were spun down and resuspended in sterile PBS. After removing appropriate aliquots for gating and compensation controls fixed cells were incubated with biotinylated anti-NeuN antibody (1:1000, Milipore) and Hoechst (1:1000, Sigma) while rotating at 4°C. Cells were pelleted and washed with PBS. Cell suspensions were incubated with secondary allophycocyanin (APC)-labeled streptavidin (1:1000, Invitrogen) for 30 minutes while rotating at 4°C. Cells were pelleted and washed twice with cold PBS.

Flow Cytometry

A FACS Aria II (BD Biosciences) was used for cell sorting (Flow Cytometry Core at Yerkes National Primate Center). A portion of cells collected from wild-type mice was used to gate based on FSC and SSC light scattering and Hoechst fluorescence characteristics. Another portion of wild-type cells incubated exclusively in secondary antibody was used to set threshold for nonspecific binding of APC-streptavadin binding and auto fluorescence in the 488nm channel. Finally, stained cells collected from Thy1-eYFP mice were sorted and samples collected. For initial characterization, samples were collected in PBS and samples

examined under fluorescent microscope to verify correct sorting. Thereafter, cells were sorted directly into lysis media of RNeasy Micro Kit (Qiagen) and kept at 4°C. After sorting was completed RNA was isolated according to manufacturer's instructions including on-column DNase treatment. Samples were combined into single tube and RNA quantity and quality were determined using Bioanalyzer pico chip (Agilent).

Real Time PCR

RNA was reverse transcribed and amplified using SMARTer HV kit (Clonetech). Quantitative PCR was performed on cDNA with each sample run in triplicate technical replicates. Reactions contained 12µl Taqman Gene Expression Master Mix (Applied Biosystems), 1µl of each forward and reverse primer, 1 µl of 5ng ul^{-1} cDNA, and 6 µl water. Primers were proprietary FAM labeled probes from Life Technologies. Quantification of qPCR was performed on Applied Biosystems 7500 Real-Time PCR System. Cycling parameters were 10 minutes at 95°C, 40 cycles of amplification of 15s at 95°C and 60 at 60°C, and a dissociation step of 15s 95°C, 60s at 60°C, 15s 95°C. Fold changes of YFP + over YFP - groups were calculated as ΔΔCT values normalized to levels of Actin B mRNA. Values presented as fold change +/- s.e.m.

Immunohistochemistry

For visualization of Decorin and RSPO2, Thy1-eYFP mice were perfused and brains were post-fixed for 2 hours using Zamboni Fixative. For all other visualizations mice were perfused and brains were post-fixed for 2 hours with 4% paraformaldehyde. 35um free-floating brain sections were rinsed in PBS, then in blocking solution (PBS, 10% Normal Goat Serum, 0.25% Tween-20, 0.4% Triton-X 100) for 1h at room temperature, and

incubated for 24h at 4C with the following antibodies in PBST: DKK3 (1:200, Abcam), TGFB2 (1:5000, Abcam), Wnt7a (1:5000, Santa Cruz), RSPO2 (1:200, Abcam), NTR2 (1:500, Santa Cruz), Decorin (1:1000, Santa Cruz). Sections stained for NTR2 underwent an amplification process, which consisted of a PBS rinse, 30min incubation in Peroxidase labeled goat anti-rabbit (1:1000, Vector Labs) at room temperature, another PBS rinse and 10min in Fluorophore Tyramide Working Solution (TSA Plus Cyanine3 System)
All other sections were rinsed in PBS and incubated for 2h at room temperature with either Alexa-Fluor 568 donkey anti-goat (1:1000, Invitrogen) or Alexa-Fluor 594 goat anti-rabbit (1:1000, Invitrogen) depending on the primary antibody's host. Following another PBS rinse, sections were mounted, then stained with Hoechst (1:1000, Sigma) before being given a final PB rinse and cover-slipped with Mowiol mounting medium.

RNA-Seq Library Preparation

Libraries were generated from 1 ng of Total RNA using the SMARTer HV kit (Clonetech), barcoding and sequencing primers were added using NexteraXT DNA kit. Libraries were validated by microelectrophoresis, quantified, pooled and clustered on Illumina TruSeq v3 flowcell. Clustered flowcell was sequenced on an Illumina HiSeq 1000 in 100-base single-read reactions.

Analysis of RNA Sequencing Data

RNA sequencing data was analyzed using Tuxedo DESeq analysis software. Differential expression between YFP + and YFP – groups were obtained and used for further analysis. Using the q value of less than .05 as a cut-off, only highly significant returns were used for further analysis. In order to ensure that genes had a large enough difference in expression

to warrant pharmacological manipulation, only those with differences in expression greater than $2^{.5}$ or ~141% were considered. Next using the 'Drug Gene Interaction Database' returns were examined for having a known pharmacological agent that modifies its activity. Genes lacking viable pharmacological modulators were eliminated.

Statistics

Statistical analyses were performed using Prism 6 by Graph Pad. All data presented as mean +/- s.e.m. Differential c-fos expression was examined using a Two-way ANOVA with behavioral condition as the between-subjects factor and Sidak's multiple comparisons test versus Home Cage. For comparison of eight c-fos expression groups, two-way ANOVA was performed followed by Sidak's post-hock multiple comparisons test. All behavioral experiments were examined using a repeated-measures ANOVA with drug or optogenetic stimulation as the between-subjects factor and tone presentation as the within subject factor. Open field activity (time in center and distance traveled) was compared using a Students t test between carrier and non-carrier groups. For qPCR delta delta CT's of data were compared by Students t-test between YFP + and YFP – groups. For all tests statistical significance was set at $p < .05$.

Analysis of BLA Thy1-Cre Projections

Three months post-viral infusion animals were sacrificed and tissue was prepared as above. Slices were initially examined to confirm that cell bodies were labeled primarily in the BLA and that sight of expression conformed with target area. Slices were examined broadly with no *a priori* hypotheses about projection patterns. Images were taken using consistent exposure times within subject to preserve consistency of brightness of staining.

Images at lower exposure time were taken of BLA for publication purposes to avoid over-exposure of YFP expressing cell bodies. Areas were characterized broadly as having either strong or weak fluorescent expression. From areas found to have strong expression, those known to play a role in fear learning and expression are highlighted in text.

4.7 Figures

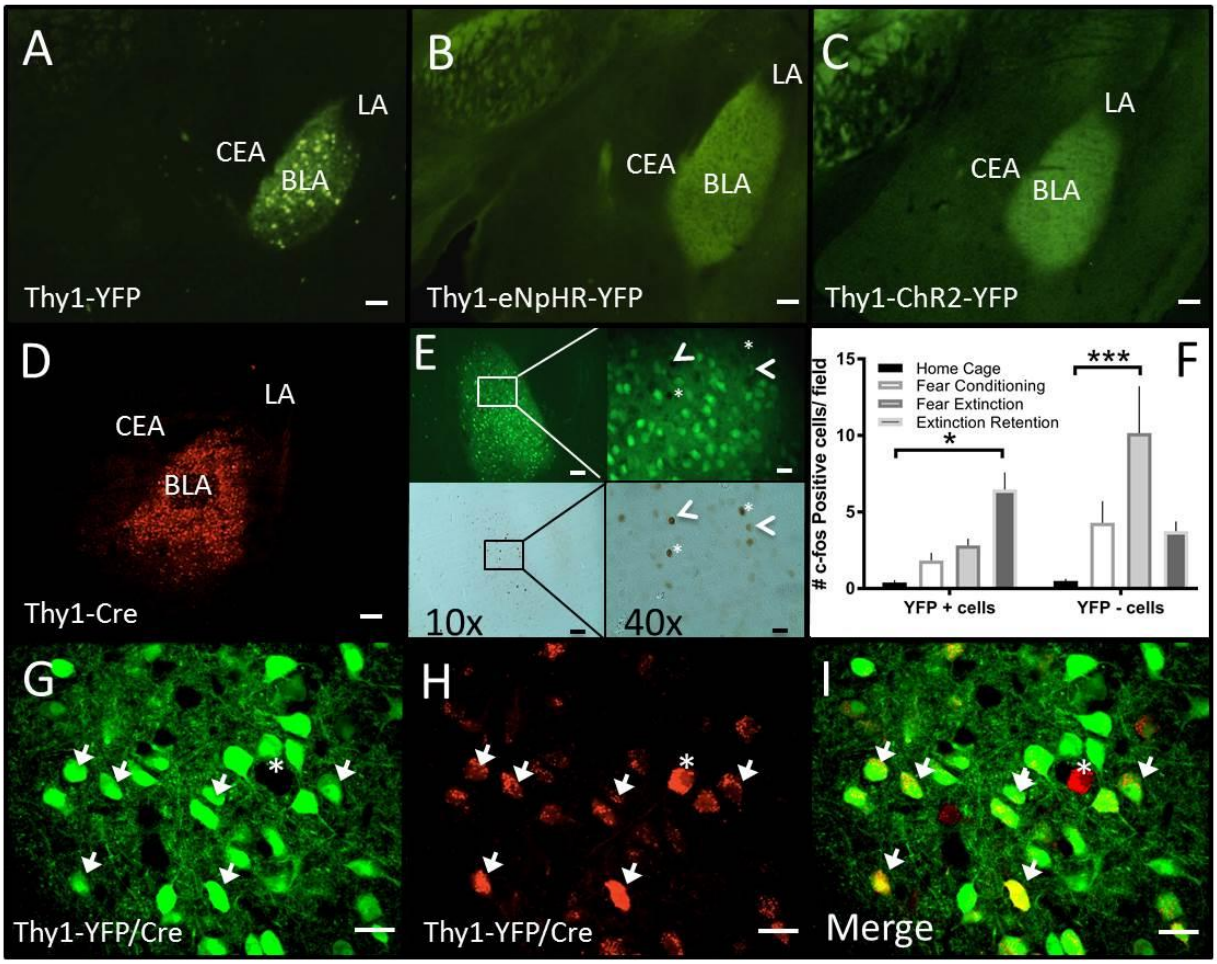

Figure 4-1. Thy1 lines mark BLA population that is active during expression of fear extinction.

A. Thy1-eYFP, **B.** Thy1-eNpHR, **C.** Thy1-ChR2, each have strong expression enriched in the BLA. **D.** Cre recombinase driven by the Thy1.2 cassette in the Thy1-cre mouse, when

visualized via infusion of AAV- hSyn-DIO-rM3D (Gs)-mCherry, marks the same regional population as marked by the Thy1-eYFP mouse. **E.** Representative images of a field of view analyzed for c-fos staining in the BLA of Thy1-YFP mouse after fear expression. Co-localization was manually scored at 40x magnification, 10x images are for reference. Upper panels: YFP+ expression in BLA of examined Thy-1 YFP mice. Green neurons in upper panels are YFP+ neurons while black c-fos+ nuclei are depicted in lower panels. Fields for analysis were chosen at random within strongly YFP expressing area. Fields of were visually inspected for co-labeling of c-fos and YFP. Example neurons identified: arrowhead indicates c-fos+/YFP+ cell while asterisk indicates c-fos +/YFP- cell. **F.** Quantification of co-labeling of YFP or non-YFP marked cells with c-fos in Thy1-eYFP mouse. Counts represented as number of positive events per field analyzed. BLA sections were analyzed after 1) untrained home cage controls (HC), 2) fear conditioning (FC), 3) fear extinction (FE), or 4) fear extinction retention (FR). Thy1-eYFP+ neurons are cfos+ significantly more often after fear extinction testing vs. home cage while eYFP- marked neurons stain for c-fos significantly more often during fear expression (2-way ANOVA, $F_{(3,40)}$ p=.0017, when significant main or interaction effects were found by the ANOVAs, Sidak's post hoc tests were carried out to locate simple effects. Sidak's multiple comparisons vs. homecage: $p < .05$, error bars indicate +/- s.e.m. Sidak's multiple comparison post hoc analysis: YFP+ HC vs. YFP- FE $p < .05$, YFP+ FC vs YFP- FE $p<.05$, YFP + FE vs YFP- FE: $p< .05$, YFP- HC vs. YFP- FE $p<.05$, YFP- FE vs YFP- FR: $p<.05$, Error Bars indicate mean +/- s.e.m.). **G-I.** Infusion of AAV-EF1a-DIO mCherry into double transgenic Thy1-eYFP/Thy1-Cre mouse allows colocalization of neurons marked by each transgene. Arrows indicate neurons with colocalization. Asterisks indicate neuron marked only by mCherry. Scale Bar =100 um for

A-D E upper left and lower left, 20 um for G-I and E upper right and lower right.

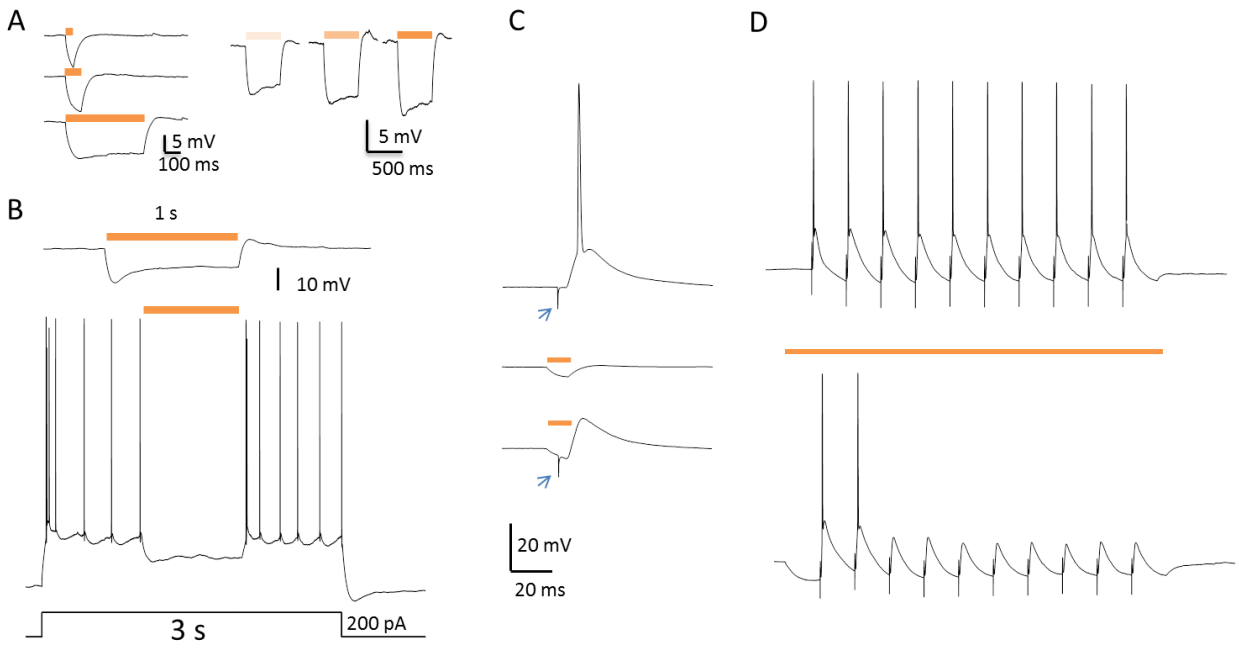

Figure 4-2. Halorhodopsin inhibition of BLA Thy-1 neurons.

A. Light activation of halorhodopsin (593 nm) induced membrane hyperpolarization in a Thy-1 neuron; strength of hyperpolarization is time and intensity-dependent **B**. Halorhodopsin activation abolished inward current injection-induced firing; **C.** upper, electrical stimulation of lateral amygdala induced action potential in a BLA Thy-1 neuron; middle, light evoked membrane hyperpolarization in Thy-1 neuron; bottom, the action potential was abolished by light illumination; arrowheads indicate stimulus artifact from LA stimulation. **D.** upper, a train of action potentials induced by 10 Hz electrical stimulation of LA, lower, the firing was reduced by concurrent halorhodopsin activation. Delays in action potential suppression are likely due to transient and complex dynamics of intrinsic

ion channels during eNpHR facilitated hyperpolarization. Similar delays were found in original characterizations of Thy1-NpHR mouse lines. For additional characterization of NpHR and eNpHR in Thy1 mouse lines please see: (Gradinaru et al., 2008; Zhao et al., 2008).

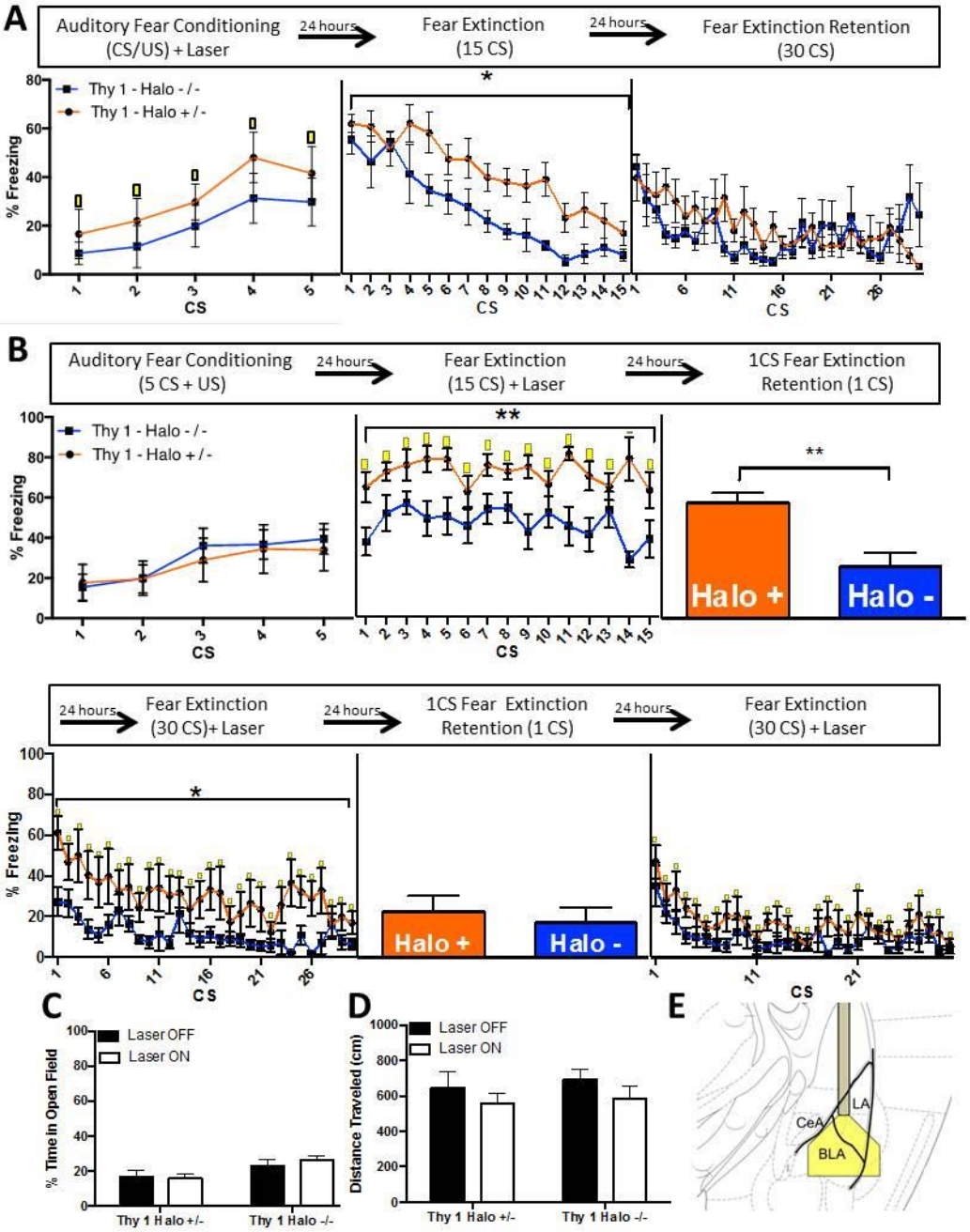

Figure 4-3. *In Vivo* inhibition of Thy1 neurons.

Inhibition of Thy1 neurons enhances fear consolidation and fear expression while blunting fear extinction consolidation. BLA neurons of mice expressing halorhodopsin under the control of the Thy1.2 expression cassette were silenced during select phases of fear

conditioning to determine their precise role in behavior. This change in fear behavior was not caused my changes in anxiety-like behavior. **A.** Silencing BLA Thy1 neurons during weak fear acquisition results in no significant within-session changes in behavior; however, 24-hours later mice carrying the Thy1-halorhodopsin gene express significantly more fear during fear extinction (Two-way RM ANOVA, $F_{(1,14)}$ =5.827 ,*= $p < .05$). **B.** Mice weakly fear conditioned in the absence of laser stimulation show no within session behavioral differences; however, 24-hours later when laser stimulation is applied during CS-on period of extinction, mice carrying the Thy1-halorhodopsin gene express significantly more fear (Two-way RM ANOVA, $F_{(1,12)}$=10.08,**= $p < .01$). Thy1-halorhodopsin carrying mice exhibit significantly enhanced fear 24-hours later in the absence of laser stimulation (Students t-test, **= $p<.01$). 24-hours later, enhanced freezing is measured throughout the extinction retention session when laser stimulation is provided during CS on period (Two-way RM ANOVA, $F_{(1,11)}$= 7.75, * = $p < .05$). 24-hours later no difference in freezing to CS is detected in the absence of laser stimulation. A final extinction session with laser stimulation during CS presentation reveals no differences in freezing. **C.** Inhibition of BLA Thy 1 neurons was not accompanied by any change in anxiety-like behavior or **D** ambulation. Thy1-halorhodopsin carriers spent the same amount of time in the center of an open field as controls whether laser light was on or off. Thy1-halorhodopsin carriers traveled the same distance whether laser light was on or off. **E.** Schematic of optical fiber placed dorsal to the BLA providing yellow laser illumination during experimental procedures. Light is estimated to maintain > 10mW power within .5 mm of the fiber optic tip. In all panels Error Bars indicate mean +/- s.e.m.

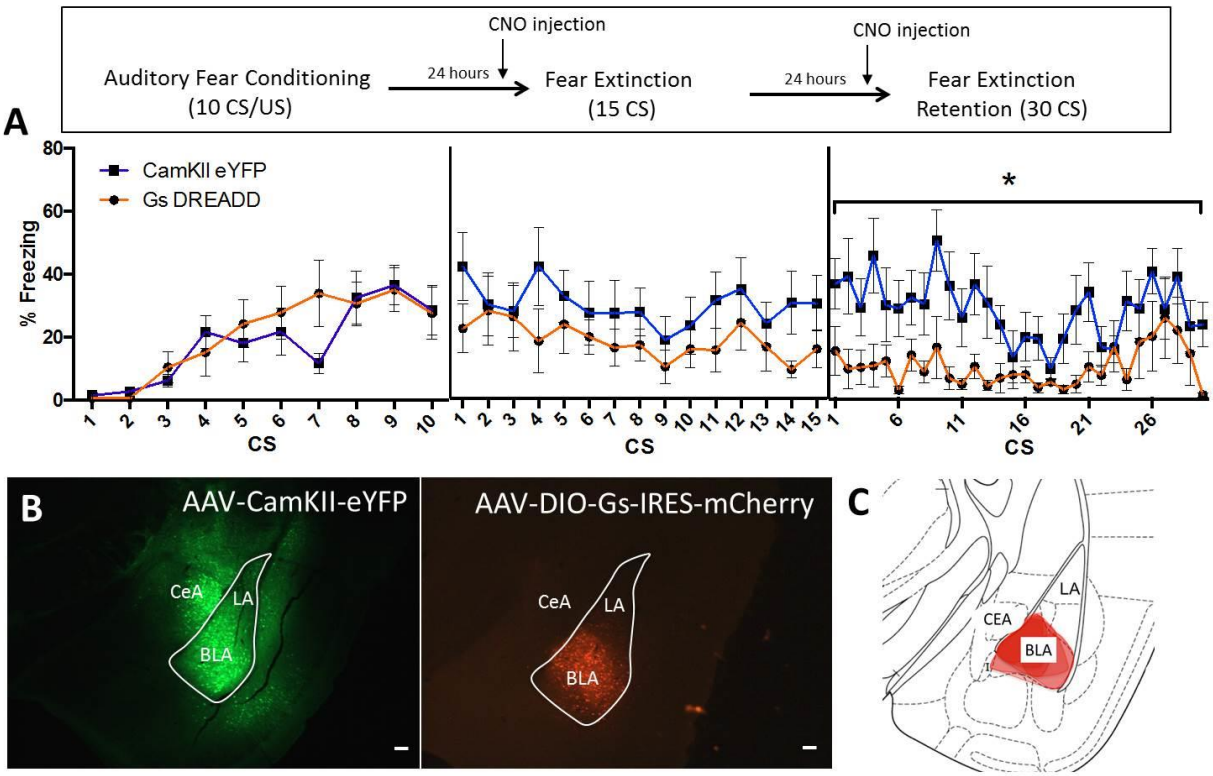

Figure 4-4. Enhancing excitability of BLA Thy1 neurons using DREADDs.

Mice harboring the Thy1-cre gene were infected with AAV-EF1a-DIO-rM3D (Gs)-mCherry or control virus AAV-CamKII-eYFP. Mice were auditory fear conditioned then administered Clozapine-N-Oxide 30 minutes before fear extinction and fear extinction retention sessions. **A.** Tonic enhancement of excitability of BLA Thy-1 neurons during fear extinction enhances consolidation of learned extinction as measured 24-hours later during fear extinction session (Two-way RM ANOVA, $F_{(1,14)} = 6.200$, $p < .05$). **B.** Location of Gs DREADD or control virus is visualized using mCherry or YFP tag. Cre-dependent recombination causes expression of Gs-DREADD-mCherry to be isolated to BLA Thy1 neurons while control virus has widespread expression throughout amygdala. Scale Bar = 100um. **C.** Depiction of aggregated expression patterns in left BLA of strong cre-dependent mCherry expression at

-1.8 DV in AAV-EF1a-DIO-rM3D (Gs)-mCherry infused animals. Scale Bar = 100um. In all panels Error Bars indicate mean +/- s.e.m.

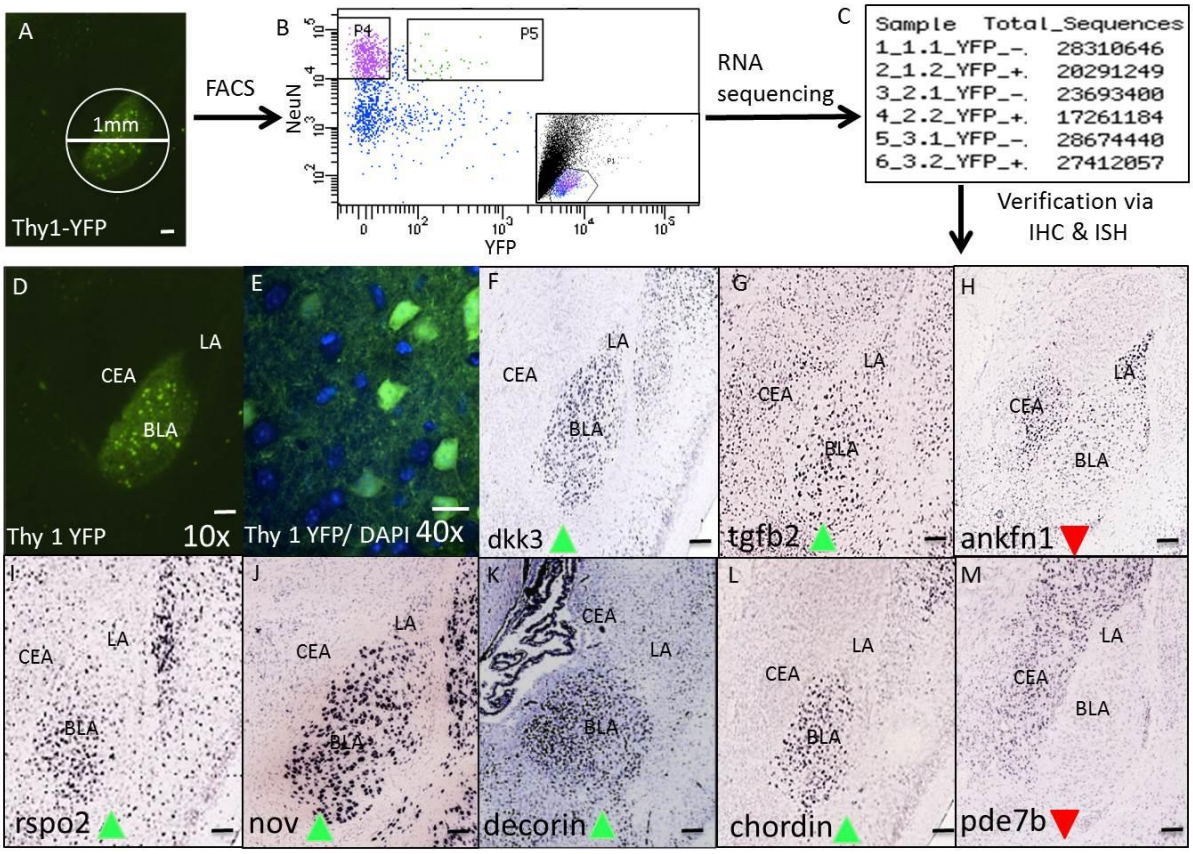

Figure 4-5. Workflow describing FACS sorting and sequencing of RNA of Thy1-eYFP cell bodies Cell-type specific RNA sequencing and identification of differentially regulated gene transcripts.

A. Schematic indicating location of tissue punch. The bilateral amygdala of Thy1-eYFP mice were obtained via bilateral 1mm punches centered over the basolateral amygdala. These tissue samples were dissociated into single cell suspensions, fixed and stained for neuronal marker, NeuN. Cell suspensions were sorted based on fluorescent profiles and NeuN+/YFP– and NeuN+/YFP + populations were collected for RNA analysis. **B.**

Representative scatterplot generated during FACS. Box P4 indicates NeuN+/YFP- events, Box P5 indicates NeuN+/YFP+ events. Inset: representative FSC/SSC; neuron cell bodies were present in small population at bottom. **C.** Chart demonstrating total number of sequences yielded with RNAseq collected by each sample with FACS. **D.** Image of YFP expression in Thy1-YFP mouse amygdala Scale Bar =100um. **E.** 40x magnification of Thy1-YFP expression demonstrating that only a subset of cell bodies (indicated by DAPI; blue) express YFP (Green) Scale Bar = 20um. **F-M** Examples of genes identified as differentially regulated. RNA sequencing yielded a list of hundreds of differentially regulated genes. After refinement using a predetermined set of exclusion criteria (see Supplementary Figure 3) RNA expression patterns of genes were examined using the Allen Brain Map for enriched expression within the BLA. Green arrows indicate genes up regulated in Thy1-eYFP neurons vs. all other neurons (*Dkk3, Tgfb, Rspo2, Nov, Dcn*, and *Chrd*). Red arrows indicate genes down regulated in Thy1-eYFP neurons vs. all other neurons (*Ankfn1* and *Pde7)*. Image Credit: Allen Institute (; 2; 3; 4; 5; 6; 7). Scale Bar = approximately 100um.

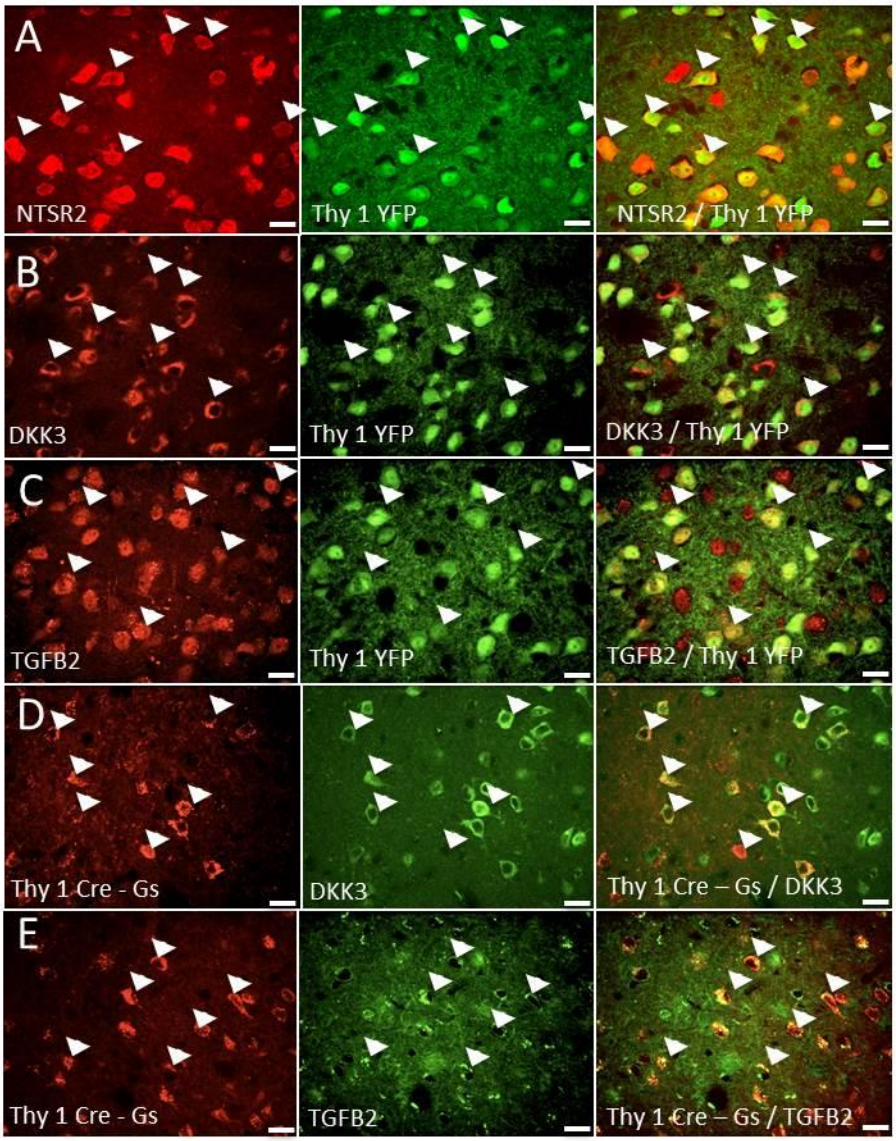

Figure 4-6. Molecular characterization of basolateral amygdala Thy1 neurons.

Examination of co-localization with protein products of identified differentially expressed genes. Molecular characterization of Thy1-eYFP expressing neurons of the basolateral amygdala was completed on tissue from Thy1-eYFP line H mice. Coronal sections were stained for protein of interested using immunohistochemistry visualized using secondary antibodies emitting in the red spectrum. Thy1-eYFP strongly co-localizes with **A.** NTSR2 **B.** DKK3 **C.** TGFB2. Tissue taken from Thy1-Cre expressing animals infused bilaterally with

AAV-EF1a-DIO-rM3D (Gs)-mCherry allows visualization (red) of Thy1-Cre expressing neurons. Coronal sections of this tissue was stained above for **D.** DKK3 and **E.** TGFB2 revealing that these markers co-localize to similar extent with both Thy1-eYFP and Thy1-Cre. All. Scale Bar = 20um.

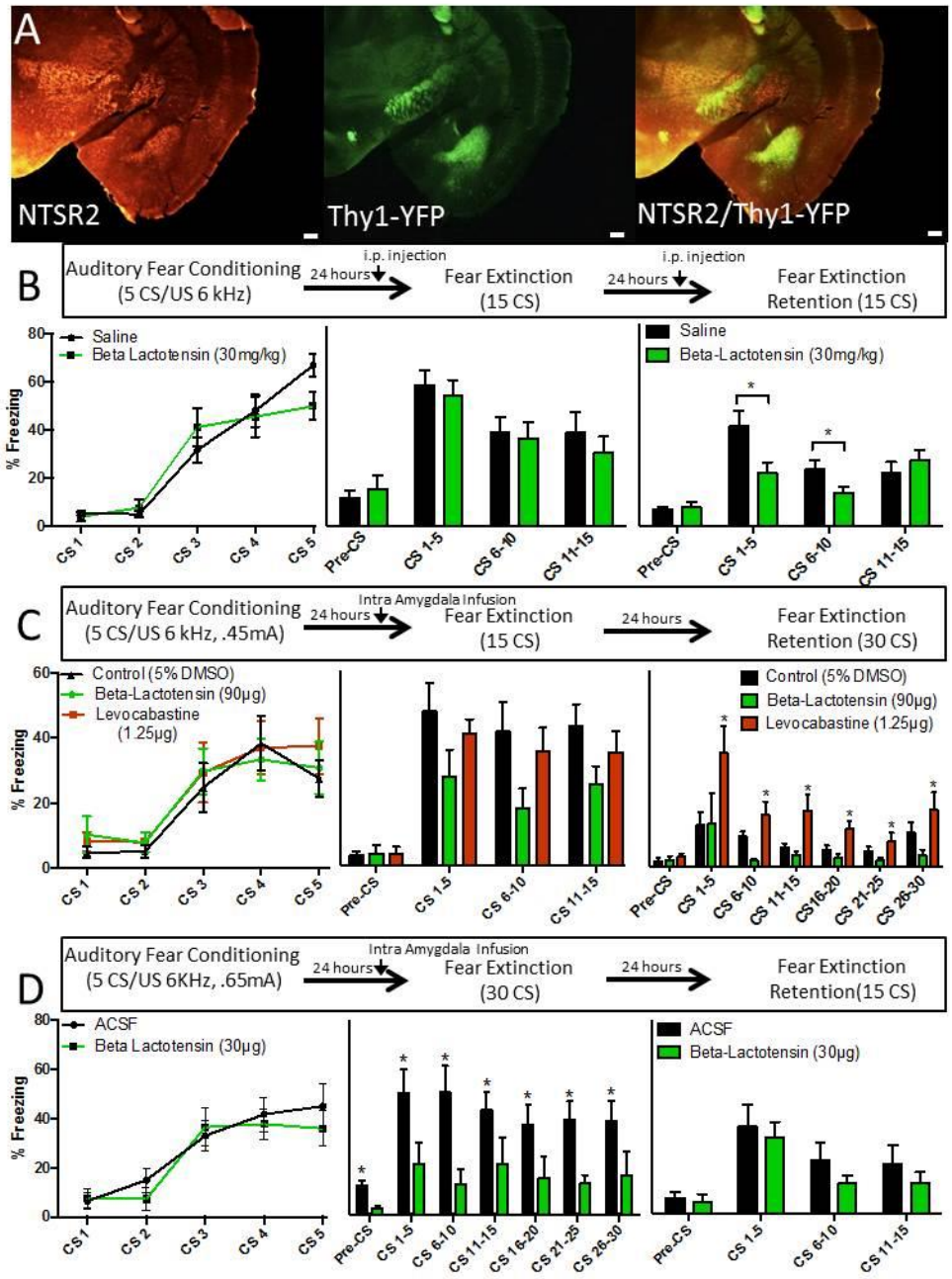

Figure 4-7. Modulating Neurotensin Receptor 2 activity alters fear expression and consolidation.

A. Regionally NTSR2 has an overlapping regional expression pattern to Thy1-eYFP along the rostral-caudal axis of the amygdala. Scale Bar = 200 um. **B.** Beta-Lactotensin, a NTSR2 agonist, was given i.p. 2 at hours before fear extinction and fear extinction retention sessions. This enhanced consolidation of fear extinction as measured by significantly decreased fear expression during first 10 CS presentations of fear extinction retention session (Two-way RM ANOVA, $F_{(1,19)}= 5.39$, *=$p < .05$). **C.** Intra-amygdala infusion of 90µg per hemisphere Beta-Lactotensin 30 minutes before fear extinction test yields near significant decreases in within session freezing expression (Two-way RM ANOVA, $F_{(2,32)}= 2.707$, $p = .085$); however, infusion of 1.5 µg per hemisphere Levocabastine causes no within session effects, but blunts fear extinction consolidation as measured by increased freezing during fear extinction retention session (Two-way RM ANOVA, $F_{(2,20)}= 6.633$, $p < .01$, Dunnetts multiple comparison test vs. control * = $p < .05$). **D.** To ensure prior training did not cause previous results, and to test a lower dose of drug, naïve animals received bilateral infusion of 30µg per hemisphere Beta-Lactotensin or saline control. Infusion of this lower dose of Beta-Lactotensin again resulted in dramatic reductions in within session freezing (Two-way RM ANOVA, $F_{(1,9)}= 13.28$, *= $p < .01$). In all panels Error Bars indicate mean +/- s.e.m.

4.8 Supplemental Discussion

Across mouse lines, the Thy1 expression cassette causes transgene expression in convergent populations of neurons. It is important to acknowledge that the generation of

Thy1 transgenic lines by insertion of the Thy1.2 expression cassette can yield mice with drastically different transgene expression patterns (Feng et al., 2000). The most well characterized Thy1-eYFP line, line-H, has strong expression in layer 5/6 cortical neurons as well as hippocampal and amygdala populations (Porrero et al., 2010). It is likely that similar expression patterns across mouse lines result from coincidental marking of a common developmental population originating from the pallial zones of the telencephalon (Porrero et al., 2010). Thus, we do not claim that Thy1 is a marker of the amygdala Fear-Off population, but rather that these mouse lines conveniently mark a common developmental population generating a population of neurons including the Fear-Off pyramidal neurons within the BLA in adulthood. Previously, using ISH and IHC we have demonstrated that both the Thy1-ChR2 and Thy1-eYFP lines mark a subset of CaMKII expressing excitatory neurons (Jasnow 2013). These lines do not mark the entire excitatory population of the BLA; however, a large proportion of the total population is marked.

Characterization of Thy1-Cre expression patterns using post-natal Cre-recombinase dependent reporter viruses revealed expression patterns consistent with other lines. However, limited expression in the BLA of Thy1-Cre mice contrasts with the original characterization of this line and our own characterizations using developmentally available Cre-recombinase dependent reporter lines (*data not shown*). These expression patterns suggest that the Thy1 cassette is expressed much more promiscuously in the Thy1-Cre line during development, but takes on a more constrained expression pattern during adulthood. The use of reporter viruses to characterize Cre-recombinase expression provides further evidence to support the above observation. AAV-hSyn-DIO-rM3D (Gs)-mCherry and AAV-EIF1-DIO-mCherry were each infused separately into the BLA of Thy1-Cre or Thy1-

eYFP/Thy1-Cre mice respectively. The resulting expression from an hSyn promoter was primarily constrained to the BLA. EF1a promoter virus produces strong BLA expression as well as weaker expression in a medial LA population and a small population in the capsular region of the CeA (Figure S14). It is likely that the Thy1.2 cassette is able to drive some basal expression in most neurons, but surrounding control regions limit significant expression to the previously discussed developmental population. Expression patterns detected in Thy1-Cre mice indicate that the Thy1 promoter drives Cre-Recombinase expression primarily in the described BLA pattern with some minimal expression in other neuron populations. As a single molecule of Cre-Recombinase may be sufficient to drive recombination, depending on the sensitivity of the viral construct, different expression patterns of fluorescent marker are revealed in the Thy1-Cre mouse. These observations, taken with convergent behavioral data across four Thy1 transgenic lines, suggests that Thy1 lines used in the present study mark a common regional population that contains fear inhibition circuitry.

On a technical note, crossing the Thy1-eYFP and Thy1-Cre mouse lines results in the appearance of a weak red fluorescent signal in all Thy1-eYFP labeled cells, even in the absence of red fluorescent reporter virus (Figure S15). This is easily distinguishable from transgenic mCherry expression described above, as it is quite weak and is found in Thy1-eYFP neurons throughout the brain. This signal likely results from a red shifting of a small percentage of transgenically expressed YFP. The cause of this red-shifting in unknown, but may result from a change in the intracellular conditions caused by the additive cellular stress of expressing two transgenes at high levels (Elowitz, Surette, Wolf, Stock, & Leibler, 1997).

Examination of c-fos expression after fear behaviors demonstrates that Thy1-eYFP labeled neurons are recruited specifically during fear extinction expression whereas unlabeled cells are recruited preferentially during fear expression. The necessity of these neurons is examined by using a Thy1-NpHR mouse to optogenetically silence Thy1 neurons during behavior. Inhibition of labeled Thy1 neurons during CS presentations within the fear conditioning session leads to enhanced fear consolidation as measured the next day during a fear expression test. Silencing Thy1 neurons during the fear expression session leads to within-session increases in fear expression as well as blunted fear extinction consolidation the next day during the unstimulated fear expression test. This is in contrast to reports that muscimol administration, pharmacologically inhibiting the basal amygdala and BMA, prior to training has no effect on behavior and prior to extinction prevents fear expression (Sierra-Mercado et al., 2011). However, more limited micro-iontophoresis of muscimol specifically into BLA does not produce within session effects, but does blunt fear extinction consolidation (Herry et al., 2008). Selective inhibition of Thy1 neurons appears to allow maintenance of activity of the previously silenced Fear-On circuitry. Thus, the fear circuit may be artificially unbalanced, and we observe enhanced within-session fear expression in addition to previously observed deficits in extinction consolidation. Optical inhibition is unilateral, thus we do not see complete lack of extinction consolidation, as the contralateral amygdala is fully functional. It is important to highlight the temporal specificity of this approach, where Thy1 neurons are silenced only during CS presentation, suggesting that it is specifically the association between the CS and US that is being over-expressed and over-consolidated.

The use of cell-type specific whole genome expression analysis allows in-depth interrogation of the molecular identity of a neural population of interest (Guez-Barber et al., 2011; Guez-Barber et al., 2012). Thy1-eYFP neurons were dissociated and sorted based upon their expression of a neuronal marker, NeuN, and Thy1 driven YFP. This allowed for the isolation of high quality RNA from a large number of Thy1-eYFP (YFP+, NeuN+) and other (YFP-, NeuN+) neurons. Of all cell bodies interrogated, 40% were NeuN positive while only ~2% were NeuN and YFP double positive. This approach has the advantage that the RNA sequencing data represents the average RNA content of Thy1-eYFP cells across the anterior-posterior axis of the amygdala as 8000-12,000 cells are isolated for each sample. However, because tissue punches likely contain cells from the CeA, LA, and BMA this method lacks the sensitivity to identify many transcripts specifically down-regulated in non-Thy1 neurons of the BLA that may have divergent functional roles. Furthermore by homogenizing non-Thy1-eYFP neurons into a single group this method washes out many differences between Thy1 neurons and other specific nuclei of the amygdala.

RNA sequencing yielded hundreds of transcripts that are differentially regulated between the Thy1-eYFP and other amygdala neurons. These were prioritized based upon a workflow designed to identify transcripts specifically upregulated in BLA Thy1 neurons that have previously been associated with pharmacological modulators (Figure S3). Of those examined for protein expression patterns, *Tgfb2* (Fukushima, Liu, & Byrne, 2007) and *Dcn* (Esmaeili, Berry, Logan, & Ahmed, 2014) have complex interactions with TGF-Beta signaling, cell cycle and axon growth; *Wnt7a* (Fernando et al., 2014), *Dkk3 (Diep, Hoen, Backman, Machon, & Krauss, 2004),* and *Rspo*-2 (Kazanskaya et al., 2004) regulate wnt/Beta-catenin signaling previously associated with fear modulation (Maguschak &

Ressler, 2008), as well as synaptic remodeling and plasticity, and possibly bipolar disorder; and *Ntsr2* (Ferraro et al., 2008) has complex signaling roles that influence the neuroendocrine and dopamine systems.

Examination of the protein products of these genes using immunohistochemistry revealed consistent regional overlap with Thy1 neurons. Importantly, although all genes had strong expression within the BLA, the extra amygdala expression patterns varied widely, suggesting that overlapping expression is a feature unique to BLA neurons. When investigated at a cellular level, all proteins examined had almost complete overlap with Thy1-eYFP expressing neurons although all marked some non-YFP expressing cells as well, suggesting that Thy1-eYFP marks a sub-set of these neurons. Quantification of co-localization was performed so that a 20μm thick slice was analyzed and labeled cells intersecting top (Z-axis) plane and two sides of the image were not counted (Figure S6). Tissue used in DREADD experiments was stained for DKK3 and TGFB2 demonstrating that Thy1-Cre neurons similarly co-localize with these markers. Overall, immunolabeling suggests expression diversity within BLA neurons representing what may amount to a hierarchical system that delineates functionally divergent sub-populations. Importantly, when co-localization was examined with Thy1-eYFP neuron images taken in areas of strong YFP expression, many genes maintained expression outside the strict BLA pattern seen in Thy1-eYFP; therefore, counts of co-localization only apply to the BLA.

Data presented here demonstrate functional and molecular characterization of the BLA Thy1 population and identifies NTSR2 as a possible functional marker of a BLA Fear-Off population. Across several Thy1 transgenic lines, strong overlap in regional and cellular expression was observed. Manipulation using optogenetics and chemogenetics confirmed a

consistent functional role in behavior suggesting that the Thy1 labeled neurons contain a BLA Fear-Off population. Genetic tracing reveals projection patterns to NAc, mPFC and ITCm, avoiding CeA, consistent with a Fear-Off / positive valence circuit. Isolation and RNA profiling of Thy1-eYFP neurons revealed a number of candidate genes that are upregulated in Thy1 neurons. Neurotensin Receptor 2 is strongly expressed in all Thy1-eYFP neurons and pharmacological manipulation using agonists or antagonists is able to enhance or suppress freezing respectively. These findings confirm that NTSR2, like Thy1, labels a population of the BLA containing functional Fear-Off circuitry, and activating the NTSR2 population may provide a novel approach to the clinical reduction of fear and enhancement of fear extinction.

4.9 Supplemental Figures

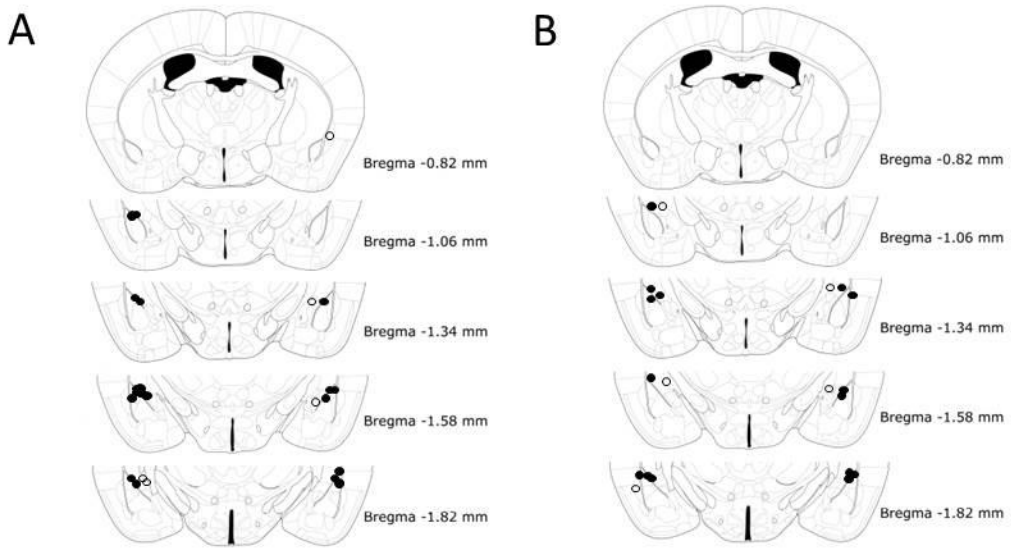

Supplemental Figure 4-1. Schematic of fiber optic fiber tip placement.

Schematic of locations of fiber optic tip location for **A.** inhibition with yellow laser light during fear acquisition and **B.** inhibition with yellow laser light during fear extinction sessions. Hits scored marked by filled circles and misses marked as open circles.

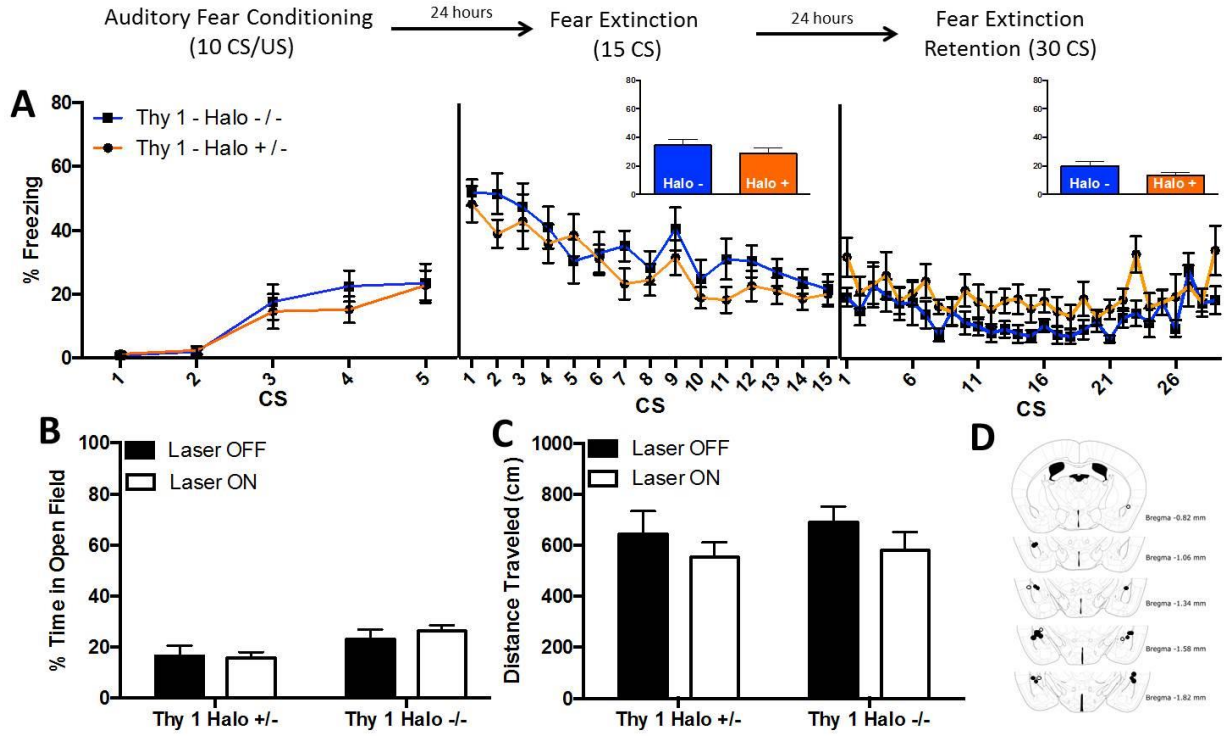

Supplemental Figure 4-2. Genetic effects are not responsible for changes in fear expression of Thy1-eNpHR mice.

A. Thy1-eNpHR carriers and non-carrier littermates that were cannulated and fear conditioned do not express any differences in fear behaviors in the absence of light stimulation. **B.** Mice exhibit no differences in anxiety like behavior as indicated by similar time spent in the center of an open field chamber regardless of genotype or status of laser (ON or OFF). **C.** Mice exhibit no differences distance traveled in open field chamber regardless of genotype or status of laser (ON or OFF). **D.** Schematic of fiber optic tip placement. Hits scored marked by filled circles and misses marked as open circles.

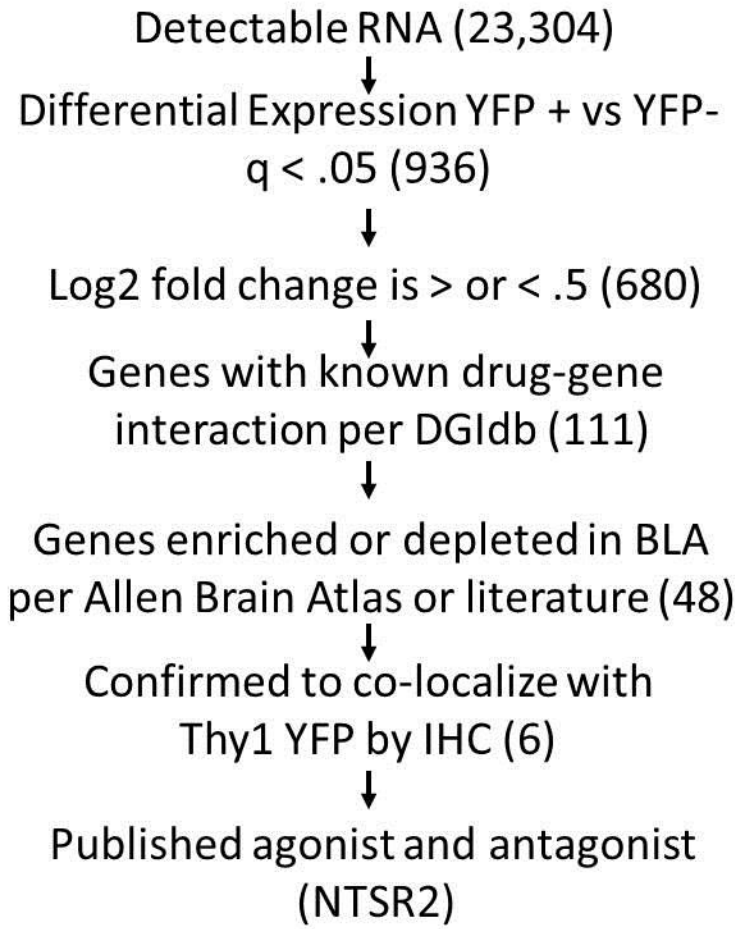

Supplemental Figure 4-3. Flow chart of strategy for analysis of RNA sequencing differential expression data.

First, only highly significant genes were taken so that any difference score with q>.05 was discarded. Next, only genes whose expression differed from control by more than 2^.5 were taken. Genes of interest were entered into the DGIdb drug-gene interaction tool and any gene without a pharmacological modulator was discarded. Genes on resulting list were examined for expression patterns on the Allen Brain Atlas or in the published literature. Those with visibly enriched expression in one or more amygdalar nuclei were selected. Finally based upon the previous two criteria, genes were chosen for protein analysis with

immunohistochemistry. NTSR2 was selected for pharmacological analysis based upon published reports of both an agonist and antagonist.

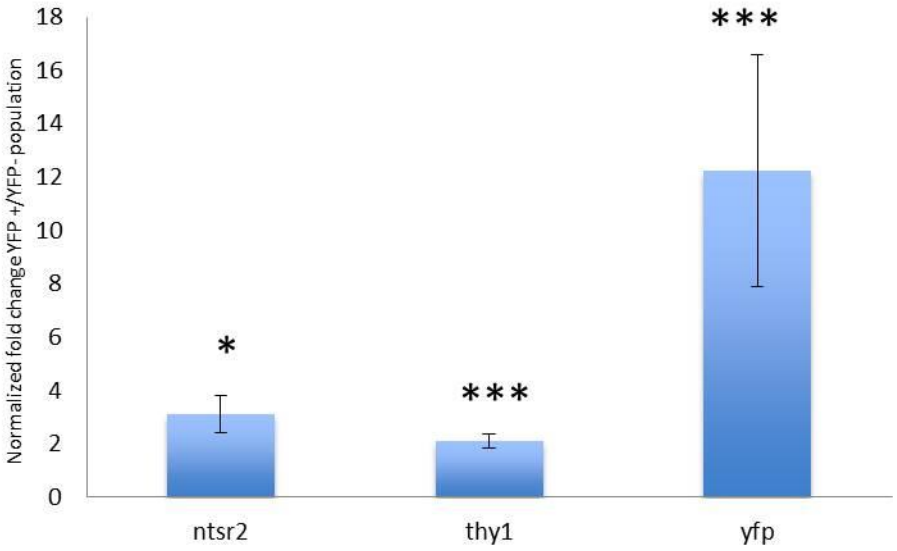

Supplemental Figure 4-4. Replication of RNA sequencing results with qPCR.

Amplified cDNA generated from RNA taken from FACS sorted neurons was analyzed with qPCR. Resulting fold changes of gene expression in RNA taken from YFP positive neurons vs. YFP negative neurons are represented in bar graph.

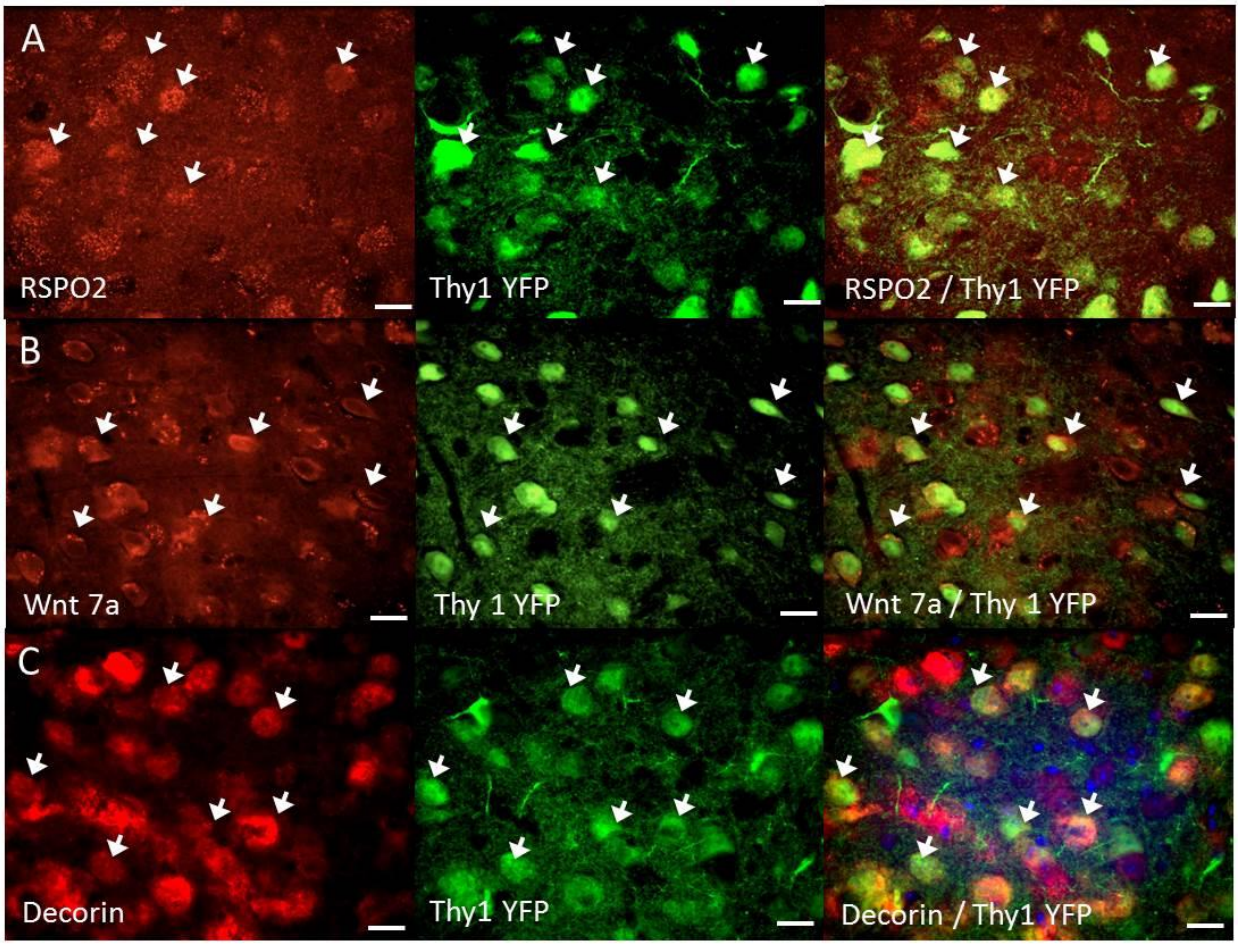

Supplemental Figure 4-5. Co-localization of Thy1-eYFP with additional differentially expressed genes.

Molecular characterization of Thy1-eYFP expressing neurons of the basolateral amygdala was completed on tissue from Thy1-eYFP line H mice. Coronal sections were stained for protein of interested using immunohistochemistry visualized using secondary antibodies emitting in the red spectrum. Thy1-eYFP strongly co-localizes with **A.** RSPO2, **B.** Wnt 7a, and **C.** Decorin. Images were captured using a confocal microscope.

	YFP + DAPI	DAPI alone
Thy 1 YFP vs. DAPI	17.1	83.5

B

Protein of Interest	P+ / YFP-	P+ /YFP +	P- / YFP+
TGFB2	9.8	15.6	.2
Dkk3	4.3	16.8	0
Wnt 7a	6.6	16.4	0
NTSR2	3.6	17.3	0
RSPO2	3.8	17.1	0.1
Decorin	4.7	18.8	0.2

Counts of expression presented as raw averages of counts per field examined.

C

	YFP +
Thy 1 YFP vs. DAPI	100%

Protein of Interest	P+ / YFP-	P+ /YFP +	P- / YFP+
TGFB2	38.3%	60.9%	0.7%
Dkk3	20.4%	79.6%	0%
Wnt 7a	28.7%	71.3%	0%
NTSR2	17.2%	82.8%	0%
RSPO2	18.1%	81.4%	0.4%
Decorin	19.8%	79.3%	0.8%

Counts of expression presented as a percentage of total fluorescent positive cells counted (X/((P+) + (YFP+))).

Supplemental Figure 4-6. Quantification of co-localization between Thy1-eYFP and additional proteins of interest.

Immunoreactivity was analyzed in a volumetric manner using confocal microcopy where neurons intersecting with the proximal Z-plane and two boarders were excluded. Cells expressing either green or red fluorescence were counted as single positive respectively

while cells expressing both red and green fluorescence were counted as double positive. Single positive Thy1-eYFP and gene of interest neurons were counted as well as double positive neurons. Counts represent the average number (n=15) of fluorescent neurons counted per stack.

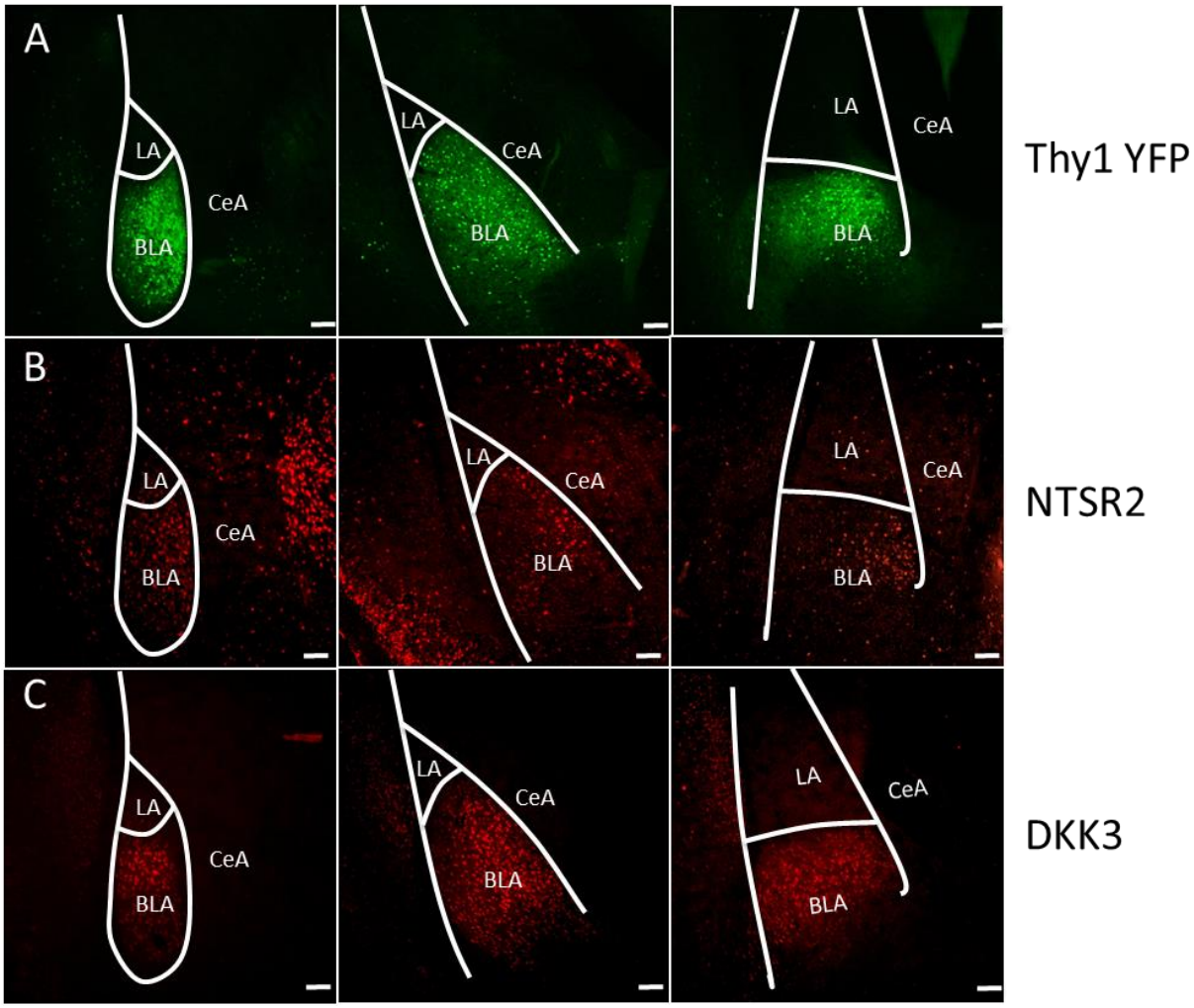

Supplemental Figure 4-7. Regional similarities in Thy1-eYFP, NTSR2, and DKK3 expression.

Images were captured at lower magnification across the anterior-posterior axis of the amygdala. Both **B.** NTSR2 and **C.** DKK3 have similar expression patterns to Thy1-eYFP across the length of the amygdala.

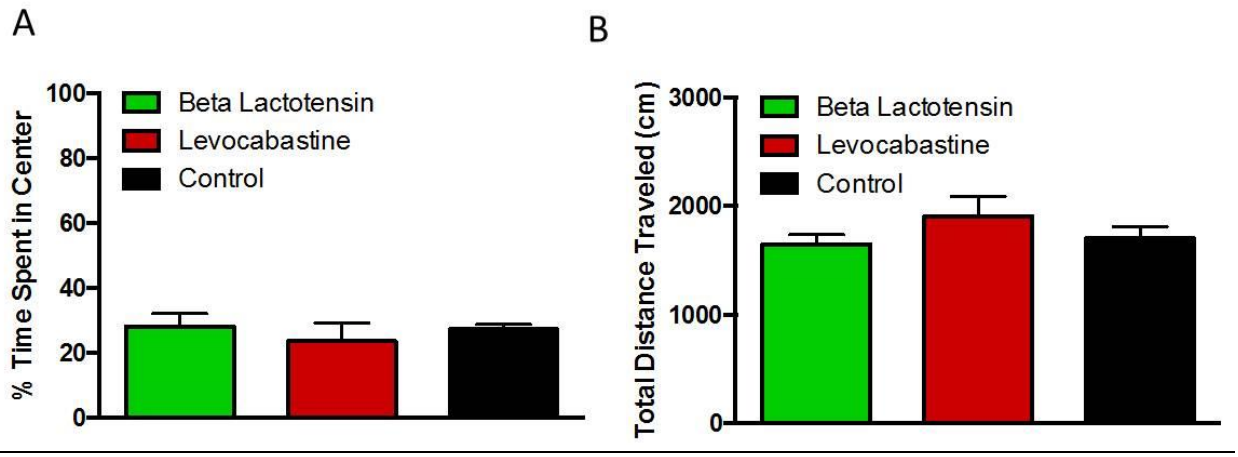

Supplemental Figure 4-8. Differences in fear behavior after drug delivery are not due to anxiety like behavior after drug administration.

Mice infused with Beta-Lactotensin, Levocabastine or vehicle 30 minutes before being placed in Open-Field box for 10 minutes express no differences in **A.** time spent in center or **B.** total distance traveled throughout 10 minute session were detected.

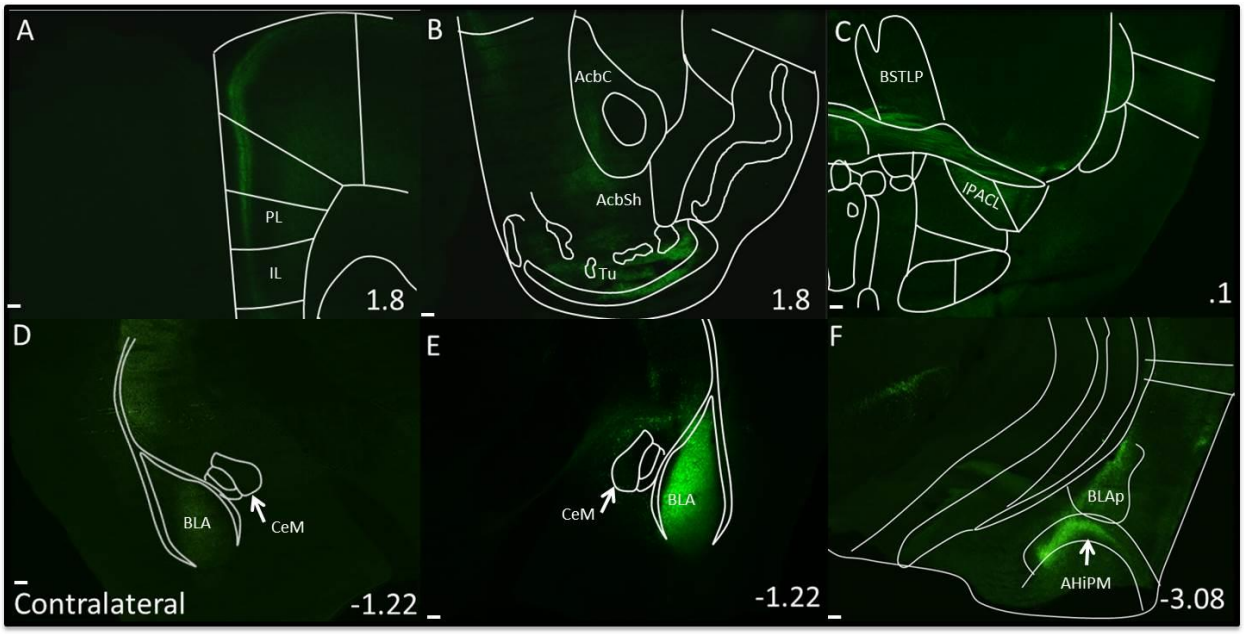

Supplemental Figure 4-9. Infusion of AAV-DIO-YFP into Anterior BLA Thy1-Cre mouse.

Infusions of AAV-DIO-YFP centered on the anterior aspect of the BLA (-1.0 A/P) label populations that have moderate projections to the superficial layers of the PFC (**A)** and the NAc (**B)**. Also observed are moderate projections to elements of the bed nucleus of the stria teminalis (BNST), the claustrum and the anterior insula (AI) (**C**). Additional fluorescence can be found in the contralateral BLA (**D**) and caudally in the posterior medial amygdalohippocampal area (**F**). Cell bodies are labeled around infusion site (**E**)

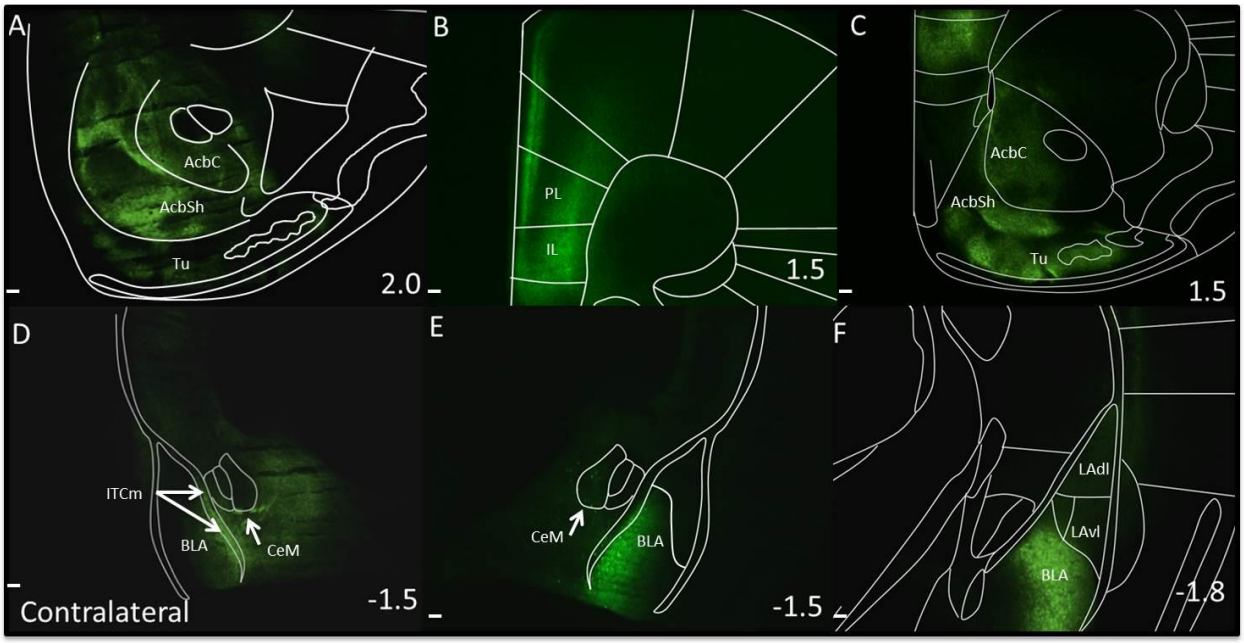
A
AcbC
AcbSh
Tu
2.0
B
PL
IL
1.5
C
AcbC
AcbSh
Tu
1.5
D
ITCm
BLA
CeM
Contralateral
-1.5
E
CeM
BLA
-1.5
F
LAdl
LAvl
BLA
-1.8

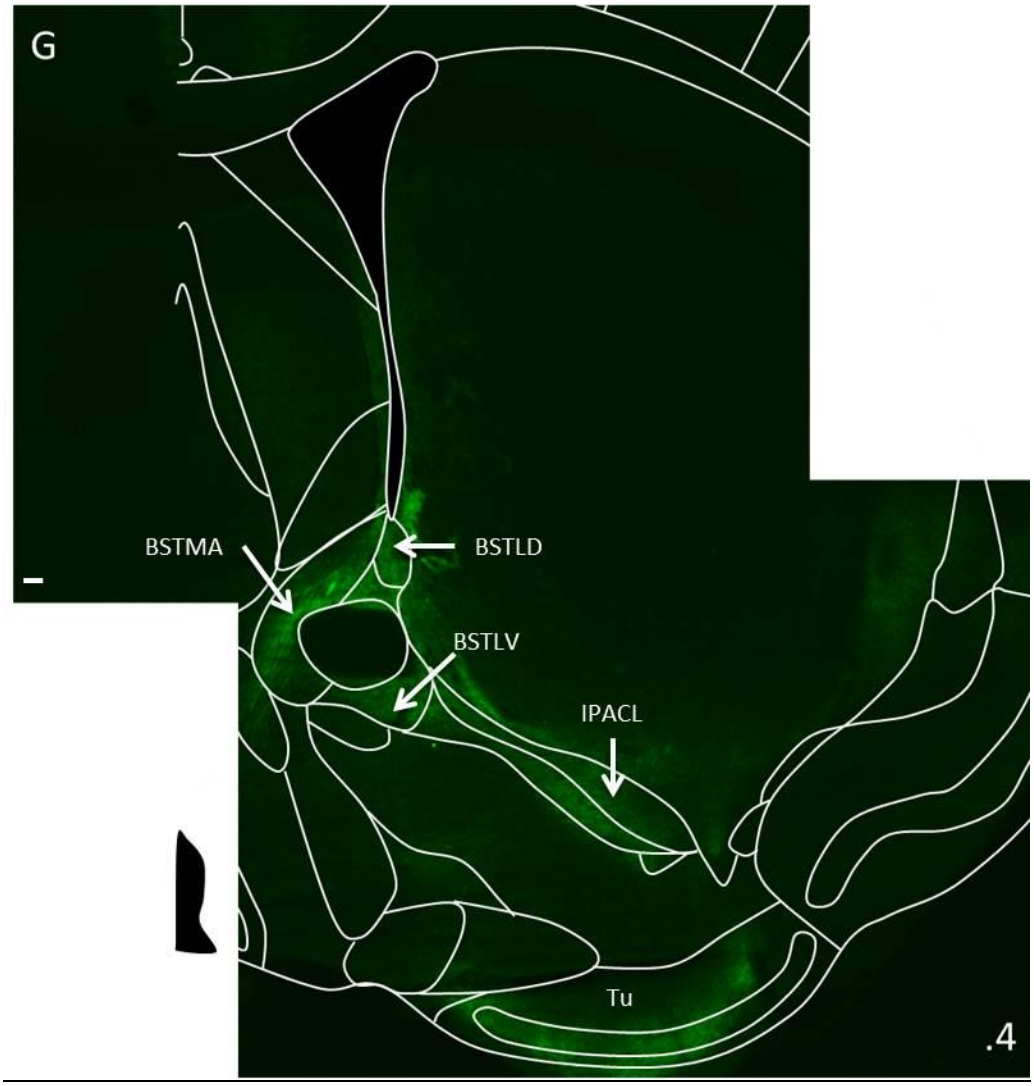

Supplemental Figure 4-10. Infusion of AAV-DIO-YFP into BLA Thy1-Cre mouse.

Infusions of AAV-DIO-YFP at -1.5 A/P label populations that project very strongly to the NAc (**A** and **C**). Projections the superficial layers of the PFC remain although there are additional projections to the deeper layers of the vmPFC (**B**). Interestingly, these infusions appear to mark neurons that project very strongly to the contralateral ITC, BLA and MeA (**D**). Projections from marked neurons project strongly to several regions of the BNST (**G**). Cell bodies are labeled around infusion site (**E** and **F**).

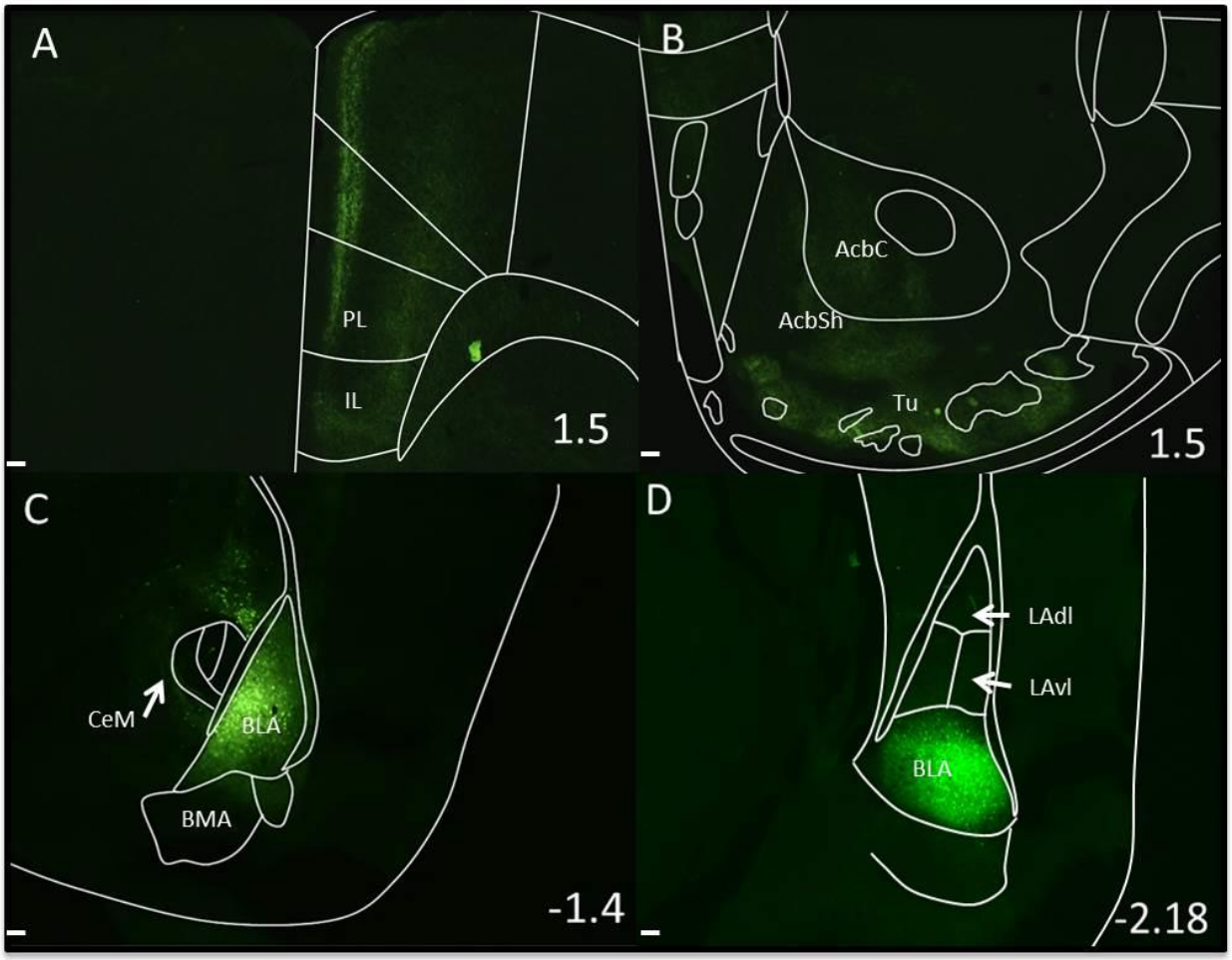

Supplemental Figure 4-11. Infusion of AAV-DIO-YFP into Posterior BLA Thy1-Cre mouse.

Infusions of AAV-DIO-YFP into the caudal aspect of the BLA (-2.0 A/P) label populations that project to the superficial layers of the PFC as well as to the deeper layers of the vmPFC (**A**). Labeled neurons additionally project to the NAc (**B**). Cell bodies are labeled around infusion site (**C** and **D**).

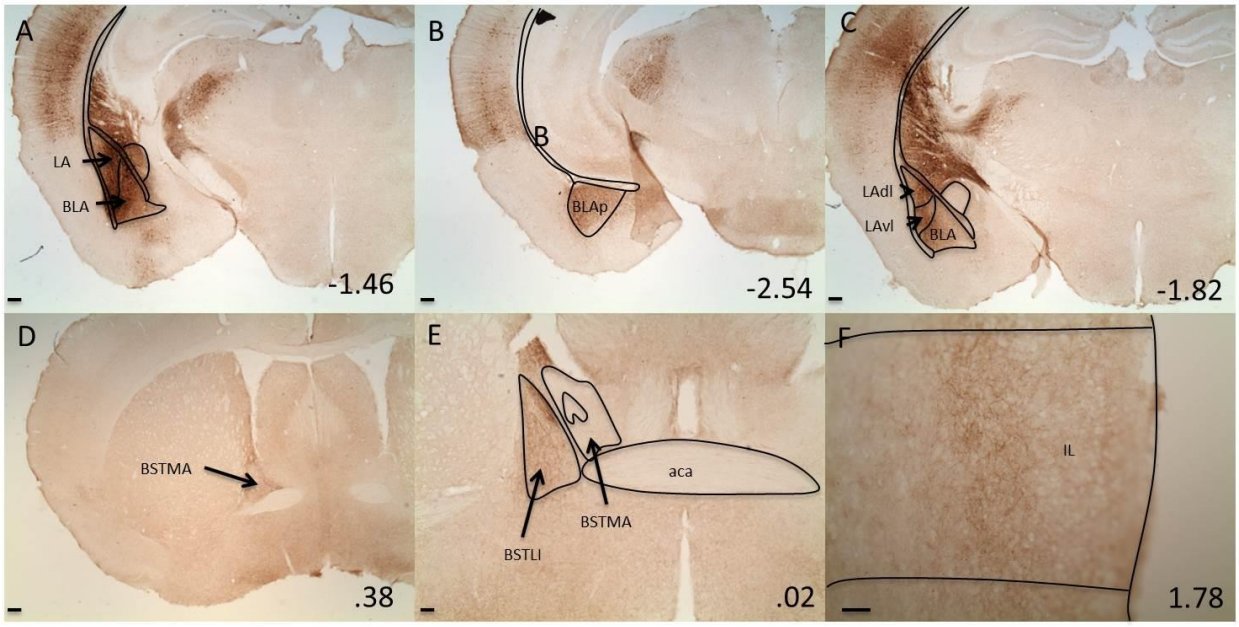

Supplemental Figure 4-12. Infusion of BDA into Anterior BLA.

Infusions of BDA (light field) into anterior aspect of BLA (-1.5 A/P) label populations with strong projections to posterior elements of the BLP. Infusion site (**A** and **C**). Some projections can be found in some nuclei of BNST (**D** and **E**). Moderate numbers of projections are observed in infralimbic cortex (**F**).

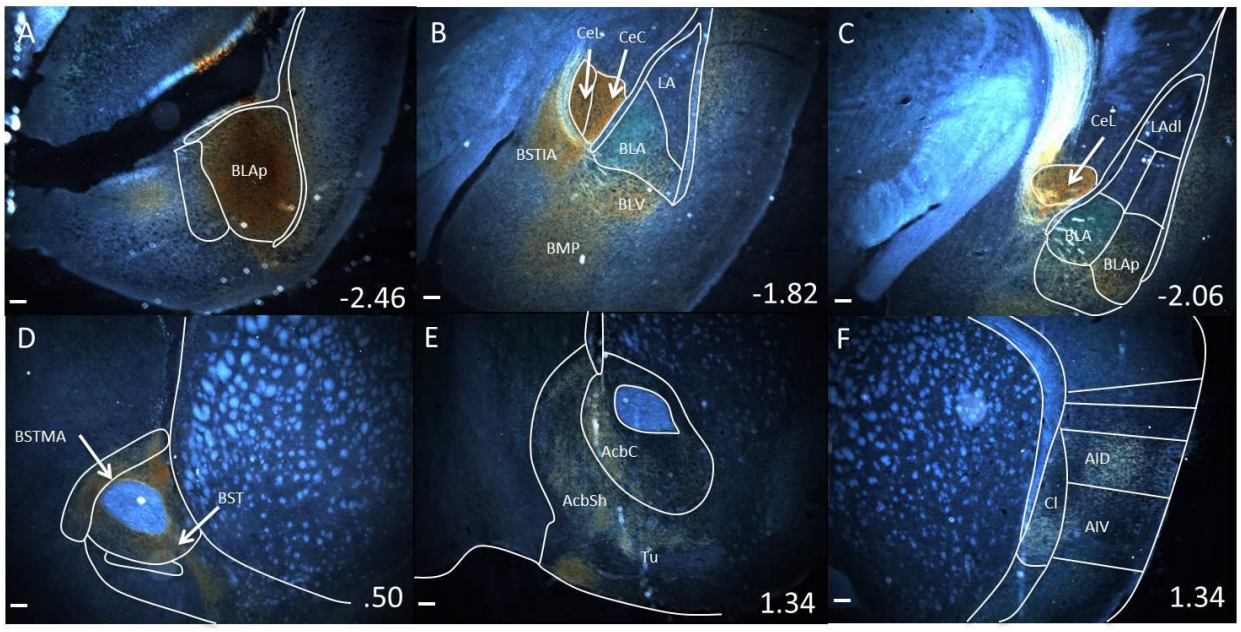

Supplemental Figure 4-13. Infusion of BDA into Posterior BLA.

Infusion of BDA (dark field) into posterior aspect of BLA (-2.5). Site of infusion (**A**). BDA labels a population with strong projections to the CeA (**B** and **C**). Strong projections to the BNST (**D**), NAc (**E**) and anterior insula (**F**) are also observed.

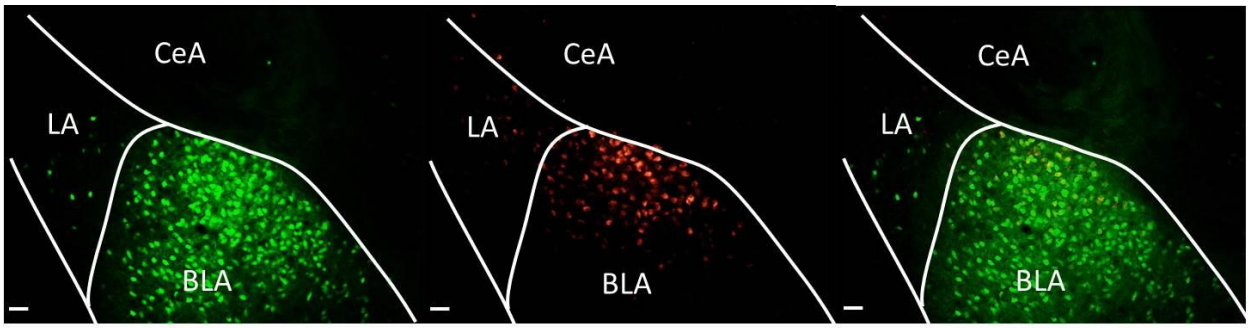

Supplemental Figure 4-14. Regional specificity of cre-recombinase mediated mCherry expression.

Cre-dependent mCherry expression resulting from infusion of AAV-EF1a-DIO-mCherry into Thy1-cre mouse. mCherry expression is observed strongly in BLA as well as weakly in the LA and a Paracapsular region of the CeA.

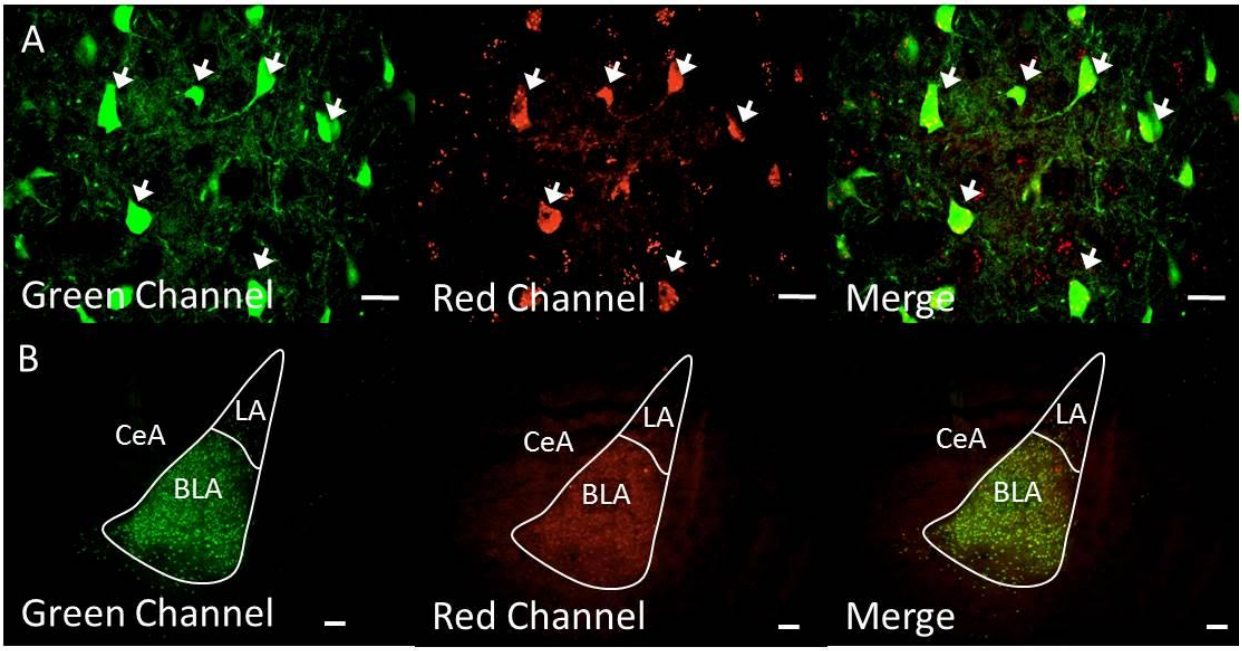

Supplemental Figure 4-15. Double transgenic Thy1-eYFP/ Thy1-Cre mice have red-shifted expression in Thy1-eYFP neurons.

Examination of tissue from double transgenic mice reveals the presence of a red-emitting fluorophore that completely overlaps with Thy1-eYFP expression at a **A.** cellular level and **B.** regional level. This expression is detected in all Thy1-eYFP neurons throughout the brain.

Chapter 5: Conclusion, Discussion and Future Directions.

5.1 Summary of Results

Findings presented in Chapter 2 represent a significant and necessary step towards a complete understanding of the identities of sub-populations present in the CeA. Our findings indicate that expression of *Prkcd* and *Drd2* are found primarily in the CeC and CeL. These markers do not extensively co-express with any other marker examined in any sub-nuclei of the CeA. Conversely, *Sst, Nts, Tac2,* and *Crf* labeled cells are found primarily in the CeL and CeM. These populations overlap extensively within the CeL but not within the CeM. Statistical analysis reveals that within the CeL, *Nts, Tac2,* and *Crf* populations are not significantly different from the *Sst* population. This suggests that the *Sst* population may contain, to a great extent, the other three gene markers. Interestingly, *Sst, Nts, Tac2,* and *Crf* do not extensively co-express with *Prkcd* or *Drd2,* confirming reports in the literature that these populations are distinct.

Findings in Chapter 3 provide an in-depth behavioral and molecular characterization of CeA *Drd2* neurons. Evidence presented in Chapter 2 suggests this population is not the same as any others examined to this point and thus may play a distinct role in behavior. *Drd2* was found primarily within the CeC and CeL in contrast to *Drd1*, which is found in the CeM, ITCs and BLA. Chemogenetic activation of *Drd2* neurons reveals these neurons to have a fear-promoting phenotype supporting fear expression and blocking fear extinction. Profiling of changes in actively translating RNAs following fear conditioning produces a set of high quality targets for cell-type specific, learning-specific pharmacological manipulation of this population. Pharmacological manipulation of D2R and of $A_{2A}R$ confirm the profile of *Drd2* neuron function generated through chemogenetic

activation, mainly that activity in this population is sufficient and necessary for fear expression and is sufficient to block fear extinction.

Findings in Chapter 4 approach an additional population found in the BLA, The Thy-1 population. This population had previously been identified to block fear learning and enhance extinction suggesting it may have a role as a fear inhibiting population. Further optogenetic and chemogenetic manipulation of this population confirms this initial finding. Profiling of RNA specifically collected from Thy-1 neurons compared to RNA from all other neurons in the amygdala generates an in-depth expression profile of this population. Co-staining for proteins identified to be up-regulated in the Thy-1 population confirms the quality and specificity of findings. Pharmacological manipulation of one of these receptors, NTSR2, recapitulates the fear suppression profile initially identified using direct optogenetic and chemogenetic manipulation.

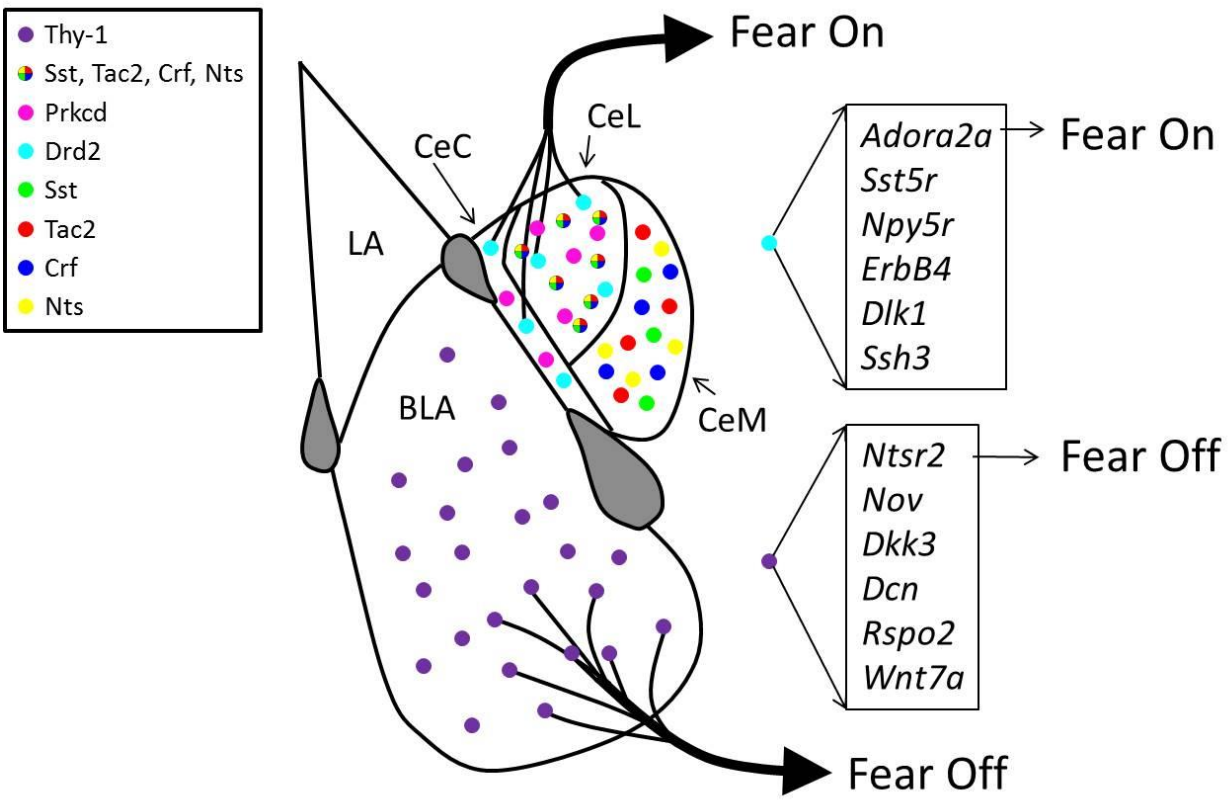

Figure 5-1. Summary of Findings.

5.2 Integration of Findings

Findings presented in Chapter 2 are especially pertinent to those found in Chapter 3 and elsewhere in the literature. Several groups have described cell-type specific manipulations and electrophysiological characterizations of CeA populations that appear to have distinct roles in fear behavior. However, limited work has been completed to confirm that these populations are indeed unique and not simply a replication of previous work. Data from Chapter 2 suggests that within the CeL, researchers must be especially careful to differentiate between CeL and CeM neurons as many of the populations examined within the CeL extensively overlap. Importantly, the *Drd2* population was not found to extensively overlap with other populations of interest suggesting that findings obtained by manipulating this population are unique.

Important differences between the approaches taken in Chapter 3 and Chapter 4 limit the direct comparison of results presented in those sections. Each approach taken to isolate RNA from populations of interest has significant advantages. Isolation of whole cell RNA, as was done in Chapter 4, gives a complete picture of the expression profile of those neurons compared to others in the area. On the other hand, isolation of transcripts being actively transcribed has the advantage of giving an extremely temporally precise snapshot of the transcriptional activity of a cell at the time of sacrifice. This technique is very useful when interrogating changes in neuron transcription and translation following a behavioral learning event. This may lead to the identification of more translationally robust pharmacological targets as the most common time point for pharmacological intervention is following trauma or therapy.

5.3 Future Directions

Data presented here represents first steps in characterization of amygdala sub-populations.

Future experiments examining sub-populations of CeA neurons will take three important forms. First, additional markers of sub-populations will be examined for co-expression with previously examined markers. These should include many additional neuropeptides such as enkephalins and endorphins as well as receptors for the signaling moieties already examined. Second, examination of dynamic changes in the levels of expression of examined RNAs following behavior. Important information may be gleaned regarding the function of the proteins encoded by examined RNAs when level of expression in each sub-nucleus is measured following fear or extinction learning. Third, dynamic circadian changes in RNA levels. Several of the proteins encoded by examined RNAs are

known to cycle with circadian phase. Changes in population overlap are possible if somewhat unlikely; however, precise measurement of changes in mRNA expression level throughout circadian phase will yield important information regarding its role in behavior.

Future experiments examining the CeA *Drd2* population should be focused on three primary goals. First, examination of the connectivity with other populations within the CeA will reveal how this population functions in behavior and how it fits into current hypothetical CeA circuitries. Second, additional in-depth examination of the behavioral function of this population during fear, anxiety-like and appetitive behavior using optogenetic, chemogenetic and pharmacological manipulations. Data presented here demonstrate the role of these neurons in fear expression, but as dopamine has diverse roles in behavior and learning it is likely that these neurons play important roles in a variety of behaviors. Third, examination of additional identified, cell-type specific, differentially regulated genes. Many of the genes identified to be differentially regulated following fear conditioning are known to play important roles in cell function and behavior. Further examination of gene function in this population may yield valuable new tools for modulating fear behavior.

Future experiments examining the BLA Thy-1 population should focus most closely on two goals. First, examination of genes identified to be upregulated in this population for additional, translationally relevant targets for pharmacological manipulation will yield important information regarding avenues for increasing activity in fear controlling populations of the amygdala. Second, further examination of the specific projections of this population to other brain regions potentially involved in fear and reward signaling.

Optogenetic and chemogenetic manipulation of specific projections of this population may yield important information about the nature of fear extinction circuitries.

References:

1.). from Experiment Detail :: Allen Brain Atlas: Mouse Brain. Mouse.brain-map.org (2016). at http://mouse.brain-map.org/experiment/show/34

2.). from Experiment Detail :: Allen Brain Atlas: Mouse Brain. Mouse.brain-map.org (2016). at http://mouse.brain-map.org/experiment/show/70927304

3.). from Experiment Detail :: Allen Brain Atlas: Mouse Brain. Mouse.brain-map.org (2016). at http://mouse.brain-map.org/experiment/show/74047714

4.). from Experiment Detail :: Allen Brain Atlas: Mouse Brain. Mouse.brain-map.org (2016). at http://mouse.brain-map.org/experiment/show/71016632

5.). from Experiment Detail :: Allen Brain Atlas: Mouse Brain. Mouse.brain-map.org (2016). at http://mouse.brain-map.org/experiment/show/69120620

6.). from Experiment Detail :: Allen Brain Atlas: Mouse Brain. Mouse.brain-map.org (2016). at http://mouse.brain-map.org/experiment/show/257

7.). from Experiment Detail :: Allen Brain Atlas: Mouse Brain. Mouse.brain-map.org (2016). at http://mouse.brain-map.org/experiment/show/71670683

Abraham, A. D., Neve, K. A., & Lattal, K. M. (2014). Dopamine and extinction: a convergence of theory with fear and reward circuitry. *Neurobiol Learn Mem, 108*, 65-77. doi: 10.1016/j.nlm.2013.11.007

Alexander, G. M., Rogan, S. C., Abbas, A. I., Armbruster, B. N., Pei, Y., Allen, J. A., . . . Roth, B. L. (2009). Remote control of neuronal activity in transgenic mice expressing evolved G protein-coupled receptors. *Neuron, 63* (1), 27-39. doi: 10.1016/j.neuron.2009.06.014

Amar, S., Kitabgi, P., & Vincent, J. P. (1987). Stimulation of inositol phosphate production by neurotensin in neuroblastoma N1E115 cells: implication of GTP-binding proteins and relationship with the cyclic GMP response. *J Neurochem, 49* (4), 999-1006.

Ambroggi, F., Ishikawa, A., Fields, H. L., & Nicola, S. M. (2008). Basolateral amygdala neurons facilitate reward-seeking behavior by exciting nucleus accumbens neurons. *Neuron, 59* (4), 648-661. doi: 10.1016/j.neuron.2008.07.004

Amir, A., Amano, T., & Pare, D. (2011). Physiological identification and infralimbic responsiveness of rat intercalated amygdala neurons. *J Neurophysiol, 105* (6), 3054-3066. doi: 10.1152/jn.00136.2011

Andero, R., Daniel, S., Guo, J. D., Bruner, R. C., Seth, S., Marvar, P. J., . . . Ressler, K. J. (2016). Amygdala-Dependent Molecular Mechanisms of the Tac2 Pathway in Fear Learning. *Neuropsychopharmacology, 41* (11), 2714-2722. doi: 10.1038/npp.2016.77

Andero, R., Dias, B. G., & Ressler, K. J. (2014). A Role for Tac2, NkB, and Nk3 Receptor in Normal and Dysregulated Fear Memory Consolidation. *Neuron*. doi: 10.1016/j.neuron.2014.05.028

Antonelli, T., Fuxe, K., Tomasini, M. C., Mazzoni, E., Agnati, L. F., Tanganelli, S., & Ferraro, L. (2007). Neurotensin receptor mechanisms and its modulation of glutamate transmission in the brain: relevance for neurodegenerative diseases and their treatment. *Prog Neurobiol, 83* (2), 92-109. doi: 10.1016/j.pneurobio.2007.06.006

Aoyama, S., Kase, H., & Borrelli, E. (2000). Rescue of locomotor impairment in dopamine D2 receptor-deficient mice by an adenosine A2A receptor antagonist. *J Neurosci, 20* (15), 5848-5852.

Arenkiel, B. R., Peca, J., Davison, I. G., Feliciano, C., Deisseroth, K., Augustine, G. J., . . . Feng, G. (2007). In vivo light-induced activation of neural circuitry in transgenic mice expressing channelrhodopsin-2. *Neuron, 54* (2), 205-218. doi: 10.1016/j.neuron.2007.03.005

Arruda-Carvalho, M., & Clem, R. L. (2014). Pathway-selective adjustment of prefrontal-amygdala transmission during fear encoding. *J Neurosci, 34* (47), 15601-15609. doi: 10.1523/jneurosci.2664-14.2014

Arruda-Carvalho, M., & Clem, R. L. (2015). Prefrontal-amygdala fear networks come into focus. *Front Syst Neurosci, 9*, 145. doi: 10.3389/fnsys.2015.00145

Asan, E. (1993). Comparative single and double immunolabelling with antisera against catecholamine biosynthetic enzymes: criteria for the identification of dopaminergic, noradrenergic and adrenergic structures in selected rat brain areas. *Histochemistry, 99* (6), 427-442. doi: 10.1007/bf00274095

Association, American Psychiatric. (2013). *Diagnostic and statistical manual of mental disorders (DSM-5®)*: American Psychiatric Pub.

Barch, D. M., Pagliaccio, D., & Luking, K. (2016). Mechanisms Underlying Motivational Deficits in Psychopathology: Similarities and Differences in Depression and Schizophrenia. *Curr Top Behav Neurosci, 27*, 411-449. doi: 10.1007/7854_2015_376

Blaesse, P., Goedecke, L., Bazelot, M., Capogna, M., Pape, H. C., & Jungling, K. (2015). mu-Opioid Receptor-Mediated Inhibition of Intercalated Neurons and Effect on Synaptic Transmission to the Central Amygdala. *J Neurosci, 35* (19), 7317-7325. doi: 10.1523/JNEUROSCI.0204-15.2015

Blanchard, D. C., & Blanchard, R. J. (1972). Innate and conditioned reactions to threat in rats with amygdaloid lesions. *J Comp Physiol Psychol, 81* (2), 281-290.

Blanchard, Robert J., & Blanchard, D. Caroline. (1969). Crouching as an index of fear. *Journal of Comparative and Physiological Psychology, 67* (3), 370-375. doi: 10.1037/h0026779

Botta, P., Demmou, L., Kasugai, Y., Markovic, M., Xu, C., Fadok, J. P., . . . Luthi, A. (2015). Regulating anxiety with extrasynaptic inhibition. *Nat Neurosci, 18* (10), 1493-1500. doi: 10.1038/nn.4102

Bourgeais, L., Gauriau, C., & Bernard, J. F. (2001). Projections from the nociceptive area of the central nucleus of the amygdala to the forebrain: a PHA-L study in the rat. *Eur J Neurosci, 14* (2), 229-255.

Bouton, M. E., Westbrook, R. F., Corcoran, K. A., & Maren, S. (2006). Contextual and temporal modulation of extinction: behavioral and biological mechanisms. *Biol Psychiatry, 60* (4), 352-360. doi: 10.1016/j.biopsych.2005.12.015

Bowers, M. E., Choi, D. C., & Ressler, K. J. (2012). Neuropeptide regulation of fear and anxiety: Implications of cholecystokinin, endogenous opioids, and neuropeptide Y. *Physiol Behav, 107* (5), 699-710. doi: 10.1016/j.physbeh.2012.03.004

Boyden, E. S. (2011). A history of optogenetics: the development of tools for controlling brain circuits with light. *F1000 Biol Rep, 3*, 11. doi: 10.3410/B3-11

Boyden, E. S., Zhang, F., Bamberg, E., Nagel, G., & Deisseroth, K. (2005). Millisecond-timescale, genetically targeted optical control of neural activity. *Nat Neurosci, 8* (9), 1263-1268. doi: 10.1038/nn1525

Brigman, J. L., Wright, T., Talani, G., Prasad-Mulcare, S., Jinde, S., Seabold, G. K., . . . Holmes, A. (2010). Loss of GluN2B-containing NMDA receptors in CA1 hippocampus and cortex impairs long-term depression, reduces dendritic spine density, and disrupts learning. *J Neurosci, 30* (13), 4590-4600. doi: 10.1523/jneurosci.0640-10.2010

Busti, D., Geracitano, R., Whittle, N., Dalezios, Y., Manko, M., Kaufmann, W., . . . Ferraguti, F. (2011). Different fear states engage distinct networks within the intercalated cell clusters of the amygdala. *J Neurosci, 31* (13), 5131-5144. doi: 10.1523/jneurosci.6100-10.2011

Cai, H., Haubensak, W., Anthony, T. E., & Anderson, D. J. (2014). Central amygdala PKC-delta (+) neurons mediate the influence of multiple anorexigenic signals. *Nat Neurosci, 17* (9), 1240-1248. doi: 10.1038/nn.3767

Campeau, S., & Davis, M. (1995). Involvement of the central nucleus and basolateral complex of the amygdala in fear conditioning measured with fear-potentiated startle in rats trained concurrently with auditory and visual conditioned stimuli. *J Neurosci, 15* (3 Pt 2), 2301-2311.

Campsall, K. D., Mazerolle, C. J., De Repentigny, Y., Kothary, R., & Wallace, V. A. (2002). Characterization of transgene expression and Cre recombinase activity in a panel of Thy-1 promoter-Cre transgenic mice. *Dev Dyn, 224* (2), 135-143. doi: 10.1002/dvdy.10092

Cassell, M. D., Freedman, L. J., & Shi, C. (1999). The intrinsic organization of the central extended amygdala. *Ann N Y Acad Sci, 877*, 217-241.

Cassell, M. D., Gray, T. S., & Kiss, J. Z. (1986). Neuronal architecture in the rat central nucleus of the amygdala: a cytological, hodological, and immunocytochemical study. *J Comp Neurol, 246* (4), 478-499. doi: 10.1002/cne.902460406

Chhatwal JP, Hammack SE, Jasnow AM, Rainnie DG, Ressler KJ. Apr;14 (7):575-83. (2007). Identification of cell-type-specific promoters within the brain using lentiviral vectors. *Gene Ther., 14* (7), 575-583.

Cho, J. H., Deisseroth, K., & Bolshakov, V. Y. (2013). Synaptic encoding of fear extinction in mPFC-amygdala circuits. *Neuron, 80* (6), 1491-1507. doi: 10.1016/j.neuron.2013.09.025

Ciocchi, S., Herry, C., Grenier, F., Wolff, S. B., Letzkus, J. J., Vlachos, I., . . . Luthi, A. (2010). Encoding of conditioned fear in central amygdala inhibitory circuits. *Nature, 468* (7321), 277-282. doi: 10.1038/nature09559

Cruz, F. C., Koya, E., Guez-Barber, D. H., Bossert, J. M., Lupica, C. R., Shaham, Y., & Hope, B. T. (2013). New technologies for examining the role of neuronal ensembles in drug addiction and fear. *Nat Rev Neurosci, 14* (11), 743-754. doi: 10.1038/nrn3597

Davis, M., Walker, D. L., Miles, L., & Grillon, C. (2010). Phasic vs sustained fear in rats and humans: role of the extended amygdala in fear vs anxiety. *Neuropsychopharmacology, 35* (1), 105-135. doi: 10.1038/npp.2009.109

Day, H. E., Curran, E. J., Watson, S. J., Jr., & Akil, H. (1999). Distinct neurochemical populations in the rat central nucleus of the amygdala and bed nucleus of the stria terminalis: evidence for their selective activation by interleukin-1beta. *J Comp Neurol, 413* (1), 113-128.

de la Mora, M. P., Gallegos-Cari, A., Arizmendi-Garcia, Y., Marcellino, D., & Fuxe, K. (2010). Role of dopamine receptor mechanisms in the amygdaloid modulation of fear and anxiety: Structural and functional analysis. *Prog Neurobiol, 90* (2), 198-216. doi: 10.1016/j.pneurobio.2009.10.010

Di Ciano, P., & Everitt, B. J. (2004). Direct interactions between the basolateral amygdala and nucleus accumbens core underlie cocaine-seeking behavior by rats. *J Neurosci, 24* (32), 7167-7173. doi: 10.1523/jneurosci.1581-04.2004

Diep, D. B., Hoen, N., Backman, M., Machon, O., & Krauss, S. (2004). Characterisation of the Wnt antagonists and their response to conditionally activated Wnt signalling in the developing mouse forebrain. *Brain Res Dev Brain Res, 153* (2), 261-270. doi: 10.1016/j.devbrainres.2004.09.008

Do-Monte, F. H., Manzano-Nieves, G., Quinones-Laracuente, K., Ramos-Medina, L., & Quirk, G. J. (2015). Revisiting the role of infralimbic cortex in fear extinction with optogenetics. *J Neurosci, 35* (8), 3607-3615. doi: 10.1523/JNEUROSCI.3137-14.2015

Dong, H. W., Petrovich, G. D., & Swanson, L. W. (2001). Topography of projections from amygdala to bed nuclei of the stria terminalis. *Brain Res Brain Res Rev, 38* (1-2), 192-246.

Drane, L., Ainsley, J. A., Mayford, M. R., & Reijmers, L. G. (2014). A transgenic mouse line for collecting ribosome-bound mRNA using the tetracycline transactivator system. *Front Mol Neurosci, 7*, 82. doi: 10.3389/fnmol.2014.00082

Duvarci, S., & Pare, D. (2014). Amygdala microcircuits controlling learned fear. *Neuron, 82* (5), 966-980. doi: 10.1016/j.neuron.2014.04.042
Dymecki, S. M., Ray, R. S., & Kim, J. C. (2010). Mapping cell fate and function using recombinase-based intersectional strategies. *Methods Enzymol, 477*, 183-213. doi: 10.1016/s0076-6879 (10)77011-7
Ehrlich, I., Humeau, Y., Grenier, F., Ciocchi, S., Herry, C., & Luthi, A. (2009). Amygdala inhibitory circuits and the control of fear memory. *Neuron, 62* (6), 757-771. doi: 10.1016/j.neuron.2009.05.026
Elowitz, M. B., Surette, M. G., Wolf, P. E., Stock, J., & Leibler, S. (1997). Photoactivation turns green fluorescent protein red. *Curr Biol, 7* (10), 809-812.
Esmaeili, M., Berry, M., Logan, A., & Ahmed, Z. (2014). Decorin treatment of spinal cord injury. *Neural Regen Res, 9* (18), 1653-1656. doi: 10.4103/1673-5374.141797
Fanselow, M. S. (1980). Conditioned and unconditional components of post-shock freezing. *Pavlov J Biol Sci, 15* (4), 177-182.
Felix-Ortiz, A. C., Burgos-Robles, A., Bhagat, N. D., Leppla, C. A., & Tye, K. M. (2015). Bidirectional modulation of anxiety-related and social behaviors by amygdala projections to the medial prefrontal cortex. *Neuroscience*. doi: 10.1016/j.neuroscience.2015.07.041
Feng, G., Mellor, R. H., Bernstein, M., Keller-Peck, C., Nguyen, Q. T., Wallace, M., . . . Sanes, J. R. (2000). Imaging neuronal subsets in transgenic mice expressing multiple spectral variants of GFP. *Neuron, 28* (1), 41-51.
Fenno, Lief E., Mattis, Joanna, Ramakrishnan, Charu, Hyun, Minsuk, Lee, Soo Yeun, He, Miao, . . . Deisseroth, Karl. (2014). Targeting cells with single vectors using multiple-feature Boolean logic. *Nat Meth, 11* (7), 763-772. doi: 10.1038/nmeth.2996
http://www.nature.com/nmeth/journal/v11/n7/abs/nmeth.2996.html#supplementary-information
Ferguson, S. M., & Neumaier, J. F. (2012). Grateful DREADDs: engineered receptors reveal how neural circuits regulate behavior. *Neuropsychopharmacology, 37* (1), 296-297. doi: 10.1038/npp.2011.179
Fernandez, R. S., Boccia, M. M., & Pedreira, M. E. (2016). The fate of memory: Reconsolidation and the case of Prediction Error. *Neurosci Biobehav Rev, 68*, 423-441. doi: 10.1016/j.neubiorev.2016.06.004
Fernando, C. V., Kele, J., Bye, C. R., Niclis, J. C., Alsanie, W., Blakely, B. D., . . . Parish, C. L. (2014). Diverse roles for Wnt7a in ventral midbrain neurogenesis and dopaminergic axon morphogenesis. *Stem Cells Dev, 23* (17), 1991-2003. doi: 10.1089/scd.2014.0166
Ferraro, L., Tomasini, M. C., Mazza, R., Fuxe, K., Fournier, J., Tanganelli, S., & Antonelli, T. (2008). Neurotensin receptors as modulators of glutamatergic transmission. *Brain Res Rev, 58* (2), 365-373. doi: 10.1016/j.brainresrev.2007.11.001
Fukushima, T., Liu, R. Y., & Byrne, J. H. (2007). Transforming growth factor-beta2 modulates synaptic efficacy and plasticity and induces

phosphorylation of CREB in hippocampal neurons. *Hippocampus, 17* (1), 5-9. doi: 10.1002/hipo.20243

Gafford, G. M., & Ressler, K. J. (2015). GABA and NMDA receptors in CRF neurons have opposing effects in fear acquisition and anxiety in central amygdala vs. bed nucleus of the stria terminalis. *Horm Behav, 76*, 136-142. doi: 10.1016/j.yhbeh.2015.04.001

Gentile, C. G., Jarrell, T. W., Teich, A., McCabe, P. M., & Schneiderman, N. (1986). The role of amygdaloid central nucleus in the retention of differential pavlovian conditioning of bradycardia in rabbits. *Behav Brain Res, 20* (3), 263-273.

Giustino, T. F., & Maren, S. (2015). The Role of the Medial Prefrontal Cortex in the Conditioning and Extinction of Fear. *Front Behav Neurosci, 9*, 298. doi: 10.3389/fnbeh.2015.00298

Glotzbach-Schoon, E., Andreatta, M., Reif, A., Ewald, H., Troger, C., Baumann, C., . . . Pauli, P. (2013). Contextual fear conditioning in virtual reality is affected by 5HTTLPR and NPSR1 polymorphisms: effects on fear-potentiated startle. *Front Behav Neurosci, 7*, 31. doi: 10.3389/fnbeh.2013.00031

Goosens, K. A., & Maren, S. (2001). Contextual and auditory fear conditioning are mediated by the lateral, basal, and central amygdaloid nuclei in rats. *Learn Mem, 8* (3), 148-155. doi: 10.1101/lm.37601

Gradinaru, V., Thompson, K. R., & Deisseroth, K. (2008). eNpHR: a Natronomonas halorhodopsin enhanced for optogenetic applications. *Brain Cell Biol, 36* (1-4), 129-139. doi: 10.1007/s11068-008-9027-6

Guarraci, F. A., Frohardt, R. J., Falls, W. A., & Kapp, B. S. (2000). The effects of intra-amygdaloid infusions of a D2 dopamine receptor antagonist on Pavlovian fear conditioning. *Behav Neurosci, 114* (3), 647-651.

Guez-Barber, D., Fanous, S., Golden, S. A., Schrama, R., Koya, E., Stern, A. L., . . . Hope, B. T. (2011). FACS identifies unique cocaine-induced gene regulation in selectively activated adult striatal neurons. *J Neurosci, 31* (11), 4251-4259. doi: 10.1523/JNEUROSCI.6195-10.2011

Guez-Barber, D., Fanous, S., Harvey, B. K., Zhang, Y., Lehrmann, E., Becker, K. G., . . . Hope, B. T. (2012). FACS purification of immunolabeled cell types from adult rat brain. *J Neurosci Methods, 203* (1), 10-18. doi: 10.1016/j.jneumeth.2011.08.045

Guzowski, J. F., McNaughton, B. L., Barnes, C. A., & Worley, P. F. (1999). Environment-specific expression of the immediate-early gene Arc in hippocampal neuronal ensembles. *Nat Neurosci, 2* (12), 1120-1124. doi: 10.1038/16046

Haaker, J., Lonsdorf, T. B., & Kalisch, R. (2015). Effects of post-extinction l-DOPA administration on the spontaneous recovery and reinstatement of fear in a human fMRI study. *Eur Neuropsychopharmacol, 25* (10), 1544-1555. doi: 10.1016/j.euroneuro.2015.07.016

Haaker, Jan, Gaburro, Stefano, Sah, Anupam, Gartmann, Nina, Lonsdorf, Tina B., Meier, Kolja, . . . Kalisch, Raffael. (2013). Single dose of l-

dopa makes extinction memories context-independent and prevents the return of fear. *Proceedings of the National Academy of Sciences of the United States of America, 110* (26), E2428-E2436. doi: 10.1073/pnas.1303061110

Han, J. H., Kushner, S. A., Yiu, A. P., Cole, C. J., Matynia, A., Brown, R. A., . . . Josselyn, S. A. (2007). Neuronal competition and selection during memory formation. *Science, 316* (5823), 457-460. doi: 10.1126/science.1139438

Han, S., Soleiman, M. T., Soden, M. E., Zweifel, L. S., & Palmiter, R. D. (2015). Elucidating an Affective Pain Circuit that Creates a Threat Memory. *Cell, 162* (2), 363-374. doi: 10.1016/j.cell.2015.05.057

Haubensak, W., Kunwar, P. S., Cai, H., Ciocchi, S., Wall, N. R., Ponnusamy, R., . . . Anderson, D. J. (2010). Genetic dissection of an amygdala microcircuit that gates conditioned fear. *Nature, 468* (7321), 270-276. doi: 10.1038/nature09553

Heiman, M., Kulicke, R., Fenster, R. J., Greengard, P., & Heintz, N. (2014). Cell type-specific mRNA purification by translating ribosome affinity purification (TRAP). *Nat Protoc, 9* (6), 1282-1291. doi: 10.1038/nprot.2014.085

Heiman, Myriam, Kulicke, Ruth, Fenster, Robert J., Greengard, Paul, & Heintz, Nathaniel. (2014). Cell-Type-Specific mRNA Purification by Translating Ribosome Affinity Purification (TRAP). *Nature protocols, 9* (6), 1282-1291. doi: 10.1038/nprot.2014.085

Hempel, C. M., Sugino, K., & Nelson, S. B. (2007). A manual method for the purification of fluorescently labeled neurons from the mammalian brain. *Nat Protoc, 2* (11), 2924-2929. doi: 10.1038/nprot.2007.416

Herry, C., Ciocchi, S., Senn, V., Demmou, L., Muller, C., & Luthi, A. (2008). Switching on and off fear by distinct neuronal circuits. *Nature, 454* (7204), 600-606. doi: 10.1038/nature07166

Hirsch, M. R., d'Autreaux, F., Dymecki, S. M., Brunet, J. F., & Goridis, C. (2013). A Phox2b::FLPo transgenic mouse line suitable for intersectional genetics. *Genesis, 51* (7), 506-514. doi: 10.1002/dvg.22393

Hohoff, C., Mullings, E. L., Heatherley, S. V., Freitag, C. M., Neumann, L. C., Domschke, K., . . . Deckert, J. (2010). Adenosine A (2A) receptor gene: evidence for association of risk variants with panic disorder and anxious personality. *J Psychiatr Res, 44* (14), 930-937. doi: 10.1016/j.jpsychires.2010.02.006

Hou, I. C., Suzuki, C., Kanegawa, N., Oda, A., Yamada, A., Yoshikawa, M., . . . Ohinata, K. (2011). beta-Lactotensin derived from bovine beta-lactoglobulin exhibits anxiolytic-like activity as an agonist for neurotensin NTS (2) receptor via activation of dopamine D (1) receptor in mice. *J Neurochem, 119* (4), 785-790. doi: 10.1111/j.1471-4159.2011.07472.x

Hou, I. C., Yoshikawa, M., & Ohinata, K. (2009). beta-Lactotensin derived from bovine beta-lactoglobulin suppresses food intake via the CRF

system followed by the CGRP system in mice. *Peptides, 30* (12), 2228-2232. doi: 10.1016/j.peptides.2009.08.018

Huff, M. L., Emmons, E. B., Narayanan, N. S., & LaLumiere, R. T. (2016). Basolateral amygdala projections to ventral hippocampus modulate the consolidation of footshock, but not contextual, learning in rats. *Learn Mem, 23* (2), 51-60. doi: 10.1101/lm.039909.115

Huff, M. L., Miller, R. L., Deisseroth, K., Moorman, D. E., & LaLumiere, R. T. (2013). Posttraining optogenetic manipulations of basolateral amygdala activity modulate consolidation of inhibitory avoidance memory in rats. *Proc Natl Acad Sci U S A, 110* (9), 3597-3602. doi: 10.1073/pnas.1219593110

Izquierdo, I., & Medina, J. H. (1997). Memory formation: the sequence of biochemical events in the hippocampus and its connection to activity in other brain structures. *Neurobiol Learn Mem, 68* (3), 285-316. doi: 10.1006/nlme.1997.3799

Jasnow, A. M., Ehrlich, D. E., Choi, D. C., Dabrowska, J., Bowers, M. E., McCullough, K. M., . . . Ressler, K. J. (2013). Thy1-expressing neurons in the basolateral amygdala may mediate fear inhibition. *J Neurosci, 33* (25), 10396-10404. doi: 10.1523/JNEUROSCI.5539-12.2013

Jensen, P., & Dymecki, S. M. (2014). Essentials of recombinase-based genetic fate mapping in mice. *Methods Mol Biol, 1092*, 437-454. doi: 10.1007/978-1-60327-292-6_26

Johansen, J. P., Cain, C. K., Ostroff, L. E., & LeDoux, J. E. (2011). Molecular mechanisms of fear learning and memory. *Cell, 147* (3), 509-524. doi: 10.1016/j.cell.2011.10.009

Johansen, J. P., Hamanaka, H., Monfils, M. H., Behnia, R., Deisseroth, K., Blair, H. T., & LeDoux, J. E. (2010). Optical activation of lateral amygdala pyramidal cells instructs associative fear learning. *Proc Natl Acad Sci U S A, 107* (28), 12692-12697. doi: 10.1073/pnas.1002418107

Jolkkonen, E., & Pitkanen, A. (1998). Intrinsic connections of the rat amygdaloid complex: projections originating in the central nucleus. *J Comp Neurol, 395* (1), 53-72.

Jungling, K., Seidenbecher, T., Sosulina, L., Lesting, J., Sangha, S., Clark, S. D., . . . Pape, H. C. (2008). Neuropeptide S-mediated control of fear expression and extinction: role of intercalated GABAergic neurons in the amygdala. *Neuron, 59* (2), 298-310. doi: 10.1016/j.neuron.2008.07.002

Katz, I. K., & Lamprecht, R. (2015). Fear conditioning leads to alteration in specific genes expression in cortical and thalamic neurons that project to the lateral amygdala. *J Neurochem, 132* (3), 313-326. doi: 10.1111/jnc.12983

Kazanskaya, O., Glinka, A., del Barco Barrantes, I., Stannek, P., Niehrs, C., & Wu, W. (2004). R-Spondin2 is a secreted activator of Wnt/beta-catenin signaling and is required for Xenopus myogenesis. *Dev Cell, 7* (4), 525-534. doi: 10.1016/j.devcel.2004.07.019

Kessler, R. C., Berglund, P., Demler, O., Jin, R., Merikangas, K. R., & Walters, E. E. (2005). LIfetime prevalence and age-of-onset distributions of dsm-iv disorders in the national comorbidity survey replication. *Archives of General Psychiatry, 62* (6), 593-602. doi: 10.1001/archpsyc.62.6.593

Kim, H. S., Cho, H. Y., Augustine, G. J., & Han, J. H. (2016). Selective Control of Fear Expression by Optogenetic Manipulation of Infralimbic Cortex after Extinction. *Neuropsychopharmacology, 41* (5), 1261-1273. doi: 10.1038/npp.2015.276

Kim, S. Y., Adhikari, A., Lee, S. Y., Marshel, J. H., Kim, C. K., Mallory, C. S., . . . Deisseroth, K. (2013). Diverging neural pathways assemble a behavioural state from separable features in anxiety. *Nature, 496* (7444), 219-223. doi: 10.1038/nature12018

Kitamura, Takashi, Sun, Chen, Martin, Jared, Kitch, Lacey J, Schnitzer, Mark J, & Tonegawa, Susumu. Entorhinal Cortical Ocean Cells Encode Specific Contexts and Drive Context-Specific Fear Memory. *Neuron, 87* (6), 1317-1331. doi: 10.1016/j.neuron.2015.08.036

Knobloch, H. S., Charlet, A., Hoffmann, L. C., Eliava, M., Khrulev, S., Cetin, A. H., . . . Grinevich, V. (2012). Evoked axonal oxytocin release in the central amygdala attenuates fear response. *Neuron, 73* (3), 553-566. doi: 10.1016/j.neuron.2011.11.030

Krashes, M. J., Koda, S., Ye, C., Rogan, S. C., Adams, A. C., Cusher, D. S., . . . Lowell, B. B. (2011). Rapid, reversible activation of AgRP neurons drives feeding behavior in mice. *J Clin Invest, 121* (4), 1424-1428. doi: 10.1172/jci46229

Kravitz, A. V., Tye, L. D., & Kreitzer, A. C. (2012). Distinct roles for direct and indirect pathway striatal neurons in reinforcement. *Nat Neurosci, 15* (6), 816-818. doi: 10.1038/nn.3100

Kunwar, P. S., Zelikowsky, M., Remedios, R., Cai, H., Yilmaz, M., Meister, M., & Anderson, D. J. (2015). Ventromedial hypothalamic neurons control a defensive emotion state. *Elife, 4*. doi: 10.7554/eLife.06633

Kwon, J. T., Nakajima, R., Kim, H. S., Jeong, Y., Augustine, G. J., & Han, J. H. (2014). Optogenetic activation of presynaptic inputs in lateral amygdala forms associative fear memory. *Learn Mem, 21* (11), 627-633. doi: 10.1101/lm.035816.114

Kwon, O. B., Lee, J. H., Kim, H. J., Lee, S., Lee, S., Jeong, M. J., . . . Kim, J. H. (2015). Dopamine Regulation of Amygdala Inhibitory Circuits for Expression of Learned Fear. *Neuron, 88* (2), 378-389. doi: 10.1016/j.neuron.2015.09.001

Lafrance, M., Roussy, G., Belleville, K., Maeno, H., Beaudet, N., Wada, K., & Sarret, P. (2010). Involvement of NTS2 receptors in stress-induced analgesia. *Neuroscience, 166* (2), 639-652. doi: 10.1016/j.neuroscience.2009.12.042

LeDoux, J. E. (2014). Coming to terms with fear. *Proc Natl Acad Sci U S A, 111* (8), 2871-2878. doi: 10.1073/pnas.1400335111

LeDoux, J. E., Farb, C., & Ruggiero, D. A. (1990). Topographic organization of neurons in the acoustic thalamus that project to the amygdala. *J Neurosci, 10* (4), 1043-1054.

LeDoux, J. E., Iwata, J., Cicchetti, P., & Reis, D. J. (1988). Different projections of the central amygdaloid nucleus mediate autonomic and behavioral correlates of conditioned fear. *J Neurosci, 8* (7), 2517-2529.

LeDoux, J. E., Ruggiero, D. A., & Reis, D. J. (1985). Projections to the subcortical forebrain from anatomically defined regions of the medial geniculate body in the rat. *J Comp Neurol, 242* (2), 182-213. doi: 10.1002/cne.902420204

Lee, H., Kim, D. W., Remedios, R., Anthony, T. E., Chang, A., Madisen, L., . . . Anderson, D. J. (2014). Scalable control of mounting and attack by Esr1+ neurons in the ventromedial hypothalamus. *Nature, 509* (7502), 627-632. doi: 10.1038/nature13169

Lein, Ed S, Hawrylycz, Michael J, Ao, Nancy, Ayres, Mikael, Bensinger, Amy, Bernard, Amy, . . . Byrnes, Emi J. (2007). Genome-wide atlas of gene expression in the adult mouse brain. *Nature, 445* (7124), 168-176.

Lein, Ed S., Hawrylycz, Michael J., Ao, Nancy, Ayres, Mikael, Bensinger, Amy, Bernard, Amy, . . . Jones, Allan R. (2007). Genome-wide atlas of gene expression in the adult mouse brain. *Nature, 445* (7124), 168-176. doi: http://www.nature.com/nature/journal/v445/n7124/suppinfo/nature05453_S1.html

Lenka, A., Arumugham, S. S., Christopher, R., & Pal, P. K. (2016). Genetic substrates of psychosis in patients with Parkinson's disease: A critical review. *J Neurol Sci, 364*, 33-41. doi: 10.1016/j.jns.2016.03.005

Lesting, J., Narayanan, R. T., Kluge, C., Sangha, S., Seidenbecher, T., & Pape, H. C. (2011). Patterns of coupled theta activity in amygdala-hippocampal-prefrontal cortical circuits during fear extinction. *PLoS One, 6* (6), e21714. doi: 10.1371/journal.pone.0021714

Letzkus, J. J., Wolff, S. B., & Luthi, A. (2015). Disinhibition, a Circuit Mechanism for Associative Learning and Memory. *Neuron, 88* (2), 264-276. doi: 10.1016/j.neuron.2015.09.024

Letzkus, J. J., Wolff, S. B., Meyer, E. M., Tovote, P., Courtin, J., Herry, C., & Luthi, A. (2011). A disinhibitory microcircuit for associative fear learning in the auditory cortex. *Nature, 480* (7377), 331-335. doi: 10.1038/nature10674

Li, H., Penzo, M. A., Taniguchi, H., Kopec, C. D., Huang, Z. J., & Li, B. (2013). Experience-dependent modification of a central amygdala fear circuit. *Nat Neurosci, 16* (3), 332-339. doi: 10.1038/nn.3322

Li, L., Bao, Y., He, S., Wang, G., Guan, Y., Ma, D., . . . Yang, J. (2016). The Association Between Genetic Variants in the Dopaminergic System and Posttraumatic Stress Disorder: A Meta-Analysis. *Medicine (Baltimore), 95* (11), e3074. doi: 10.1097/md.0000000000003074

Likhtik, E., Popa, D., Apergis-Schoute, J., Fidacaro, G. A., & Pare, D. (2008). Amygdala intercalated neurons are required for expression of fear extinction. *Nature, 454* (7204), 642-645. doi: 10.1038/nature07167

Linke, R., Braune, G., & Schwegler, H. (2000). Differential projection of the posterior paralaminar thalamic nuclei to the amygdaloid complex in the rat. *Exp Brain Res, 134* (4), 520-532.

Liu, X., Ramirez, S., Pang, P. T., Puryear, C. B., Govindarajan, A., Deisseroth, K., & Tonegawa, S. (2012). Optogenetic stimulation of a hippocampal engram activates fear memory recall. *Nature, 484* (7394), 381-385. doi: 10.1038/nature11028

Luo, L., Salunga, R. C., Guo, H., Bittner, A., Joy, K. C., Galindo, J. E., . . . Erlander, M. G. (1999). Gene expression profiles of laser-captured adjacent neuronal subtypes. *Nat Med, 5* (1), 117-122. doi: 10.1038/4806

Maguschak, K. A., & Ressler, K. J. (2008). Beta-catenin is required for memory consolidation. *Nat Neurosci, 11* (11), 1319-1326. doi: 10.1038/nn.2198

Marcellino, D., Frankowska, M., Agnati, L., Perez de la Mora, M., Vargas-Barroso, V., Fuxe, K., & Larriva-Sahd, J. (2012). Intercalated and paracapsular cell islands of the adult rat amygdala: a combined rapid-Golgi, ultrastructural, and immunohistochemical account. *Neuroscience, 226*, 324-347. doi: 10.1016/j.neuroscience.2012.08.067

Marchant, N. J., Densmore, V. S., & Osborne, P. B. (2007). Coexpression of prodynorphin and corticotrophin-releasing hormone in the rat central amygdala: evidence of two distinct endogenous opioid systems in the lateral division. *J Comp Neurol, 504* (6), 702-715. doi: 10.1002/cne.21464

Maren, S., & Fanselow, M. S. (1996). The amygdala and fear conditioning: has the nut been cracked? *Neuron, 16* (2), 237-240.

McCullough, K. M., Morrison, F. G., & Ressler, K. J. (2016). Bridging the Gap: Towards a cell-type specific understanding of neural circuits underlying fear behaviors. *Neurobiol Learn Mem, 135*, 27-39. doi: 10.1016/j.nlm.2016.07.025

McDonald, A. J. (1982). Cytoarchitecture of the central amygdaloid nucleus of the rat. *J Comp Neurol, 208* (4), 401-418. doi: 10.1002/cne.902080409

McDonald, A. J. (1984). Neuronal organization of the lateral and basolateral amygdaloid nuclei in the rat. *J Comp Neurol, 222* (4), 589-606. doi: 10.1002/cne.902220410

McDonald, A. J. (1998). Cortical pathways to the mammalian amygdala. *Prog Neurobiol, 55* (3), 257-332.

McDonald, A. J., & Mott, D. D. (2016). Functional neuroanatomy of amygdalohippocampal interconnections and their role in learning and memory. *J Neurosci Res*. doi: 10.1002/jnr.23709

Merali, Z., McIntosh, J., Kent, P., Michaud, D., & Anisman, H. (1998). Aversive and appetitive events evoke the release of corticotropin-

releasing hormone and bombesin-like peptides at the central nucleus of the amygdala. *J Neurosci, 18* (12), 4758-4766.
Methods of Behavior Analysis in Neuroscience. (2009). (e. Buccafusco JJ Ed. 2nd edition ed.). Boca Raton (FL): CRC Press/Taylor & Francis.
Millhouse, O. E. (1986). The intercalated cells of the amygdala. *J Comp Neurol, 247* (2), 246-271. doi: 10.1002/cne.902470209
Morozov, A., Sukato, D., & Ito, W. (2011). Selective suppression of plasticity in amygdala inputs from temporal association cortex by the external capsule. *J Neurosci, 31* (1), 339-345. doi: 10.1523/JNEUROSCI.5537-10.2011
Muller, J., Corodimas, K. P., Fridel, Z., & LeDoux, J. E. (1997). Functional inactivation of the lateral and basal nuclei of the amygdala by muscimol infusion prevents fear conditioning to an explicit conditioned stimulus and to contextual stimuli. *Behav Neurosci, 111* (4), 683-691.
Myers, K. M., & Davis, M. (2007). Mechanisms of fear extinction. *Mol Psychiatry, 12* (2), 120-150. doi: 10.1038/sj.mp.4001939
Nagel, G., Szellas, T., Huhn, W., Kateriya, S., Adeishvili, N., Berthold, P., . . . Bamberg, E. (2003). Channelrhodopsin-2, a directly light-gated cation-selective membrane channel. *Proceedings of the National Academy of Sciences, 100* (24), 13940-13945. doi: 10.1073/pnas.1936192100
Namburi, P., Beyeler, A., Yorozu, S., Calhoon, G. G., Halbert, S. A., Wichmann, R., . . . Tye, K. M. (2015). A circuit mechanism for differentiating positive and negative associations. *Nature, 520* (7549), 675-678. doi: 10.1038/nature14366
Nieh, E. H., Kim, S. Y., Namburi, P., & Tye, K. M. (2013). Optogenetic dissection of neural circuits underlying emotional valence and motivated behaviors. *Brain Res, 1511*, 73-92. doi: 10.1016/j.brainres.2012.11.001
Nomura, H., Hara, K., Abe, R., Hitora-Imamura, N., Nakayama, R., Sasaki, T., . . . Ikegaya, Y. (2015). Memory formation and retrieval of neuronal silencing in the auditory cortex. *Proc Natl Acad Sci U S A, 112* (31), 9740-9744. doi: 10.1073/pnas.1500869112
Okaty, B. W., Freret, M. E., Rood, B. D., Brust, R. D., Hennessy, M. L., deBairos, D., . . . Dymecki, S. M. (2015). Multi-Scale Molecular Deconstruction of the Serotonin Neuron System. *Neuron, 88* (4), 774-791. doi: 10.1016/j.neuron.2015.10.007
Oude-Ophuis, Ralph J, Boender, Arjen J, van Rozen, Rea, & Adan, Roger A. (2014). Cannabinoid, melanocortin and opioid receptor expression on DRD1 and DRD2 subpopulations in rat striatum. *Frontiers in Neuroanatomy, 8*. doi: 10.3389/fnana.2014.00014
Oude Ophuis, R. J. A., Boender, A. J., van Rozen, A. J., & Adan, R. A. H. (2014). Cannabinoid, melanocortin and opioid receptor expression on DRD1 and DRD2 subpopulations in rat striatum. *Front Neuroanat, 8*.
Palomares-Castillo, E., Hernandez-Perez, O. R., Perez-Carrera, D., Crespo-Ramirez, M., Fuxe, K., & Perez de la Mora, M. (2012). The intercalated

paracapsular islands as a module for integration of signals regulating anxiety in the amygdala. *Brain Res, 1476*, 211-234. doi: 10.1016/j.brainres.2012.03.047

Pape, H. C., & Pare, D. (2010). Plastic synaptic networks of the amygdala for the acquisition, expression, and extinction of conditioned fear. *Physiol Rev, 90* (2), 419-463. doi: 10.1152/physrev.00037.2009

Pare, D., & Duvarci, S. (2012). Amygdala microcircuits mediating fear expression and extinction. *Curr Opin Neurobiol, 22* (4), 717-723. doi: 10.1016/j.conb.2012.02.014

Pare, D., Quirk, G. J., & Ledoux, J. E. (2004). New vistas on amygdala networks in conditioned fear. *J Neurophysiol, 92* (1), 1-9. doi: 10.1152/jn.00153.2004

Penzo, M. A., Robert, V., & Li, B. (2014). Fear conditioning potentiates synaptic transmission onto long-range projection neurons in the lateral subdivision of central amygdala. *J Neurosci, 34* (7), 2432-2437. doi: 10.1523/jneurosci.4166-13.2014

Perez de la Mora, M., Gallegos-Cari, A., Crespo-Ramirez, M., Marcellino, D., Hansson, A. C., & Fuxe, K. (2012). Distribution of dopamine D (2)-like receptors in the rat amygdala and their role in the modulation of unconditioned fear and anxiety. *Neuroscience, 201*, 252-266. doi: 10.1016/j.neuroscience.2011.10.045

Petrovich, GD, & Swanson, LW. (1997). Projections from the lateral part of the central amygdalar nucleus to the postulated fear conditioning circuit. *Brain research, 763* (2), 247-254.

Picciotto, M. R., & Wickman, K. (1998). Using knockout and transgenic mice to study neurophysiology and behavior. *Physiol Rev, 78* (4), 1131-1163.

Pikkarainen, M., Ronkko, S., Savander, V., Insausti, R., & Pitkanen, A. (1999). Projections from the lateral, basal, and accessory basal nuclei of the amygdala to the hippocampal formation in rat. *J Comp Neurol, 403* (2), 229-260.

Pitkanen, A., Savander, V., & LeDoux, J. E. (1997). Organization of intra-amygdaloid circuitries in the rat: an emerging framework for understanding functions of the amygdala. *Trends Neurosci, 20* (11), 517-523.

Ponnusamy, R., Nissim, H. A., & Barad, M. (2005). Systemic blockade of D2-like dopamine receptors facilitates extinction of conditioned fear in mice. *Learn Mem, 12* (4), 399-406. doi: 10.1101/lm.96605

Porrero, C., Rubio-Garrido, P., Avendano, C., & Clasca, F. (2010). Mapping of fluorescent protein-expressing neurons and axon pathways in adult and developing Thy1-eYFP-H transgenic mice. *Brain Res, 1345*, 59-72. doi: 10.1016/j.brainres.2010.05.061

Quirk, G. J., Likhtik, E., Pelletier, J. G., & Pare, D. (2003). Stimulation of medial prefrontal cortex decreases the responsiveness of central amygdala output neurons. *J Neurosci, 23* (25), 8800-8807.

Ramirez, S., Liu, X., Lin, P. A., Suh, J., Pignatelli, M., Redondo, R. L., . . . Tonegawa, S. (2013). Creating a false memory in the hippocampus. *Science, 341* (6144), 387-391. doi: 10.1126/science.1239073

Ramirez, S., Liu, X., MacDonald, C. J., Moffa, A., Zhou, J., Redondo, R. L., & Tonegawa, S. (2015). Activating positive memory engrams suppresses depression-like behaviour. *Nature, 522* (7556), 335-339. doi: 10.1038/nature14514

Reijmers, L. G., Perkins, B. L., Matsuo, N., & Mayford, M. (2007). Localization of a stable neural correlate of associative memory. *Science, 317* (5842), 1230-1233. doi: 10.1126/science.1143839

Repa, J. C., Muller, J., Apergis, J., Desrochers, T. M., Zhou, Y., & LeDoux, J. E. (2001). Two different lateral amygdala cell populations contribute to the initiation and storage of memory. *Nat Neurosci, 4* (7), 724-731. doi: 10.1038/89512

Riga, D., Matos, M. R., Glas, A., Smit, A. B., Spijker, S., & Van den Oever, M. C. (2014). Optogenetic dissection of medial prefrontal cortex circuitry. *Front Syst Neurosci, 8*, 230. doi: 10.3389/fnsys.2014.00230

Rodrigues, H., Figueira, I., Lopes, A., Goncalves, R., Mendlowicz, M. V., Coutinho, E. S., & Ventura, P. (2014). Does D-cycloserine enhance exposure therapy for anxiety disorders in humans? A meta-analysis. *PLoS One, 9* (7), e93519. doi: 10.1371/journal.pone.0093519

Rogan, S. C., & Roth, B. L. (2011). Remote control of neuronal signaling. *Pharmacol Rev, 63* (2), 291-315. doi: 10.1124/pr.110.003020

Ryan, T. J., Roy, D. S., Pignatelli, M., Arons, A., & Tonegawa, S. (2015). Memory. Engram cells retain memory under retrograde amnesia. *Science, 348* (6238), 1007-1013. doi: 10.1126/science.aaa5542

Sarret, P., Beaudet, A., Vincent, J. P., & Mazella, J. (1998). Regional and cellular distribution of low affinity neurotensin receptor mRNA in adult and developing mouse brain. *J Comp Neurol, 394* (3), 344-356.

Sarret, P., Perron, A., Stroh, T., & Beaudet, A. (2003). Immunohistochemical distribution of NTS2 neurotensin receptors in the rat central nervous system. *J Comp Neurol, 461* (4), 520-538. doi: 10.1002/cne.10718

Saus, E., Brunet, A., Armengol, L., Alonso, P., Crespo, J. M., Fernandez-Aranda, F., . . . Estivill, X. (2010). Comprehensive copy number variant (CNV) analysis of neuronal pathways genes in psychiatric disorders identifies rare variants within patients. *J Psychiatr Res, 44* (14), 971-978. doi: 10.1016/j.jpsychires.2010.03.007

Senn, V., Wolff, S. B., Herry, C., Grenier, F., Ehrlich, I., Grundemann, J., . . . Luthi, A. (2014). Long-range connectivity defines behavioral specificity of amygdala neurons. *Neuron, 81* (2), 428-437. doi: 10.1016/j.neuron.2013.11.006

Shilling, P. D., & Feifel, D. (2008). The neurotensin-1 receptor agonist PD149163 blocks fear-potentiated startle. *Pharmacol Biochem Behav, 90* (4), 748-752. doi: 10.1016/j.pbb.2008.05.025

Sierra-Mercado, D., Padilla-Coreano, N., & Quirk, G. J. (2011). Dissociable roles of prelimbic and infralimbic cortices, ventral hippocampus, and

basolateral amygdala in the expression and extinction of conditioned fear. *Neuropsychopharmacology, 36* (2), 529-538. doi: 10.1038/npp.2010.184

Simoes, A. P., Machado, N. J., Goncalves, N., Kaster, M. P., Simoes, A. T., Nunes, A., . . . Cunha, R. A. (2016). Adenosine A2A Receptors in the Amygdala Control Synaptic Plasticity and Contextual Fear Memory. *Neuropsychopharmacology*. doi: 10.1038/npp.2016.98

Singewald, N., Schmuckermair, C., Whittle, N., Holmes, A., & Ressler, K. J. (2015). Pharmacology of cognitive enhancers for exposure-based therapy of fear, anxiety and trauma-related disorders. *Pharmacol Ther, 149*, 150-190. doi: 10.1016/j.pharmthera.2014.12.004

Slattery, D. A., Naik, R. R., Grund, T., Yen, Y. C., Sartori, S. B., Fuchsl, A., . . . Neumann, I. D. (2015). Selective breeding for high anxiety introduces a synonymous SNP that increases neuropeptide S receptor activity. *J Neurosci, 35* (11), 4599-4613. doi: 10.1523/JNEUROSCI.4764-13.2015

Smith, Y., Bevan, M. D., Shink, E., & Bolam, J. P. (1998). Microcircuitry of the direct and indirect pathways of the basal ganglia. *Neuroscience, 86* (2), 353-387.

Soleiman, M. T. (2015). Opioid Inhibition of Intercalated Input to the Central Amygdala. *J Neurosci, 35* (39), 13272-13274. doi: 10.1523/JNEUROSCI.2578-15.2015

Sousa, N., Almeida, O. F., & Wotjak, C. T. (2006). A hitchhiker's guide to behavioral analysis in laboratory rodents. *Genes Brain Behav, 5 Suppl 2*, 5-24. doi: 10.1111/j.1601-183X.2006.00228.x

Sparta, D. R., Smithuis, J., Stamatakis, A. M., Jennings, J. H., Kantak, P. A., Ung, R. L., & Stuber, G. D. (2014). Inhibition of projections from the basolateral amygdala to the entorhinal cortex disrupts the acquisition of contextual fear. *Front Behav Neurosci, 8*, 129. doi: 10.3389/fnbeh.2014.00129

Stuber, G. D., Sparta, D. R., Stamatakis, A. M., van Leeuwen, W. A., Hardjoprajitno, J. E., Cho, S., . . . Bonci, A. (2011). Excitatory transmission from the amygdala to nucleus accumbens facilitates reward seeking. *Nature, 475* (7356), 377-380. doi: 10.1038/nature10194

Swanson, Larry W. (2003). The Amygdala and Its Place in the Cerebral Hemisphere. *Annals of the New York Academy of Sciences, 985* (1), 174-184. doi: 10.1111/j.1749-6632.2003.tb07081.x

Thompson, B. L., Erickson, K., Schulkin, J., & Rosen, J. B. (2004). Corticosterone facilitates retention of contextually conditioned fear and increases CRH mRNA expression in the amygdala. *Behav Brain Res, 149* (2), 209-215.

Toledo-Rodriguez, M., Blumenfeld, B., Wu, C., Luo, J., Attali, B., Goodman, P., & Markram, H. (2004). Correlation maps allow neuronal electrical properties to be predicted from single-cell gene expression profiles in rat neocortex. *Cereb Cortex, 14* (12), 1310-1327. doi: 10.1093/cercor/bhh092

Tonegawa, S., Liu, X., Ramirez, S., & Redondo, R. (2015). Memory Engram Cells Have Come of Age. *Neuron, 87* (5), 918-931. doi: 10.1016/j.neuron.2015.08.002

Trouche, S., Perestenko, P. V., van de Ven, G. M., Bratley, C. T., McNamara, C. G., Campo-Urriza, N., . . . Dupret, D. (2016). Recoding a cocaine-place memory engram to a neutral engram in the hippocampus. *Nat Neurosci*. doi: 10.1038/nn.4250

Tye, K. M., Prakash, R., Kim, S. Y., Fenno, L. E., Grosenick, L., Zarabi, H., . . . Deisseroth, K. (2011). Amygdala circuitry mediating reversible and bidirectional control of anxiety. *Nature, 471* (7338), 358-362. doi: 10.1038/nature09820

Viviani, D., Charlet, A., van den Burg, E., Robinet, C., Hurni, N., Abatis, M., . . . Stoop, R. (2011). Oxytocin selectively gates fear responses through distinct outputs from the central amygdala. *Science, 333* (6038), 104-107. doi: 10.1126/science.1201043

Wolff, S. B., Grundemann, J., Tovote, P., Krabbe, S., Jacobson, G. A., Muller, C., . . . Luthi, A. (2014). Amygdala interneuron subtypes control fear learning through disinhibition. *Nature, 509* (7501), 453-458. doi: 10.1038/nature13258

Yamauchi, R., Wada, E., Kamichi, S., Yamada, D., Maeno, H., Delawary, M., . . . Wada, K. (2007). Neurotensin type 2 receptor is involved in fear memory in mice. *J Neurochem, 102* (5), 1669-1676. doi: 10.1111/j.1471-4159.2007.04805.x

Yamauchi, R., Wada, E., Yamada, D., Yoshikawa, M., & Wada, K. (2006). Effect of beta-lactotensin on acute stress and fear memory. *Peptides, 27* (12), 3176-3182. doi: 10.1016/j.peptides.2006.08.009

Yao, F., Yu, F., Gong, L., Taube, D., Rao, D. D., & MacKenzie, R. G. (2005). Microarray analysis of fluoro-gold labeled rat dopamine neurons harvested by laser capture microdissection. *J Neurosci Methods, 143* (2), 95-106. doi: 10.1016/j.jneumeth.2004.09.023

Yiu, A. P., Mercaldo, V., Yan, C., Richards, B., Rashid, A. J., Hsiang, H. L., . . . Josselyn, S. A. (2014). Neurons are recruited to a memory trace based on relative neuronal excitability immediately before training. *Neuron, 83* (3), 722-735. doi: 10.1016/j.neuron.2014.07.017

Yu, K., Garcia da Silva, P., Albeanu, D. F., & Li, B. (2016). Central Amygdala Somatostatin Neurons Gate Passive and Active Defensive Behaviors. *J Neurosci, 36* (24), 6488-6496. doi: 10.1523/jneurosci.4419-15.2016

Zhang, F., Wang, L. P., Boyden, E. S., & Deisseroth, K. (2006). Channelrhodopsin-2 and optical control of excitable cells. *Nat Methods, 3* (10), 785-792. doi: 10.1038/nmeth936

Zhao, S., Cunha, C., Zhang, F., Liu, Q., Gloss, B., Deisseroth, K., . . . Feng, G. (2008). Improved expression of halorhodopsin for light-induced silencing of neuronal activity. *Brain Cell Biol, 36* (1-4), 141-154. doi: 10.1007/s11068-008-9034-7

Zhou, P., Zhang, Y., Ma, Q., Gu, F., Day, D. S., He, A., . . . Pu, W. T. (2013). Interrogating translational efficiency and lineage-specific

transcriptomes using ribosome affinity purification. *Proc Natl Acad Sci U S A, 110* (38), 15395-15400. doi: 10.1073/pnas.1304124110